Vol. 24, no. 3, 2024 eISSN 2687-1653
PEER-REVIEWED SCIENTIFIC AND PRACTICAL JOURNAL

Advanced Engineering Research (Rostov-on-Don)

Mechanics

Machine Buiding and Machine Science

Information Technology, Computer Science and Management

www.vestnik-donstu.ru
DOI 10.23947/2687-1653

Advanced Engineering Research (Rostov-on-Don)

Peer-reviewed scientific and practical journal (published since 2000)

eISSN 2687–1653
DOI: 10.23947/2687–1653

Vol. 24, no. 3, 2024

The journal is aimed at informing the readership about the latest achievements and prospects in the field of mechanics, mechanical engineering, computer science and computer technology. The publication is a forum for cooperation between Russian and foreign scientists, it contributes to the convergence of the Russian and world scientific and information space.

The journal is included in the List of the leading peer-reviewed scientific publications (Higher Attestation Commission under the Ministry of Science and Higher Education of the Russian Federation), where basic scientific results of dissertations for the degrees of Doctor and Candidate of Science in scientific specialties and their respective branches of science should be published.

The journal publishes articles in the following fields of science:

– Theoretical Mechanics, Dynamics of Machines (Engineering Sciences)
– Deformable Solid Mechanics (Engineering, Physical and Mathematical Sciences)
– Mechanics of Liquid, Gas and Plasma (Engineering Sciences)
– Mathematical Simulation, Numerical Methods and Program Systems (Engineering Sciences)
– System Analysis, Information Management and Processing, Statistics (Engineering Sciences)
– Automation and Control of Technological Processes and Productions (Engineering Sciences)
– Software and Mathematical Support of Machines, Complexes and Computer Networks (Engineering Sciences)
– Computer Modeling and Design Automation (Engineering, Physical and Mathematical Sciences)
– Computer Science and Information Processes (Engineering Sciences)
– Machine Science (Engineering Sciences)
– Machine Friction and Wear (Engineering Sciences)
– Technology and Equipment of Mechanical and Physicotechnical Processing (Engineering Sciences)
– Engineering Technology (Engineering Sciences)
– Welding, Allied Processes and Technologies (Engineering Sciences)
– Methods and Devices for Monitoring and Diagnostics of Materials, Products, Substances and the Natural Environment (Engineering Sciences)
– Hydraulic Machines, Vacuum, Compressor Equipment, Hydraulic and Pneumatic Systems (Engineering Sciences)

Indexing and Archiving	RSCI, CyberLeninka, CrossRef, Dimensions, DOAJ, EBSCO, Index Copernicus, Internet Archive, Google Scholar
Name of the Body that Registered the Publication	Extract from the Register of Registered Mass Media ЭЛ № ФС 77 – 78854 dated August 07, 2020, issued by the Federal Service for Supervision of Communications, Information Technology and Mass Media
Founder and Publisher	Federal State Budgetary Educational Institution of Higher Education Don State Technical University (DSTU)
Periodicity	4 issues per year
Address of the Founder and Publisher	1, Gagarin sq., Rostov-on-Don, 344003, Russian Federation
E-mail	vestnik@donstu.ru
Telephone	+7 (863) 2–738–372
Website	http://vestnik-donstu.ru
Date of Publication	30.09.2024

Advanced Engineering Research (Rostov-on-Don)

Рецензируемый научно-практический журнал (издается с 2000 года)

eISSN 2687–1653
DOI: 10.23947/2687–1653

Том 24, № 3, 2024

Создан в целях информирования читательской аудитории о новейших достижениях и перспективах в области механики, машиностроения, информатики и вычислительной техники. Издание является форумом для сотрудничества российских и иностранных ученых, способствует сближению российского и мирового научно-информационного пространства.

Журнал включен в перечень рецензируемых научных изданий, в котором должны быть опубликованы основные научные результаты диссертаций на соискание ученой степени кандидата наук, на соискание ученой степени доктора наук (Перечень ВАК) по следующим научным специальностям:

1.1.7 – Теоретическая механика, динамика машин (технические науки)
1.1.8 – Механика деформируемого твердого тела (технические, физико-математические науки)
1.1.9 – Механика жидкости, газа и плазмы (технические науки)
1.2.2 – Математическое моделирование, численные методы и комплексы программ (технические науки)
2.3.1 – Системный анализ, управление и обработка информации, статистика (технические науки)
2.3.3 – Автоматизация и управление технологическими процессами и производствами (технические науки)
2.3.5 – Математическое и программное обеспечение вычислительных систем, комплексов и компьютерных сетей (технические науки)
2.3.7 – Компьютерное моделирование и автоматизация проектирования (технические, физико-математические науки)
2.3.8 – Информатика и информационные процессы (технические науки)
2.5.2 – Машиноведение (технические науки)
2.5.3 – Трение и износ в машинах (технические науки)
2.5.5 – Технология и оборудование механической и физико-технической обработки (технические науки)
2.5.6 – Технология машиностроения (технические науки)
2.5.8 – Сварка, родственные процессы и технологии (технические науки)
2.5.9 – Методы и приборы контроля и диагностики материалов, изделий, веществ и природной среды (технические науки)
2.5.10 – Гидравлические машины, вакуумная, компрессорная техника, гидро- и пневмосистемы (технические науки)

Индексация и архивация	РИНЦ, CyberLeninka, CrossRef, Dimensions, DOAJ, EBSCO, Index Copernicus, Internet Archive, Google Scholar
Наименование органа, зарегистрировавшего издание	Выписка из реестра зарегистрированных средств массовой информации ЭЛ № ФС 77 – 78854 от 07 августа 2020 г., выдано Федеральной службой по надзору в сфере связи, информационных технологий и массовых коммуникаций
Учредитель и издатель	Федеральное государственное бюджетное образовательное учреждение высшего образования «Донской государственный технический университет» (ДГТУ)
Периодичность	4 выпуска в год
Адрес учредителя и издателя	344003, Российская Федерация, г. Ростов-на-Дону, пл. Гагарина, 1
E-mail	vestnik@donstu.ru
Телефон	+7 (863) 2–738–372
Сайт	http://vestnik-donstu.ru
Дата выхода в свет	30.09.2024

Contents

Содержание

ANNIVERSARY OF THE SCIENTIST
ЮБИЛЕЙ УЧЕНОГО

Alexey Nikolaevich Beskopylny, Scientist, Teacher, Expert, Leader, is 65

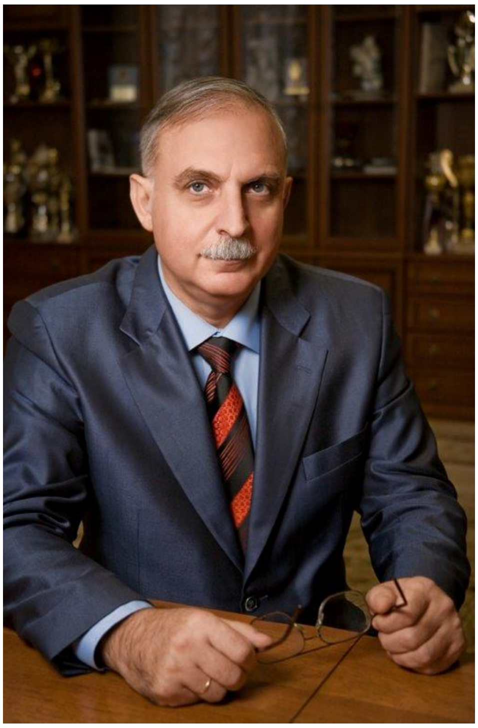

Alexey Nikolaevich Beskopylny — Doctor of Engineering Science, Professor, scientist and expert in the diagnostics and monitoring of building structures, Vice-Rector for Academic and International Affairs, Don State Technical University.

In 1981, Aleksey Nikolayevich graduated from Rostov Institute of Construction Engineering majoring in Industrial Transport Engineering. He embarked upon a career as an engineer in the industrial transport research laboratory. After completing his postgraduate studies and defending his PhD thesis, from 1986 to 1994, he worked his way up from a junior research fellow to the Head of the machine reliability management laboratory.

In 1997, A.N. Beskopylny defended his doctoral thesis on the topic "Method for determining mechanical properties and quality control of structural steels by impact indentation" at Rostov State University of Civil Engineering (RSCU). From 1997 to 1998, A.N. Beskopylny worked as a Deputy director and, from 1998 to 2005 — as Director of the Road Transport Institute, RSCU. From 2005 to 2016, he successfully performed the duties of Vice-Rector for educational work, Vice-Rector for academic affairs, and Vice-Rector for the organization of educational activities at the university.

As a result of the reorganization in early 2016, RSCU became part of the Don State Technical University (DSTU) as the Academy of Civil Engineering and Architecture, and Alexey Nikolaevich was immediately appointed its Director. From 2018 to 2021, he worked as Vice-Rector for Academic Affairs and Training of Highly Qualified Personnel, and from 2021 to the present — Vice-Rector for Academic Affairs and International Activities of DSTU.

A.N. Beskopylny made a significant contribution to the modernization and development of the system of training highly qualified personnel and strengthening collaboration with foreign partners of the flagship university, including within the framework of the "Priority–2030" program.

A.N. Beskopylny is a well-known scientist in the field of construction, non-destructive testing methods of dynamic structures. His teaching and scientific activities are reflected in 240 works, including 3 monographs, 5 textbooks and teaching aids, 9 patents. Over the past five years, he has published more than 220 scientific papers, 159 of which are indexed in the international scientometric databases Scopus and Web of Science.

With the active support of Alexey Nikolaevich, the Academy of Publication Activity and a system of scientific, organizational and financial support for authors, including young scientists and specialists, were created at DSTU; 10 scientific journals are published, 6 of which are included in the List of the State Commission for Academic Degrees and Titles. The Vice-Rector's initiatives enable the university to fulfill and exceed its publication plans, while developing and enhancing the professional competences of authors in the international scientific communication and academic writing. As Vice-Rector, Aleksey Nikolaevich made a great contribution to improving the educational process, introducing information and computer technologies, training highly qualified engineering and scientific-pedagogical personnel. Under his leadership, doctoral and candidate thesis papers were successfully prepared.

A.N. Beskopylny has developed and is currently implementing scientific and educational programs for the engineering master's degree within the framework of 14 educational projects in cooperation with industrial partners of the Don Region: PJSC Rostvertol, OJSC PK NEVZ, PJSC Tagmet, LLC KZ Rostselmash, JSC Aluminum Metallurg Rus.

The results of Alexey Nikolaevich's scientific and innovative activities have been implemented by the Ministry of Transport of the Russian Federation, the Ministry of Transport of the Rostov Region at 53 enterprises in Russia, including Scientific Research Institute of Automobile Transport LLC (Moscow), Stroyproekt Engineering Group Association (St. Petersburg), the Department of Highways and Traffic Management of the City of Rostov-on-Don, and others.

Alexey Nikolaevich Beskopylny is the recipient of the Certificate of Honor of the Ministry of Education and Science of the Russian Federation (2010), the badge "Honorary Worker of RF Higher Vocational Education" (2003), the badge "Honorary Builder of Russia" (2011), the medal "In Recognition of Development of the Construction Industry" (2011).

The Editorial team sincerely congratulates Alexey Nikolaevich Beskopylny, Editor-in-chief of the journal "Advanced Engineering Research (Rostov-on-Don)", on his 65th birthday and wishes him health, well-being, inspiration and energy for new scientific achievements for the benefit of his native university and construction education!

MECHANICS
МЕХАНИКА

UDC 620.17.4
https://doi.org/10.23947/2687-1653-2024-24-3-215-226

Original Empirical Research

Increasing the Interlayer Fracture Toughness of Polymer Fabric Composites Using Local 3D-Reinforcement (Felting)

EDN: KVEMQM

Galina A. Forental[1] ✉, **Sergey B. Sapozhnikov**[1,2]
[1] South Ural State University, Chelyabinsk, Russian Federation
[2] Central Aerohydrodynamic Institute, Zhukovsky, Russian Federation
✉gforental@mail.ru

Abstract
Introduction. One of the reasons for undesirable delamination of polymer composites with fabric reinforcement is low transverse shear properties. It is known that the reinforcement of polymer fabric composites in the *Z* direction reduces the sensitivity to delamination and increases the viscosity of interlayer fracture. Various methods of three-dimensional reinforcement of polymer fabric composites are proposed in the literature. However, they complicate the manufacturing process of the structure. The problem is solved by the method of three-dimensional reinforcement proposed in this article — felting. This is a local reinforcement of the composite in the *Z* direction with minimal production changes. The degree of *Z*-reinforcement is determined by the felting density, i.e., the number of needle punches per 1 cm^2 of the fabric package. The work is aimed at evaluating the effect of felting on the interlayer crack resistance of a composite material.
Materials and Methods. The interlayer fracture toughness G_{IIc} was determined on a cross-woven fiberglass with felting of 10 cm^{-2}. The material was impregnated with Etal-370 resin and Etal-45 hardener. Experiments according to ASTM D7905M–14 and GOST 33685–2015 standards were carried out on an Instron 5900R test machine. The stress state at the crack tip was analyzed with regard to the nonlocal strength theory in the ANSYS Workbench program (option "static strength analysis"). The finite element method (FEM) was used.
Results. The "load — displacement" curves were considered for the samples. Values G_{IIc} were calculated. The results of ENF tests for felting density of 0 cm^{-2} and 10 cm^{-2} were summarized. Control samples and felting samples were compared. In the latter case, G_{IIc} turned out to be ~33% higher. The stress state at the crack tip was calculated under DCB and ENF loading. The dependences of maximum normal and shear stresses, as well as displacements, were visualized in the form of graphs and color charts. To get the calculated "load — displacement" dependences using FEM, the reverse method of obtaining transverse shear constants was used. DCB loading showed that felting provided increasing the rupture strength in the *Z* direction to ~18%, by 39 to 46 MPa, and in the planes *XZ*— to ~16%, by 77 to 89 MPa.
Discussion and Conclusion. Felting as a method of local three-dimensional reinforcement enhances the interlayer crack resistance of polymer fabric composites. It provides reducing the area of stratifications after local impacts during the operation of structures. Flexible felting technology makes it possible to create zones with an arbitrary impact density, increasing fracture toughness only in the required places of structures. The FEM analysis of the stress state at the crack tip within the framework of the nonlocal strength theory has shown that in strength calculations, the stratification crack can be considered as a stress concentrator.

Keywords: reinforcement of polymer fabric composites, transverse shear strength, interlayer crack resistance, interlaminar fracture toughness, felting local three-dimensional reinforcement

Acknowledgements. The authors would like to thank colleagues A.V. Nikonov and A.V. Kheruvimov for their help in preparing the samples.

Funding Information. The research was done within the framework of the Program for the Creation and Development of the World-Class Scientific Center "Supersound" for 2020–2025 with the financial support of the Ministry of Education and Science of the Russian Federation (Agreement no. 075–15–2022–1023, dated May 17, 2022).

For Citation. Forental GA, Sapozhnikov SB. Increasing the Interlayer Fracture Toughness of Polymer Fabric Composites Using Local 3D-Reinforcement (Felting). *Advanced Engineering Research* (*Rostov-on-Don*). 2024;24(3):215–226. https://doi.org/10.23947/2687-1653-2024-24-3-215-226

Оригинальное эмпирическое исследование

Повышение межслойной трещиностойкости полимерных тканевых композитов с помощью локального трехмерного армирования (фелтинга)

Г.А. Форенталь[1] ✉, **С.Б. Сапожников**[1,2]

[1] Южно-Уральский государственный университет, г. Челябинск, Российская Федерация

[2] Центральный аэрогидродинамический институт имени профессора Н.Е. Жуковского, г. Жуковский, Российская Федерация

✉gforental@mail.ru

Аннотация

Введение. Одна из причин нежелательных расслоений полимерных композитов с тканевым армированием — низкие трансверсально-сдвиговые характеристики. Известно, что армирование полимерных тканевых композитов в направлении Z уменьшает чувствительность к расслоению и повышает вязкость межслойного разрушения. В литературе предлагаются разные способы трехмерного армирования полимерных тканевых композитов. Однако они усложняют процесс изготовления конструкции. Проблему решает предложенный в данной статье способ трехмерного армирования — фелтинг. Это локальное армирование композита в направлении Z при минимальных производственных изменениях. Степень Z-армирования определяется плотностью фелтинга, т.е. количеством ударов иглы на 1 см^2 тканевого пакета. Цель работы — оценить влияние фелтинга на межслойную трещиностойкость композитного материала.

Материалы и методы. Межслойную вязкость разрушения G_{IIc} определяли на стеклоткани полотняного переплетения с фелтингом 10 см$^{-2}$. Материал пропитывали смолой Этал-370 и отвердителем Этал-45. Эксперименты по стандартам ASTM D7905M–14 и ГОСТ 33685–2015 проводили на испытательной машине Instron 5900R. Напряженное состояние у вершины трещины анализировали с позиции нелокальной теории прочности в программе Ansys Workbench (опция «статический прочностной анализ»). Задействовали метод конечных элементов (МКЭ).

Результаты исследования. Для образцов рассмотрели кривые «нагрузка — перемещение». Вычислили значения G_{IIc}. Обобщили итоги ENF-испытаний для плотности фелтинга 0 см$^{-2}$ и 10 см$^{-2}$. Сравнили контрольные образцы и образцы с фелтингом. В последнем случае G_{IIc} оказалась выше на ~33 %. Рассчитали напряженное состояние у вершины трещины при DCB- и ENF-нагружении. Визуализировали в виде графиков и цветовых диаграмм зависимости максимальных нормальных и касательных напряжений, а также перемещений. Для получения расчетных зависимостей «нагрузка — перемещение» с помощью МКЭ использовали обратный метод получения трансверсально-сдвиговых констант. Нагружение по схеме DCB показало, что фелтинг позволяет увеличить предел прочности на растяжение в направлении Z на ~18 %, с 39 до 46 МПа, а в плоскости XZ — на ~16 %, с 77 МПа до 89 МПа.

Обсуждение и заключение. Фелтинг как способ локального трехмерного армирования усиливает межслойную трещиностойность полимерных тканевых композитов. Он позволяет сократить площадь расслоений после локальных ударов при эксплуатации конструкций. Гибкая технология фелтинга дает возможность создавать зоны с произвольной плотностью ударов, повышая трещиностойкость лишь в необходимых местах конструкций. МКЭ-анализ напряженного состояния у вершины трещины в рамках нелокальной теории прочности показал, что в прочностных расчетах трещину расслоения можно рассматривать как концентратор напряжений.

Ключевые слова: армирование полимерных тканевых композитов, трансверсально-сдвиговая прочность, межслойная трещиностойкость, межслоевая вязкость разрушения, фелтинговое локальное трехмерное армирование

Благодарности. Авторы выражают признательность коллегам Никонову А.В., Херувимову А.В. за помощь в изготовлении образцов для экспериментальных исследований.

Финансирование. Исследование выполнено в рамках Программы создания и развития научного центра мирового уровня «Сверхзвук» на 2020–2025 годы при финансовой поддержке Минобрнауки России (соглашение от 17 мая 2022 г. № 075–15–2022–1023).

Для цитирования. Форенталь Г.А., Сапожников С.Б. Повышение межслойной трещиностойкости полимерных тканевых композитов с помощью локального трехмерного армирования (фелтинга). *Advanced Engineering Research* (*Rostov-on-Don*). 2024;24(3):215–226. https://doi.org/10.23947/2687-1653-2024-24-3-215-226

Introduction. Fibrous polymer composites are widely used, in particular, in aviation and space engineering due to their significant rigidity and strength in the fiber orientation (plane *XY*) [1]. However, the transverse shear strength of these materials is quite low [2], as it is determined by the features of the polymer matrix [3]. Reinforcement of polymer fabric composites in the *Z* direction provides reducing the sensitivity to delamination, i.e., increasing the viscosity of interlayer fracture [4].

Various methods of three-dimensional reinforcement of polymer fabric composites are known [5]. However, they create additional difficulties in the manufacture of structures made of polymer fabric composites [6]. The method of three-dimensional reinforcement proposed in this work, felting [7], makes it possible to obtain a locally reinforced composite in the *Z* direction with minimal changes in the production process. The degree of Z-reinforcement is determined by the felting density, i.e., the number of needle punches per 1 cm^2 of the area of the fabric package [8].

The use of various methods for determining the fracture toughness of polymer composite materials [9] makes it possible to conduct studies on various samples [10] and with different loading methods [11]. One of the most common approaches is the three-point bending method. In this case, a beam-shaped delamination sample is used. We are talking about ENF tests (End-Notched Flexure — bending of a sample with edge delamination) [12], which involve transverse shear loading. This makes it possible to determine the interlayer fracture viscosity of G_{IIc} — mode II fracture. High shear stresses occur at the crack tip [13].

Another common way to determine transverse characteristics is the Double Cantilever Beam method (DCB tests). In DCB tests, the value of the interlaminar fracture toughness G_{Ic} is determined under separation loading — fracture according to mode I [14]. The delamination crack spreads due to the action of normal stresses [15].

The presented work was aimed at the evaluation of the effect of felting on the interlayer fracture toughness of a composite material. To do this, ENF tests (bending of a sample with an edge separation) of a composite material with increased crack resistance due to the use of felting were carried out. Previously, the authors studied the effect of felting on the interlayer crack resistance of a composite material during DCB tests [16]. A computational model based on the nonlocal theory of strength has been developed. It provides for the calculation of the stresses that occur in ENF and DCB samples, for cracks of various lengths, using the finite element method (FEM).

Materials and Methods

Experimental determination of interlayer crack resistance by the ENF method. The samples were made of cross-woven fiberglass with a layer thickness of 0.2 mm. A package of dry two-layered fiberglass was punched on a felting machine with a felting density of 10 cm^{-2} (10 punches with a felting machine needle per 1 cm^2 of dry glass fabric). The fiberglass package was punched in such a way that after impregnation and hardening, the initial crack did not fall on the felting area. To create an initial crack between two layers of fiberglass, an aluminum foil with a thickness of 11 µm, coated with a Vs-M parting lubricant, was placed. Fiberglass was impregnated with resin Etal-370 and hardener Etal-45. For the production of reference samples, two layers of dry fiberglass were impregnated with Etal-370 resin and Etal-45 hardener without punching on a felting machine. After impregnation, plates from glass textolite STEF (electrotechnical glass-cloth-base laminate) were glued to two layers of fiberglass (Fig. 1 *a*). Samples with a length of 150 mm and a width of 16 mm were obtained by cutting the hardened plates using a high-speed circular saw.

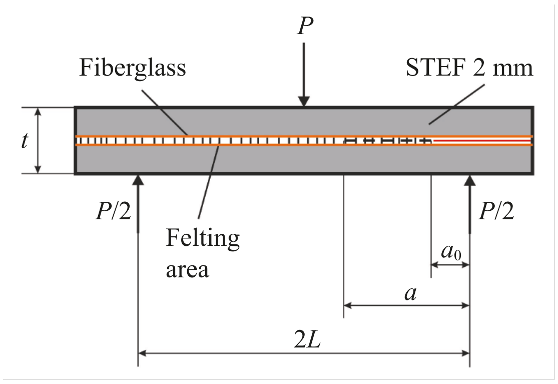

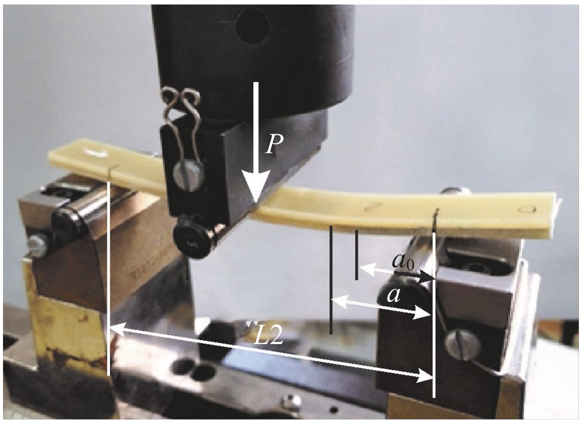

a) *b*)

Fig. 1. Configuration and parameters of ENF tests according to mode *II*:
a — loading scheme; *b* — photo of tests

The Instron 5900R test machine with a loading speed of 10 mm/min was used. The distance between the supports was $2L = 100$ mm. The initial crack length for all samples was $a_0 = 25$ mm. To perform compliance calibration over a wide range of crack lengths, one sample of each type was unloaded and reloaded. The resulting crack served as the initial crack in the next loading cycle.

Calibration recommended by ASTM D7905M–14[1] and GOST 33685–2015[2] standards was used to process the test results. This approach provided determining parameters A and m for each felting sample and each non-felting control sample from the linear dependence of two quantities — compliance of sample C and cube of the crack length a^3:

$$C\left(\delta / P(\delta)\right) = A + m \cdot a^3, \qquad (1)$$

where P — load applied to the sample; δ — displacement.

After calibration and determination of parameters A and $m,$ the crack length can be found from expression (1):

$$a = \left(\frac{C - A}{m}\right)^{1/3}. \qquad (2)$$

The moment of the delamination onset is determined by the condition $C(\delta) = C(P_{max})$. Value of the interlayer fracture toughness at the separation onset (crack development):

$$G_{\mathrm{II}c} = \frac{3m \cdot P_{max}^2 \cdot a^2}{2b}, \qquad (3)$$

where P_{max} — maximum load; a — crack length calculated by formula (2) at load P_{max}; b — sample width.

Calculation of the stress state at the crack tip under loading according to the DCB and ENF schemes. The stress state of a crack-like concentrator is estimated from the perspective of approaches that use nonlocal stresses [17], i.e., averaged on some basis [18]. The calculation model also includes the assumption of linear-elastic behavior of the material up to destruction [16].

The main hypothesis is that the strength criterion of the composite, which includes all components of stress averaged on the basis λ, is responsible for the development of a crack-like concentrator (Fig. 2):

$$\left(\frac{max\,\sigma_{z\lambda}}{Z_t}\right)^2 + \left(\frac{max\,\sigma_{x\lambda}}{X_t}\right)^2 + \left(\frac{max\,\tau_{xz\lambda}}{S}\right)^2 - \frac{max\,\sigma_{z\lambda} \cdot max\,\sigma_{x\lambda}}{Z_t \cdot X_t} \le 1, \qquad (4)$$

where Z_t and X_t — rupture strength in the Z and X directions; S — shear strength in the plane XZ.

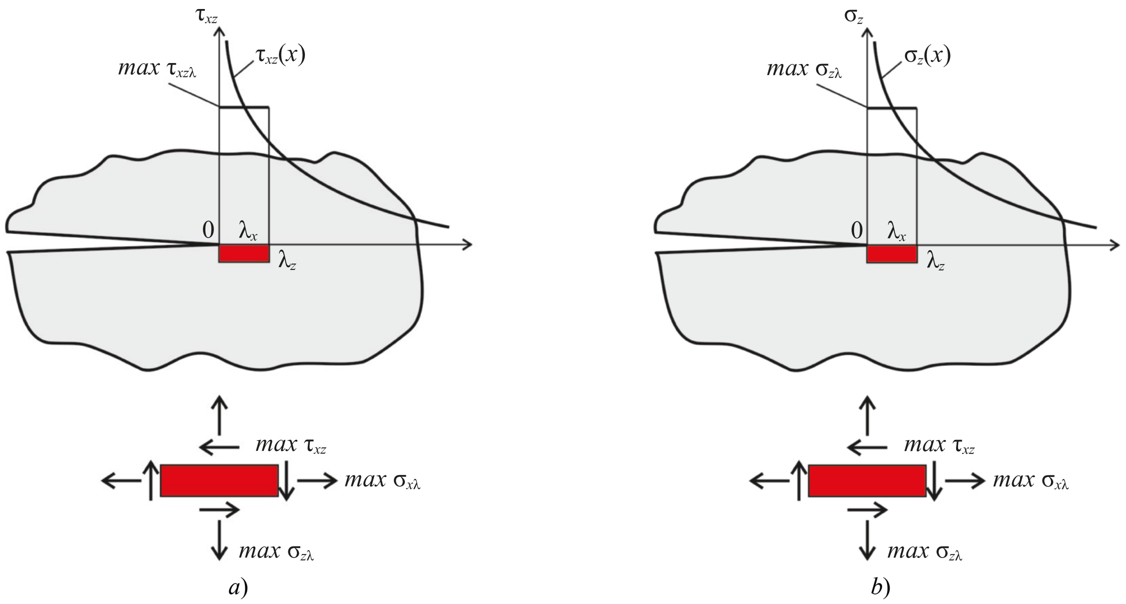

Fig. 2. Stresses averaged on the basis λ at the crack tip:
a — ENF tests; *b* — DCB tests

[1] ASTM D7905/D7905M–14. *Standard Test Method for Determination of the Mode II Interlaminar Fracture Toughness of Unidirectional Fiber-Reinforced Polymer Matrix Composites.* URL: https://cdn.standards.iteh.ai/samples/89096/03be6b5e53664f13a8703bb4342d981a/ASTM-D7905-D7905M-14.pdf (accessed: 22.04.2024).

[2] GOST 33685–2015. *Polymer Composites. Test Method for Determination of the Interlaminar Fracture Toughness under Shear.* (In Russ.) URL: https://docs.cntd.ru/document/1200127774 (accessed: 22.04.2024).

Due to the presence of symmetry planes, a three-dimensional 1/2 crack sample model was constructed for ENF loading (Fig. 3), and 1/4 crack sample — for DCB tests (Fig. 4). Calculations were performed in the ANSYS Workbench program (option "static structural").

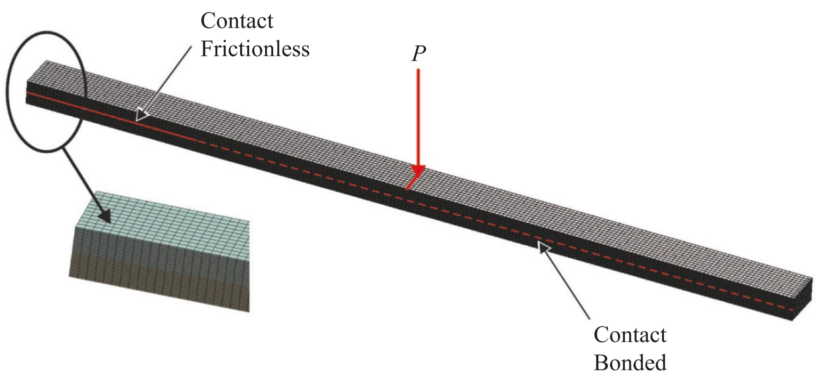

Fig. 3. Finite element model 1/2 of the sample and a fragment of the grid for ENF tests

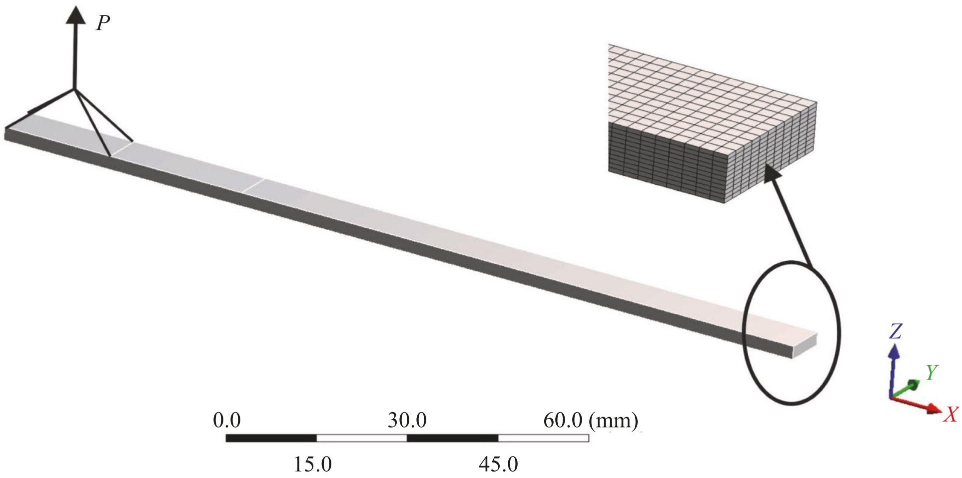

Fig. 4. Finite element model 1/4 of the sample and a fragment of the grid for DCB tests

When creating the finite element grid, parameter $\lambda_x = 0.75$ mm in width of the sample [19] and parameter $\lambda_z = 0.2$ mm in thickness of the sample were set, which corresponded to the thickness of the modified layer [20]. One finite element in the thickness of the layer was set in accordance with the layer wise theory used in assessing the strength of layers within the framework of mesomechanics of composites [21]. In ENF tests, the total displacements in the sample were much greater than the local displacements from the loading roller (Fig. 1 *b*); therefore, the grid of finite elements was not condensed at the places of application of loads and supports (Fig. 3). Properties of fiberglass used in the calculation:

- elastic modules $E_x = E_y = 23$ GPa, $E_z = 9$ GPa;
- shear modules $G_{xy} = G_{yz} = G_{xz} = 6000$ GPa;
- Poisson's coefficients $\mu_{xy} = 0.15$, $\mu_{yz} = \mu_{xz} = 0.3$ [22].

Since the volume fraction of transverse reinforcement is less than 1% [16], it is assumed in the calculations that the elastic properties of fiberglass do not change under felting.

Dependence $P(\delta)$ was calculated in accordance with the sequence described below.

1. FEM-calculation of the maximum stresses $max\sigma_{z\lambda}$, $max\sigma_{x\lambda}$ and $max\tau_{xz\lambda}$ and displacements of point δ of application of load $P = 1$ H for cracks with the given lengths in the range $a = 20\ldots90$ mm (DCB) and $a = 25\ldots40$ mm (ENF) was performed.

1. Approximation dependences $\sigma_{z\lambda} = f(a, P) = P{\cdot}b_1{\cdot}a$; $\sigma_{x\lambda} = f(a, P) = P{\cdot}b_2{\cdot}a$; $\tau_{xz\lambda} = f(a, P) = P{\cdot}b_3{\cdot}a$; $\delta = f(a, P) = P{\cdot}c_1{\cdot}a^3$·(DCB) and $\sigma_{z\lambda} = f(a, P) = P{\cdot}b_1{\cdot}a$; $\sigma_{x\lambda} = f(a, P) = P{\cdot}b_2{\cdot}a$; $\tau_{xz\lambda} = f(a, P) = P{\cdot}(b_3{\cdot}a + d_3)$; $\delta = f(a, P) = P{\cdot}(c_1{\cdot}a^3 + c_2{\cdot}a^2 + c_3{\cdot}a + c_4)$·(ENF).

2. were constructed using the least squares method.

3. Load $P_{cr}(a_0)$ and displacement δ_{cr}, at which the initial crack length a_0 would increase abruptly by $\lambda_x = 0.75$ mm upon the violation of the strength criterion, were determined (4).

4. With crack length $a_0+n\lambda$, loads $P(a_0+n\lambda)$ and displacements $\delta(n)$ for $n>0$ were determined.

Mechanics

Research Results

Results of the experimental determination of interlayer fracture toughness by the ENF method. Figure 5 shows the “load — displacement” curves for all tested samples. All “load — displacement” curves have an area with constant compliance (C_{lin}), corresponding to the linear “load — displacement” ratio. Values C_{lin} were used for calibration.

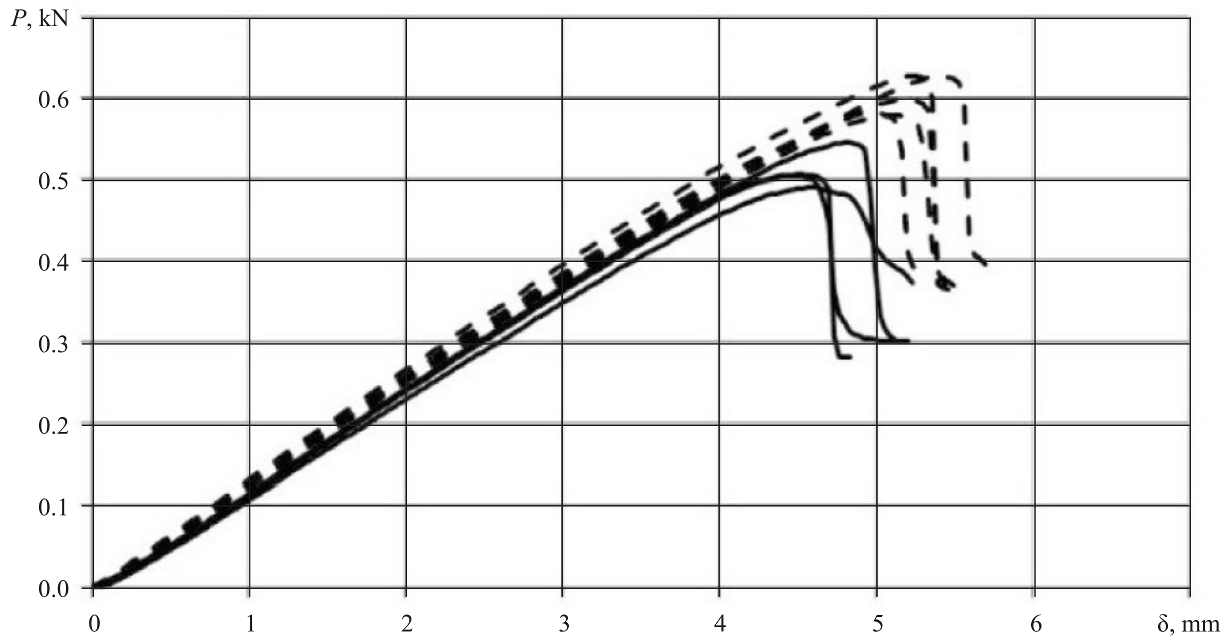

Fig. 5. “Load — displacement” diagrams of ENF tests
——— without felting; — — — — with felting

Figure 6 shows the calibration curves. For felting and non-felting samples, compliance is proportional to the cube of the crack length.

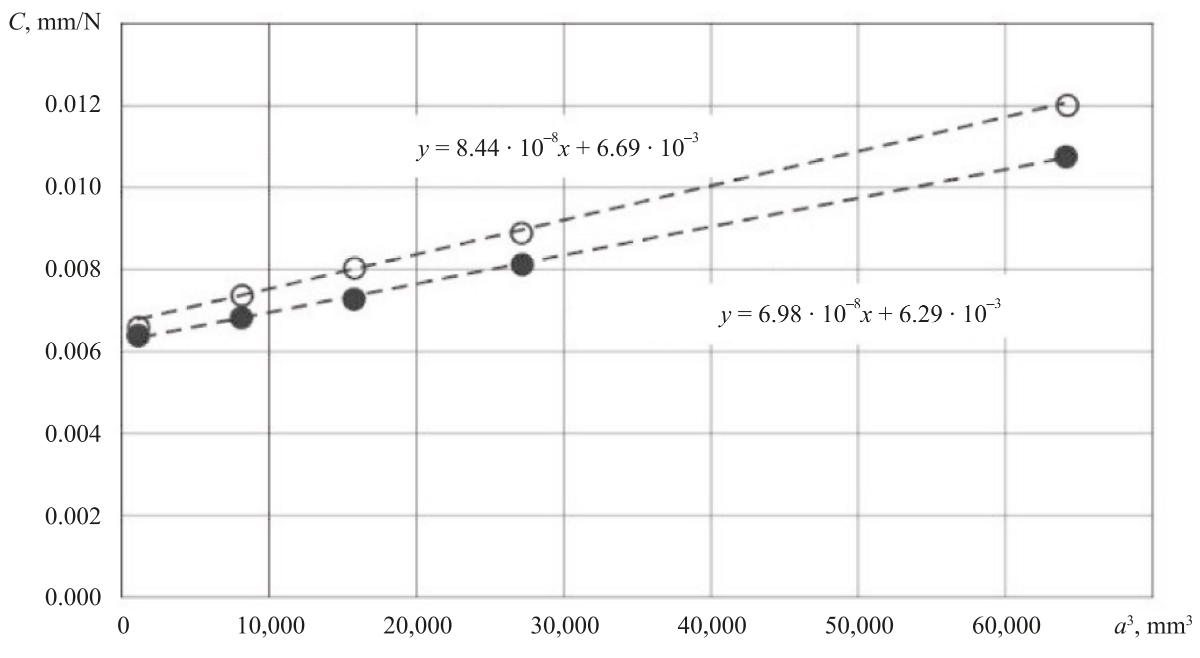

Fig. 6. Dependence of compliance of sample C on the cube of crack length a^3:
○ — without felting; ● — with felting

To calculate values of the crack length a^*, corresponding to the compliance at the delamination onset $C(P_{max})$, the obtained calibration curves and equation (2) were used. For the found values of the crack length a^*, values G_{IIc} were calculated using equation (3). The results are shown in Table 1.

Table 1

ENF Test Results

Felting Density, cm^{-2}	a_0, mm	C_{lin}, mm/N	$C_{(Pmax)}$, mm/N	a*, mm	P_{max}, N	G_{IIc}, kJ/m^2	G_{IIc} (average value), kJ/m^2 (CV)
0	25	8.032	8.845	29.4	504.6	1.723	1.840 ± 0.126 (6.9%)
0	25	7.980	8.807	29.3	544.6	1.983	
0	25	8.299	9.392	31.7	489.4	1.908	
0	25	7.905	8.900	29.7	505.2	1.746	
10	25	7.587	8.337	30.8	627.3	2.432	2.441 ± 0.154 (6.3%)
10	25	7.849	8.677	32.4	625.8	2.682	
10	25	7.937	8.811	33.0	578.4	2.376	
10	25	7.824	8.594	32.1	581.4	2.261	
10	25	7.880	8.818	33.1	589.3	2.456	
* variation coefficient							

Felting samples showed a significant (by ~33%) increase in the interlayer fracture toughness G_{IIc} compared to the control samples. After testing, felting samples were separated with a sharp knife and examined under a microscope. Micrographs of the zone without felting (area of the initial crack) and the zone with felting (area of crack development) are shown in Figure 7. When cracks develop, the fibers elongated during felting are destroyed, because their length is greater than the critical one [16].

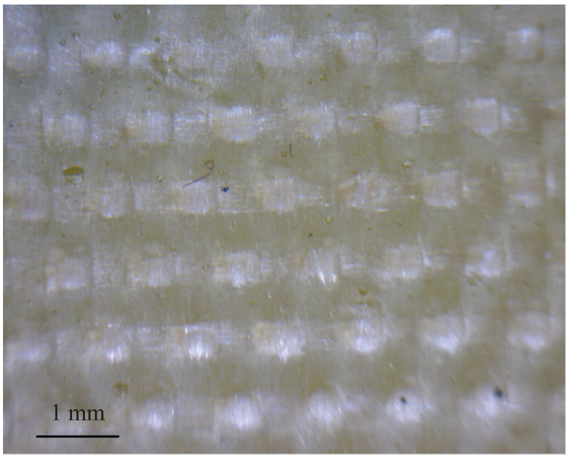

a)

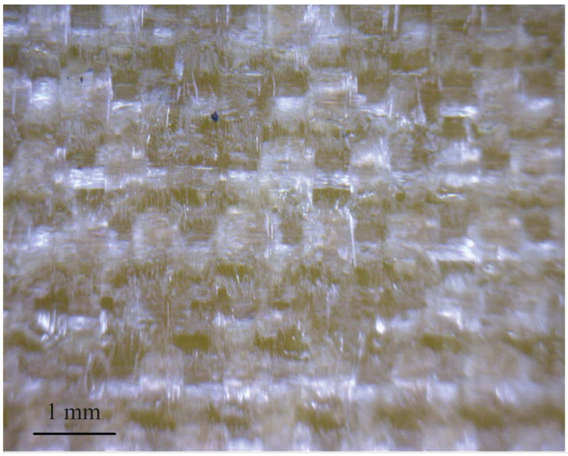

b)

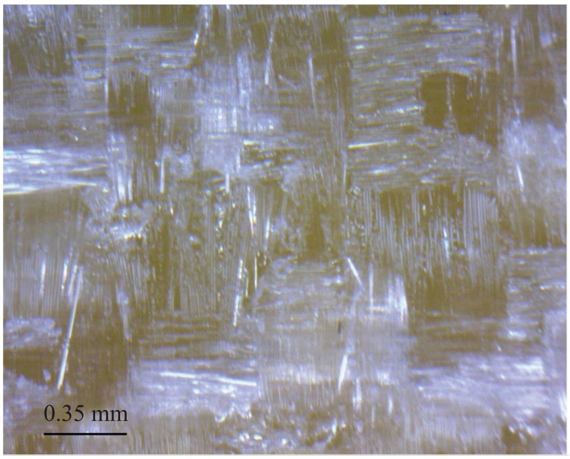

c)

Fig. 7. Micrographs of felting samples after ENF tests:
a — zone without felting (area of initial crack);
b — zone with felting (area of crack development);
c — zone with felting (enlarged scale)

Results of the calculation of the stress state at the crack tip under loading according to the DCB and ENF schemes. Figures 8–9 show the dependences of stress $max\sigma_{z\lambda}(a)$, $max\sigma_{x\lambda}(a)$, $max\tau_{xz\lambda}(a)$ and displacements $\delta(a)$. Conditions: P = 1 N, loading according to DCB and ENF schemes.

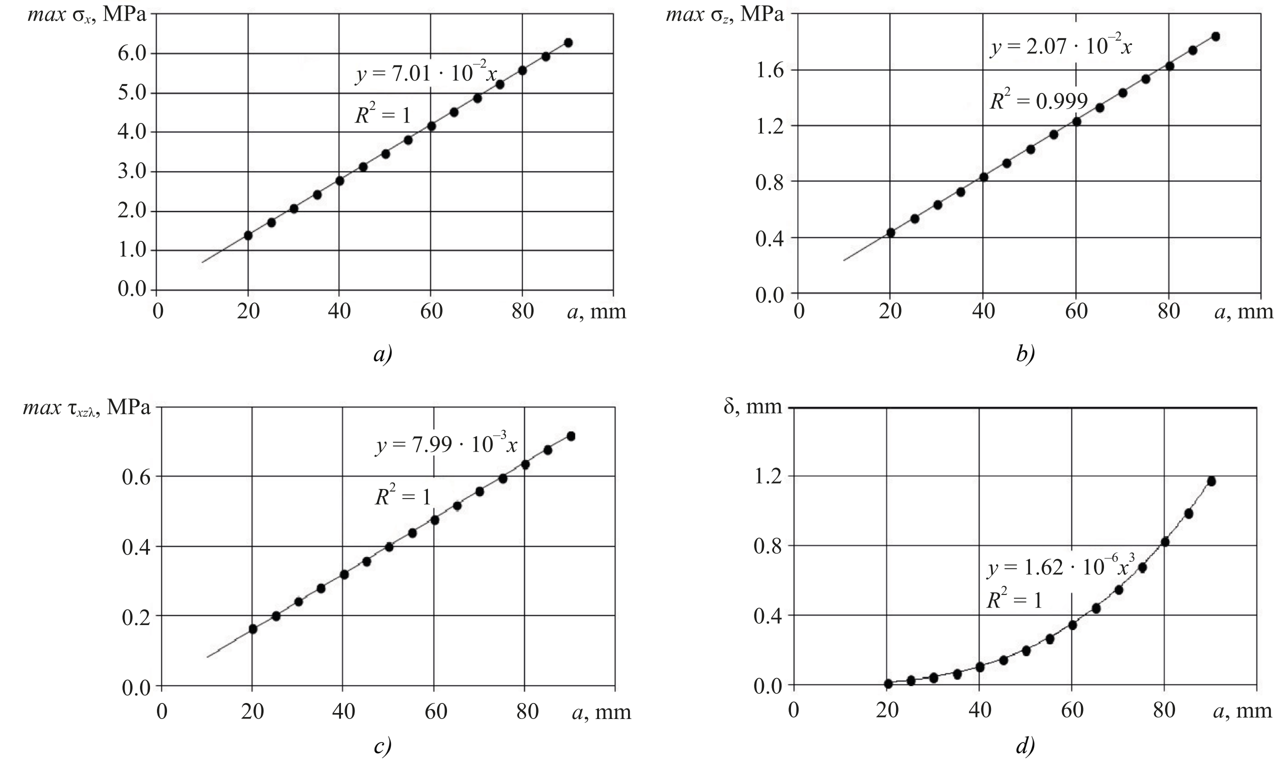

Fig. 8. DCB-loading. Dependences of maximum stresses and displacements of the crack length at P = 1 N:
a— dependence of normal stresses $max\sigma_{x\lambda}(a)$; *b* — dependence of normal stresses $max\sigma_{z\lambda}(a)$;
c — dependence of shear stresses $max\tau_{xz\lambda}(a)$; *d* — dependence of displacements $\delta(a)$

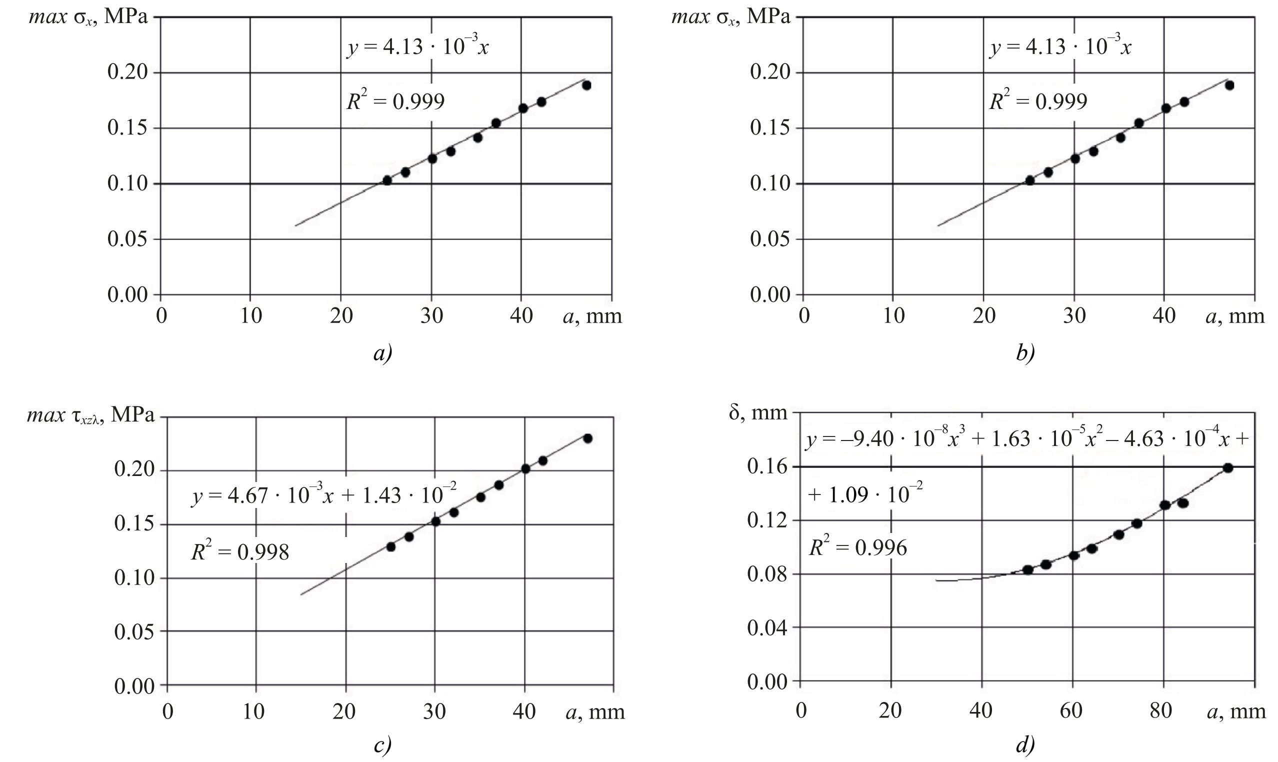

Fig. 9. ENF- loading. Dependences of maximum stresses and displacements of the crack length at P = 1 N:
a — dependence of normal stresses $max\sigma_{x\lambda}(a)$; *b* — dependence of normal stresses $max\sigma_{z\lambda}(a)$;
c — dependence of shear stresses $max\tau_{xz\lambda}(a)$; *d* — dependence of displacements $\delta(a)$

Examples of stress distribution at the crack tip are shown in Figures 10–11 with crack length a_0 = 30 mm.

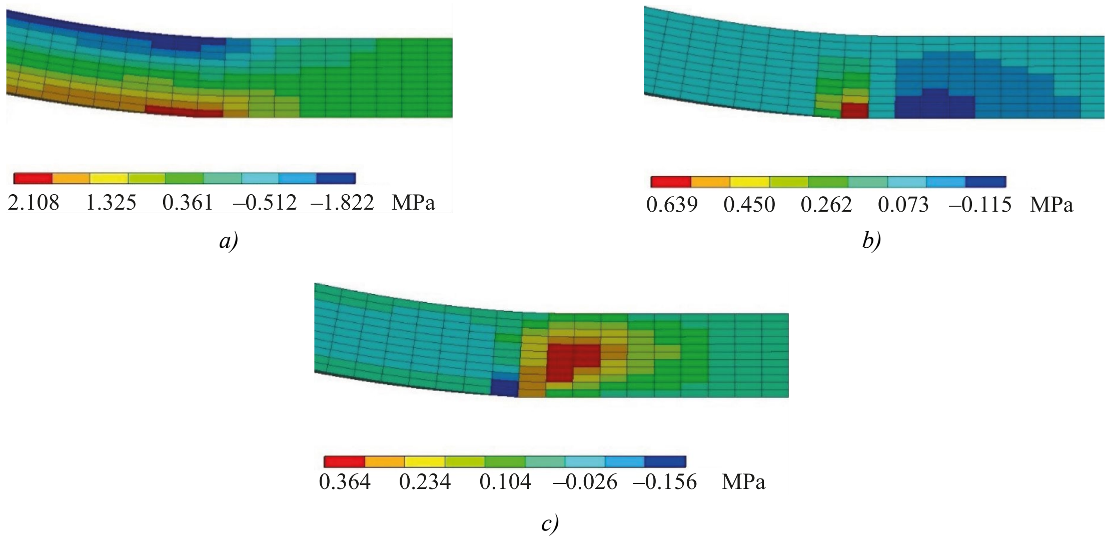

Fig. 10. Stresses at the crack tip under DCB loading: *a* — normal stresses $\sigma_{x\lambda}$;
b — normal stresses $\sigma_{z\lambda}$; *c* — shear stresses $\tau_{xz\lambda}$

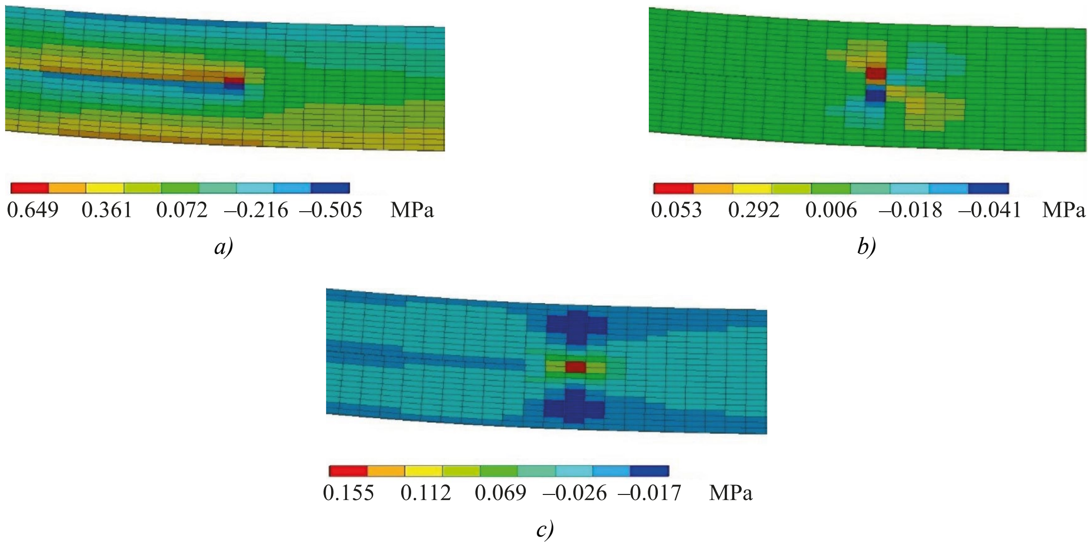

Fig. 11. Stresses at the crack tip under ENF loading: *a* — normal stresses $\sigma_{x\lambda}$;
b — normal stresses $\sigma_{z\lambda}$; *c* — shear stresses $\tau_{xz\lambda}$

To obtain the calculated "load — displacement" dependences using FEM, the strength characteristics of the composite in the main directions are taken into account, i.e., criterion (4). Direct obtaining of transverse shear constants involves a certain difficulty; therefore, the reverse method is considered below. With this approach, the constants vary, and their best combination is found. This means that the calculated and experimental loading diagrams are in good agreement (mean square deviation of displacements at specified loads is minimal).

The results of the calculation under loading according to the DCB scheme were compared to the authors' experiment, which was considered in [16]. Samples were made in the same way. The tests were carried out in accordance with GOST R 56815–2015[3] and ASTMD5528–14[4] standards.

The calculation was performed for loading according to the DCB scheme. When calculating dependence $P(\delta)$ for samples without felting, the following stress limits were found and rounded to integer values: Z_t = 39 MPa, X_t = 360 MPa, S = 82 MPa. The obtained values 360 MPa and 39 MPa correspond to the data on the strength of fiberglass specified in [23]. For felting samples (density 10 cm^{-2}), the calculated values were X_t* = 270 MPa, Z_t* = 46 MPa and S* = 97 MPa. Thus, the use of felting made it possible to increase the rupture strength in the Z direction from 39 to 46 MPa (by ~18%).

[3] GOST R 56815–2015. *Polymer Composites. Method for Determination Specific Work of Exfoliation in Tearing Off Conditions.* (In Russ.) URL: https://docs.cntd.ru/document/1200131393/titles (accessed: 22.04.2024).
[4] ASTMD5528M–21. *Standard Test Method for Mode I Interlaminar Fracture Toughness of Unidirectional Fiber-Reinforced Polymer Matrix Composites.* https://doi.org/10.1520/D5528_D5528M-21

When loading according to the DCB scheme, the shear strength limits in the plane XZ S and S^* do not make a big contribution to criterion (4); therefore, values $S = 82$ MPa and $S^* = 97$ MPa obtained in calculations according to the DCB scheme need to be clarified according to the ENF loading scheme. Note that the effect of normal stresses in the X and Z directions is insignificant compared to shear stresses under loading according to the ENF scheme. Therefore, in the calculations, when searching for the values S and S^*, values Z_t, X_t, Z_t^* and X_t^* were taken from solving the inverse problem under loading according to the DCB scheme.

Values $S = 77$ MPa (without felting) and $S^* = 89$ MPa (with felting) were determined from the condition of the best consistency of the experimental and calculated curves $P(\delta)$ (mean square deviation of displacements at given loads is minimal). Evidently, felting made it possible to increase the shear strength in the plane XZ by ~16%.

Figures 12–13 show the experimental "load — displacement" diagrams, as well as calculated dependences $P(\delta)$ for the found values of stress limits:

– $Z_t = 39$ MPa, $X_t = 360$ MPa, $S = 77$ MPa (for control samples without felting);

– $Z_t^* = 46$ MPa, $X_t^* = 270$ MPa, $S^* = 89$ MPa (for samples with felting).

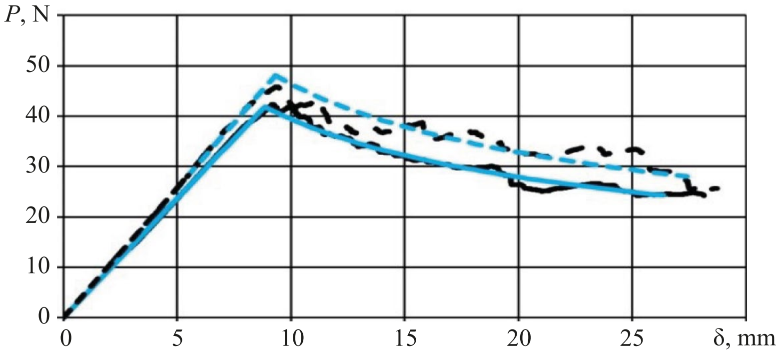

Fig. 12. Experimental diagrams "load – displacement" [16] and calculated dependences $P(\delta)$:
▬ DCB tests of samples without felting; ▬ calculation without felting ($Z_t = 39$ MPa, $X_t = 360$ MPa, $S = 77$ MPa);
- - - DCB tests of samples with felting; - - - calculation with felting ($Z_t^* = 46$ MPa, $X_t^* = 270$ MPa, $S^* = 89$ MPa)

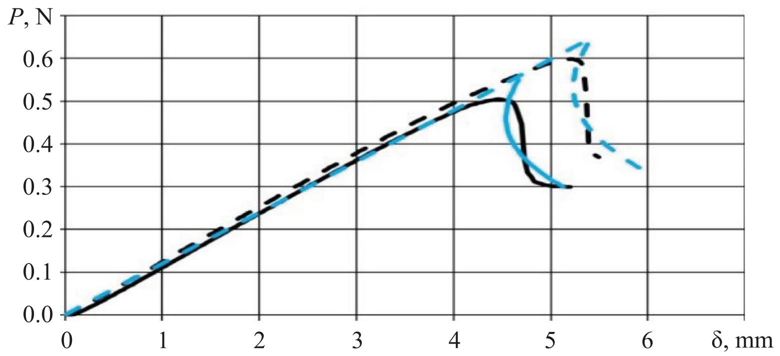

Fig. 13. Experimental diagrams "load – displacement" and calculated dependences $P(\delta)$: ▬ ENF tests of samples without felting;
▬ calculation without felting ($Z_t = 39$ MPa, $X_t = 360$ MPa, $S = 77$ MPa); - - - ENF tests of samples with felting;
- - - calculation with felting ($Z_t^* = 46$ MPa, $X_t^* = 270$ MPa, $S^* = 89$ MPa)

Discussion and Conclusion. Studies of the fabric composite have shown that felting with a density of 10 cm^{-2} increases the viscosity of the interlayer fracture G_{IIc} by ~33%.

Using FEM, the stress state was analyzed in a quasi-static elastic formulation of the problem and with a nonlocal strength theory for the developed numerical models of a beam with cracks of the known length. The distinctive feature of the calculations was that they did not use contact algorithms, but only considered the destruction of the composite layer closest to the crack, and the corresponding change in the area of gluing the layers. That is, the crack was considered as a stress concentrator. The composite strength criterion, which contained three parameters and was recorded through averaged stresses, provided using the method of step-by-step crack advancement to predict the "load — displacement" curve.

The use of felting with a density of 10 cm^{-2} increases the stress limit of the composite in the Z direction by ~18%, and the shear strength in the plane XZ — by ~16%. This became known from solving the inverse problem, i.e., searching for the strength characteristics of the material according to criterion (4) and the "load — displacement" curve.

The results of the presented research will find their practical application. They can be specifically used in problems of forecasting defects, such as delamination (e.g., in low-speed impacts on composites in aircraft skin). The research results will be useful for eliminating these defects with the help of felting.

References

1. Callister WD Jr., Rethwisch DG. *Materials Science and Engineering: An Introduction,* 10th ed. Hoboken, NJ: Wiley; 2018. 992 p. URL: https://www.wiley.com/en-us/Materials+Science+and+Engineering%3A+An+Introduction%2C+10th+Edition-p-9781119405498 (accessed: 22.04.2024).

2. Wei Tan, Falzon BG, Chiu LNS, Price M. Predicting Low Velocity Impact Damage and Compression-After-Impact (CAI) Behaviour of Composite Laminates. *Composites Part A: Applied Science and Manufacturing*. 2015;71:212–226. https://doi.org/10.1016/j.compositesa.2015.01.025

3. Balasubramani Veerappan, S Rajendra Boopathy. Prediction of Residual Tensile Strength of Laminated Composite Plates after Low Velocity Impact. *ARPN Journal of Engineering and Applied Sciences*. 2014;9(3):320–325.

4. Abrate S. *Impact on Composite Structures*. Cambridge: Cambridge University Press; 2009. 289 p. https://doi.org/10.1017/CBO9780511574504

5. Liyong Tong, Mouritz AP, Bannister MK. *3D Fibre Reinforced Polymer Composites.* Amsterdam: Elsevier Science; 2002. 254 p. https://doi.org/10.1016/B978-0-08-043938-9.X5012-1

6. Jinlian Hu. *3-D Fibrous Assemblies: Properties, Applications and Modeling of Three-Dimensional Textile Structures.* Sawston, Cambridge: Woodhead Publishing; 2008. 280 p.

7. Chen Xiaoming, Zhao Yufen, Zhang Chunyan, Wang Xiaoxu, Chen Li. Robot Needle-Punching for Manufacturing Composite Performs. *Robotics and Computer-Integrated Manufacturing*. 2018;50:132–139. https://doi.org/10.1016/j.rcim.2017.09.008

8. Forental GA, Kheruvimov AV, Nikonov AV, Sapozhnikov SB. Stack Fabric Felting to Get PCM G_{IIc} Improvement and LVI Tolerance. *IOP Conference Series: Materials Science and Engineering*. 2021;1024(1):012001. https://doi.org/10.1088/1757-899X/1024/1/012001

9. Sham MS, Venkatesha CS, Jayaraju T. Experimental Methods of Determining Fracture Toughness of Fiber Reinforced Polymer Composites under Various Loading Conditions. *Journal of Minerals and Materials Characterization and Engineering*. 2011;10(13):1263–1275. http://doi.org/10.4236/jmmce.2011.1013099

10. Pinho S, Robinson P, Iannucci L. Developing a Four Point Bend Specimen to Measure the Mode I Intralaminar Fracture Toughness of Unidirectional Laminated Composites. *Composites Science and Technology*. 2009;69(7–8):1303–1309. https://doi.org/10.1016/j.compscitech.2009.03.007

11. Issam Tawk, Jihad Rishmany, Nicolas Saba, Pablo Navarro, Jean-Francois Ferrero. Experimental Study of the Interlaminar Fracture of Composite Materials in Mode III by MSCB Test. *Composite Structures*. 2020;233:111548. https://doi.org/10.1016/j.compstruct.2019.111548

12. Hossein Saidpour, Mehdi Barikani, Multu Sezen. Mode-II Interlaminar Fracture Toughness of Carbon/Epoxy Laminates. *Iranian Polymer Journal.* 2003;12(5):389–400.

13. Sham Prasad MS, Venkatesha CS, Jayaraju T. Experimental Methods of Determining Fracture Toughness of Fiber Reinforced Polymer Composites under Various Loading Conditions. *Journal of Minerals and Materials Characterization and Engineering*. 2011;10(13):1263–1275. http://doi.org/10.4236/jmmce.2011.1013099

14. Ying Zeng, Hong-Yuan Liu, Yiu-Wing Mai, Xu-Sheng Du. Improving Interlaminar Fracture Toughness of Carbon Fibre/Epoxy Laminates by Incorporation of Nano-Particles. *Composites Part B: Engineering*. 2012;43(1):90–94. https://doi.org/10.1016/j.compositesb.2011.04.036

15. Kadhum A, Muslim ZR, Jaffer HI. Interlaminar Fracture of Micro and Nano Composites Special. *Acta Physica Polonica: Series A*. 2019;135(5):1126–1128. http://doi.org/10.12693/APhysPolA.135.1126

16. Forental GA, Sapozhnikov SB. Prospects of Felting Technology for Local 3D-Reinforcement of Polymer Fabric Composites. *Composites and Nanostructures*. 2022;14(56):233–245. https://doi.org/36.10236/1999-7590-2022-14-4-233-245233

17. Maimi P, Gonzalez EV, Gascons N, Ripoll L. Size Effect Law and Critical Distance Theories to Predict the Nominal Strength of Quasibrittle Structures. *Applied Mechanics Reviews*. 2013;65(2):020803. https://doi.org/10.1115/1.4024163

18. Hoang Thai Nguyen, A Abdullah Dönmez, Zdenek P Bazant. Structural Strength Scaling Law for Fracture of Plastic-Hardening Metals and Testing of Fracture Properties. *Extreme Mechanics Letters*. 2021;43(1):101141. https://doi.org/10.1016/j.eml.2020.101141

19. Taylor D. *The Theory of Critical Distances: A New Perspective in Fracture Mechanics.* Amsterdam: Elsevier Science; 2007. 306 p. https://doi.org/10.1016/B978-0-08-044478-9.X5000-5

20. Mahmoodi MJ, Khamehchi M. Finite Element Analysis of Free Corner Effects in Composite Laminates Based on a Global–Local Model. *Archive of Applied Mechanics*. 2023;93(12):4327–4350. http://doi.org/10.1007/s00419-023-02494-1

21. Jaehong Lee, Zafer Gurdal, O Hayden Griffin Jr. Layer-Wise Approach for the Bifurcation Problem in Laminated Composites with Delaminations. *AIAA Journal*. 1993;31(2):331–338. https://doi.org/10.2514/3.11672

22. Sapozhnikov SB. Failure of Fabric Reinforced Composite with Concentrators: Implementation of Inelastic Deformation in Numerical Simulation. *Composites and Nanostructures*. 2020;12(45):31–39. https://doi.org/10.36236/1999-7590-2020-12-2-31-39

23. Barbero EJ. *Introduction to Composite Materials Design*, 2nd ed. Boca Raton: CRC Press; 2011. 562 p. https://doi.org/10.1201/9781439894132

About the Authors:

Galina A. Forental, Research Engineer, South Ural State University (76, Lenin Ave., Chelyabinsk, 454080, Russian Federation), SPIN-code, ORCID, ScopusID, gforental@mail.ru

Sergey B. Sapozhnikov, Dr.Sci. (Eng.), Professor of the Engineering Mechanics Department, South Ural State University (76, Lenin Ave., Chelyabinsk, 454080, Russian Federation), Leading Scientist, Central Aerohydrodynamic Institute named after N.E. Zhukovsky (1, Zhukovsky Str., Zhukovsky, Moscow Region, 140180, Russian Federation), SPIN-code, ORCID, ScopusID, ResearcherID, sapozhnikovsb@susu.ru

Claimed Contributorship:

GA Forental: conducting experiments and calculations, analysis of the research results, formulation of conclusions, text preparation, layout of the paper.

SB Sapozhnikov: academic advising, revision of the text.

Conflict of Interest Statement: **the authors declare no conflict of interest.**

All authors have read and approved the final manuscript.

Об авторах:

Галина Анатольевна Форенталь, инженер-исследователь Южно-Уральского государственного университета (454080, Российская Федерация, г. Челябинск, пр. Ленина, 76), SPIN-код, ORCID, ScopusID, gforental@mail.ru

Сергей Борисович Сапожников, доктор технических наук, профессор Южно-Уральского государственного университета (454080, Российская Федерация, г. Челябинск, пр. Ленина, 76), ведущий ученый Центрального аэрогидродинамического института имени профессора Н.Е. Жуковского (140180, Российская Федерация, г. Жуковский, Московская область, ул. Жуковского, 1), SPIN-код, ORCID, ScopusID, ResearcherID, sapozhnikovsb@susu.ru

Заявленный вклад авторов:

Г.А. Форенталь: проведение экспериментов и расчетов, анализ результатов исследований, формулирование выводов, подготовка текста статьи, оформление статьи.

С.Б. Сапожников: научное руководство, корректировка текста статьи.

Конфликт интересов: **авторы заявляют об отсутствии конфликта интересов.**

Все авторы прочитали и одобрили окончательный вариант рукописи.

Received / Поступила в редакцию 03.06.2024
Reviewed / Поступила после рецензирования 27.06.2024
Accepted / Принята к публикации 05.07.2024

MECHANICS
МЕХАНИКА

UDC 539.42 539.375
https://doi.org/10.23947/2687-1653-2024-24-3-227-237

Original Empirical Research

Study of Structural Defects Evolution in Fine-Grained Concrete Using Computed Tomography Methods

EDN: AICZHY

Anastasiia V. Puzatova ✉, Maria A. Dmitrieva, Alexandr O. Tovpinets, Vladimir V. Leitsin
Immanuel Kant Baltic Federal University, Kaliningrad, Russian Federation
✉ a.v.puzatova@gmail.com

Abstract

Introduction. When studying composite materials for construction purposes, it is needed to consider the mechanisms of formation of the structure and properties of modern concretes in the process of strength development. In studies of modern composite materials based on cement binder, there is no information about the development of structural defects and destruction of the material at the initial stages of strength development. This information can be obtained using X-ray computed tomography, a promising method of nondestructive testing of the state of the material. Therefore, the objective of this work was to study the formation and propagation of cracks in samples of fine-grained concrete with different fractional composition of sand due to natural processes of cement shrinkage, as well as the mechanics of destruction of samples of modified fine-grained concrete when applying a compressive load at the early stages of strength development.

Materials and Methods. The study used fine-grained concrete mixtures of three compositions with different sand gradation. The tomography samples were made by placing fresh mixtures in polymer cylindrical containers. Tomography of the samples immediately after manufacture, as well as after 8 and 51 days, was performed in a YXLON Cheetah microfocus X-ray machine. The composition with two-fraction sand was modified by mechanical activation of the components, 20×20×20 mm cube samples were made. Further, compression tests were performed at the Instron installation after 3 and 7.5 hours, and then — tomography of the destroyed samples.

Results. It was established that the destruction of contact zones depended on the ratio of the size of the fractions. In the presence of a bulk of coarse sand grains in concrete, the destruction of contact zones was more pronounced and had a main mode. When using fine or polyfraction sand, contact zones were destroyed locally and had a visually smaller area. The images of the destroyed modified sample, tested 3 hours after manufacturing, showed clear cracks and indents on the edges, which indicated the elastic-plastic nature of the destruction. In 7.5 hours, the edges of the sample upon destruction were covered with a network of small cracks; inside the sample there were also numerous cracks and microcracks, which indicated brittle fracture. Based on the obtained images of the deformed structure of modified concrete, the mechanism of transition from elastic-plastic destruction of the material to brittle one was clearly visible.

Discussion and Conclusion. The studied dependences of the influence of the size of fine aggregate on the mechanisms of formation and propagation of structural defects contribute to the theory of the processes of destruction of fine-grained concretes. The results obtained prove the prospects of using X-ray computed tomography as a method of nondestructive testing of the internal structure of fine-grained concrete, including at the early stages of strength development.

Keywords: X-ray computed tomography, fine-grained concrete, deformation, elastic-plastic failure, brittle fracture

Acknowledgements. The authors would like to thank Maria Vladimirovna Shiryaeva, Alina Dmitrievna Kogai for their help in preparing samples of composite materials for conducting structural studies on an X-ray computed tomograph.

For Citation. Puzatova AV, Dmitrieva MA, Tovpinets AO, Leitsin VN. Study of Structural Defects Evolution in Fine-Grained Concrete Using Computed Tomography Methods. *Advanced Engineering Research (Rostov-on-Don)*. 2024;24(3):227–237. https://doi.org/10.23947/2687-1653-2024-24-3-227-237

Оригинальное эмпирическое исследование

Исследование процессов эволюции дефектов структуры мелкозернистых бетонов методами компьютерной томографии

А.В. Пузатова ✉, **М.А. Дмитриева**, **А.О. Товпинец**, **В.Н. Лейцин**
Балтийский федеральный университет имени Иммануила Канта, г. Калининград, Российская Федерация
✉ a.v.puzatova@gmail.com

Аннотация

Введение. При изучении композиционных материалов строительного назначения актуальными являются исследования механизмов формирования структуры и свойств современных бетонов в процессе набора прочности. В исследованиях современных композиционных материалов на цементном вяжущем отсутствуют сведения о развитии дефектов структуры и разрушении материала на начальных сроках набора прочности. Такие сведения можно получить с помощью рентгеновской компьютерной томографии — перспективного метода неразрушающего контроля состояния материала. Поэтому целью данной работы явилось изучение образования и распространения трещин в образцах мелкозернистого бетона с различным фракционным составом песка вследствие естественных процессов усадки цементного камня, а также механики разрушения образцов модифицированного мелкозернистого бетона при приложении сжимающей нагрузки на ранних сроках набора прочности.

Материалы и методы. В исследовании использовались мелкозернистые бетонные смеси трех композиций с различным гранулометрическим составом песка. Образцы для томографии были изготовлены путем помещения свежих смесей в полимерные цилиндрические контейнеры. Томография образцов сразу после изготовления, а также через 8 и 51 сутки проводилась в микрофокусной рентгеновской установке YXLON Cheetah. Состав с двухфракционным песком был модифицирован механической активацией компонентов, изготовлены образцы-кубики 20×20×20 мм. Далее на установке Instron проведены испытания на сжатие через 3 и 7,5 часов и затем — томография разрушенных образцов.

Результаты исследования. Установлено, что разрушение контактных зон зависит от отношения размеров фракций. В присутствии большого количества крупных частиц песка в теле бетона разрушение контактных зон более выражено и имеет магистральный характер. При использовании мелкого или полифракционного песка контактные зоны разрушаются локально и имеют визуально меньшую площадь. На изображениях разрушенного модифицированного образца, испытанного через три часа после изготовления, прослеживаются четкие трещины и выколы на гранях, что говорит об упруго-пластическом характере разрушения. Через 7,5 часов грани образца при разрушении покрываются сеткой мелких трещин, внутри образца также образуется множество трещин и микротрещин, что свидетельствует о хрупком разрушении. По полученным изображениям деформированной структуры модифицированного бетона наглядно прослеживается механизм перехода от упруго-пластического разрушения материала к хрупкому.

Обсуждение и заключение. Изученные зависимости влияния размеров мелкого заполнителя на механизмы образования и распространения дефектов структуры вносят вклад в теорию процессов разрушения мелкозернистых бетонов. Полученные результаты доказывают перспективность применения рентгеновской компьютерной томографии как метода неразрушающего контроля внутренней структуры мелкозернистого бетона, в том числе на ранних сроках набора прочности.

Ключевые слова: рентгеновская компьютерная томография, мелкозернистый бетон, деформация, упруго-пластическое разрушение, хрупкое разрушение

Благодарности. Авторы выражают благодарность Шиняевой Марии Владимировне, Когай Алине Дмитриевне за помощь в приготовлении образцов композиционных материалов для проведения исследований структуры на рентгеновском компьютерном томографе.

Для цитирования. Пузатова А.В., Дмитриева М.А., Товпинец А.О., Лейцин В.Н. Исследование процессов эволюции дефектов структуры мелкозернистых бетонов методами компьютерной томографии. *Advanced Engineering Research (Rostov-on-Don).* 2024;24(3):227–237. https://doi.org/10.23947/2687-1653-2024-24-3-227-237

Introduction. X-ray computed tomography is a promising technique of nondestructive testing of the state of the material. In the concrete industry, tomography is suitable for determining the structure of concrete samples, microcracks, internal fractures, and studying the distribution of pores and aggregate particles. X-ray computed tomography provides the construction of a model of the microstructure of cement paste, allows us to study the development of cement hydration processes [1, 2], to make forecasts of the formation of mechanical characteristics and fracture conditions [3, 4]. Computed tomography is actively used for studying the average density and porosity of high-strength lightweight concretes [5], the morphology of structural heat-insulating concrete [6], building a mesoscale 3D model of foamed concrete [7], investigating the formation and distribution of pores in lightweight concrete [8], analyzing the microstructural characteristics of concrete samples with various aggregates [9, 10], developing three-dimensional mesoscale models for constructing a finite element grid in modeling the structure of concrete [11, 12]. In comparison to standard 2D X-ray methods, the construction of 3D models of multicomponent concrete samples is promising for the study of the fundamental mechanisms of formation of the structure and properties of modern concretes.

The most vulnerable area of fine-grained concrete under loading is the contact zone — the contact areas of cement stone and aggregates. When exposed to external loads, it is from these areas that the formation of microdefects and microcracks starts, whose development causes the defect formation at the macro level, which can lead to loss of bearing capacity and structural failure. The destruction of the contact zones occurs due to the difference in characteristics of the bordering components (Young's modulus, Poisson's ratio, thermal linear expansion coefficient, sizes of the contacting phases, microdefects on the interface of the phases) [13]. The X-ray computed tomography method is promising for studying the evolution of contact zones, including at the early stages of hydration. It provides studying the structure without destroying the sample directly during the hardening process. Contact zones, as a rule, have higher porosity and low strength, as a result of which cracks are formed in these zones [4]. The strength of the contact zones is also affected by the size of the aggregate. It has been established that homogeneous and more durable contact zones are formed in concretes with combined aggregates (coarse fraction and crushed) [14]. There are numerous modern studies on the formation of contact zones of cement stone with reinforcement [15], cracks in popcorn concrete [16], defects at the contact boundary of sand-cement mortar with a coarse aggregate [17]. However, along with this, the formation of contact zones in fine-grained concretes with different fineness and packing density of sand grains is poorly studied. In the modern scientific literature, there is no description of the effect of the size of a fine aggregate on the formation of contact zone defects in fine-grained concretes. Thus, the study of the formation of defects in the structure of fine-grained concrete containing sand of aggregate fractional make-up, to obtain a visual picture of crack propagation by X-ray computed tomography is urgent.

To reduce the stresses that occur in the contact zones, microfillers, similar in their properties to cement stone, are used. These fillers, having an increased specific surface area, create additional contact zones between which the stresses arising from the hardening of the binder are redistributed. Hardening of the contact zones can be achieved through introducing mechanically activated components into the concrete mixture [13]. Mechanical activation of separate components contributes to the formation of a denser structure, the preservation of uniformity in composition, the development of initial strength due to the acceleration of the hydration reaction and the growth of crystallohydrates of cement stone, as well as the reduction in the setting time [18, 19]. The development of structural defects in fine-grained concretes modified by mechanical activation of components has also been poorly studied. Among modern scientific papers, there are very few works devoted to the study of crack propagation processes in the modified structure of fine-grained concretes at the initial stages of strength development. Therefore, the use of the computed tomography method to study the mechanics of destruction of samples of modified fine-grained concrete at the initial stages of hardening is important today.

This work was aimed at studying the formation and propagation of cracks in samples of fine-grained concrete with different fractional make-up of sand due to natural processes of shrinkage of cement stone, as well as the mechanics of destruction of samples of modified fine-grained concrete when applying a compressive load at the early stages of strength development.

Materials and Methods. In the research, to determine the defects of the contact zones of fine-grained concretes with different sand gradation, three samples of fine-grained concrete mixture of the following compositions were used:

– composition No. 1: Portland cement Eurocem 500 super; CEM I 42.5 N (“Petersburg Cement” LLC); monofraction sand (fraction 0.63–0.315 mm); water. The ratio of the mixture components was 1:2.56:0.67;

– composition No. 2: Portland cement Eurocem 500 super; CEM I 42.5 N (“Petersburg Cement” LLC); polyfraction construction sand according to GOST 8736-2014 with ISO=1.85; water. The ratio of the mixture components was1:2.56:0.67;

– composition No. 3: Portland cement Eurocem 500 super; CEM I 42.5 N (“Petersburg Cement” LLC); two-fraction sand (fraction 2.5–1.25 mm — 80% of the total mass of sand, fraction 0.63–0.315 mm — 20% of the total mass of sand; no intermediate fraction 1.25–0.63 mm); highly active metakaolin (white) (manufactured by CG “Sinergo”, Chelyabinsk region); microsilica; water. The ratio of the mixture components was 1:1.75:0.43:0.23:0.15:0.67.

Freshly-mixed compositions of fine-grained concrete mix were placed in a polymer cylindrical container with a diameter of 8 mm and a length of about 70 mm. The diameter of the container was determined in accordance with the size of the initial components of fine-grained concrete of the previously mentioned compositions based on the conditions of representativeness [20], and representativeness of the volume under study. To track changes in the structure under cement hydration and cement stone shrinkage, tomography of the samples was performed immediately after mixing the components and after 8 days of hardening. Samples at the age of 51 days were taken as the final result.

In the study on the evolution of the crack formation mechanism during the destruction of samples under the action of an external compressive force, composition No. 3 with two-fraction sand, modified by mechanical activation of the cement and sand composition, was used. Mechanical activation of the components (cement and sand) was carried out using a high energy ball mill Retsch EMax. The components were crushed at a rotation speed of the apparatus bowls of 750 rpm for 5 minutes. Cubic samples of 20×20×20 mm in size were made from concrete mortars, to which an external compressive load was applied after 3 and 7.5 hours. After applying the load, tomography of the destroyed samples was performed to trace the evolution of the fracture mode of the material.

The structure of the concrete samples was studied using a YXLON Cheetah microfocus X-ray computed tomograph with Y. Cheetah configuration. The device specifications are shown in Table 1.

Table 1

YXLON Cheetah Tomograph Specifications

Characteristic	Value
X-ray tube	Open-type
Operating voltage range, kV	25–160
Operating current range, mA	0.1–1.0
Maximum tube power, W	64
Maximum tube power on target, W	15
Detector tilt angle	±70º (segment 140°)
Magnification (geometric/maximum)	2000x/17500x
Maximum sample dimensions, mm	800x500
Time from sample loading to first image, sec	<10
Time for full tomography of the sample, sec	7
Time for laminography of the sample, sec	20
Overall dimensions, mm	1650x1400x1850
Weight, kg	2,200

From the perspective of micromechanics of composite materials, the assessment of effective characteristics can be introduced by sets of properties of a representative volume of the body under study. The test sample for tomography should correspond to a representative volume of material, which makes sense of the elementary macrovolume of a microinhomogeneous medium.

During the experiment, after X-rays pass through the sample, a set of flat X-ray images with an uneven distribution of grayness in the images is obtained. This is due to the uneven absorption of X-rays by the components of the studied material — the presence of pores, defects, dense inclusions, etc. After reconstruction of 3D images of the sample, the grayness gradient is inverted relative to conventional X-ray images: the materials that are most transparent to X-rays, e.g., pores, correspond to black, and the densest material is white. The grayness density in full-color representation is considered in the range 0–255, where 0 corresponds to black, and 255 corresponds to white. This algorithm is used to determine the minimum size of features that could be differentiated as structural components of the sample under study: porosity, cement mortar, and aggregate in volume. Further, using this grayscale, highlighting certain numerical ranges, it is possible to analyze a separate internal structure, distribution of components and porosity [21].

The shooting parameters for all the studied samples remained constant: voltage — 85 kW; current — 45 μA; approximation — 8.9; scanning angle — 360°. The survey results represent 1,024 consecutive images of the internal structure of the samples. Further processing of the resulting array of two-dimensional images took place in the "Volume Graphics Studio" program. To improve the visualization of inclusions, editing layered images by brightness and contrast levels was performed. The result of the tomography was a 3D model of the sample and its three projections with the possibility of studying the internal structure in any section.

Research Results. Images of the internal structure of samples of composition No. 1 with monofraction sand (fraction 0.63–0.315 mm) at the age of 0, 8, and 51 days obtained by X-ray tomography are shown in Figure 1. The darkest areas in the images have the lowest density, in this case, the pores. The hardest particles correspond to the lightest areas.

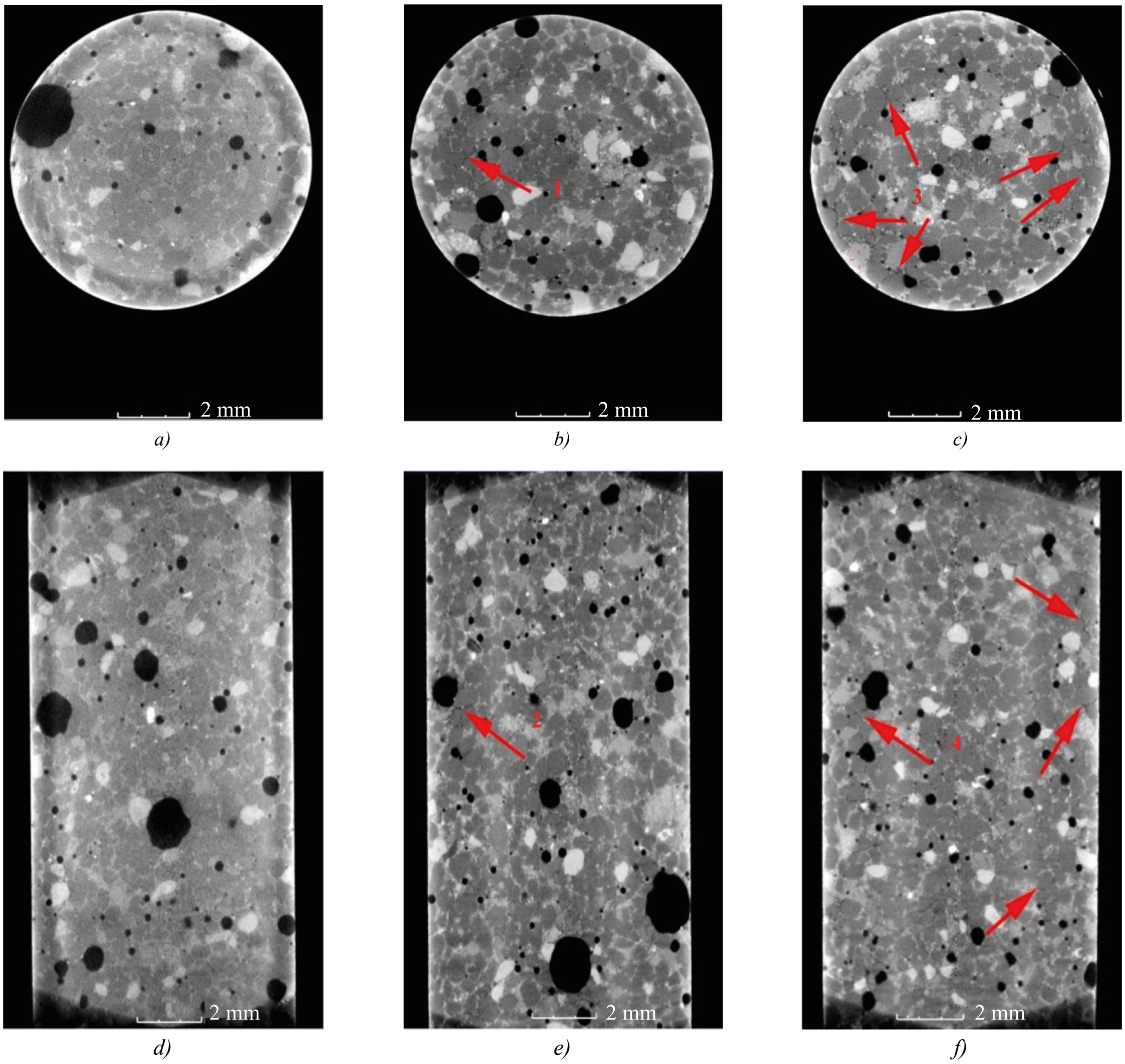

Fig. 1. Internal structure of sample No. 1 (monofraction sand): *a, d* — immediately after preparation; *b, f* — at the age of 8 days; *c, f* — at the age of 51 days

The images of the internal structure of the sample of composition No. 1 with monofraction sand showed no changes in the contact zones immediately after mixing. By the 8th and 51st days of hardening, dark stripes were visible around separate sand grains (indicated by red arrows), corresponding to voids that were formed due to shrinkage of the cement stone. Moreover, with the increasing age of concrete, such voids around the sand grains visually became more numerous. Enlarged images of separate fractured voids are shown in Figure 2.

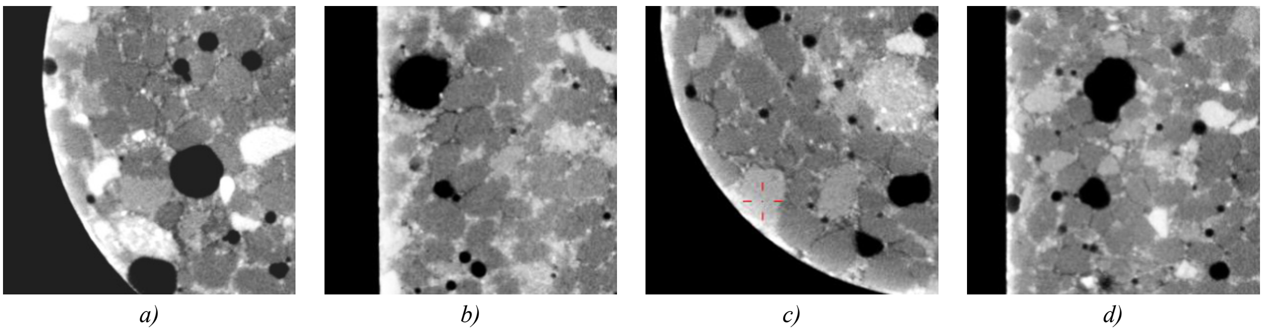

Fig. 2. Enlarged fragments of Figure 1: *a* — fragment 1; *b* — fragment 2; *c* — fragment 3; *d* — fragment 4

In fragments 3 and 4 corresponding to sample No. 1 at the age of 51 days, the mode of the manifestation of defects in the contact zones around sand particles was most pronounced. This was confirmed by the fact that by 51 days, the process of shrinkage of cement stone was almost complete, whereas at the age of 8 days, the shrinkage was in the active phase.

Images of the internal structure of samples of composition No. 2 with polyfraction sand at the age of 0, 8 and 51 days are shown in Figure 3. Separate enlarged fragments are shown in Figure 4.

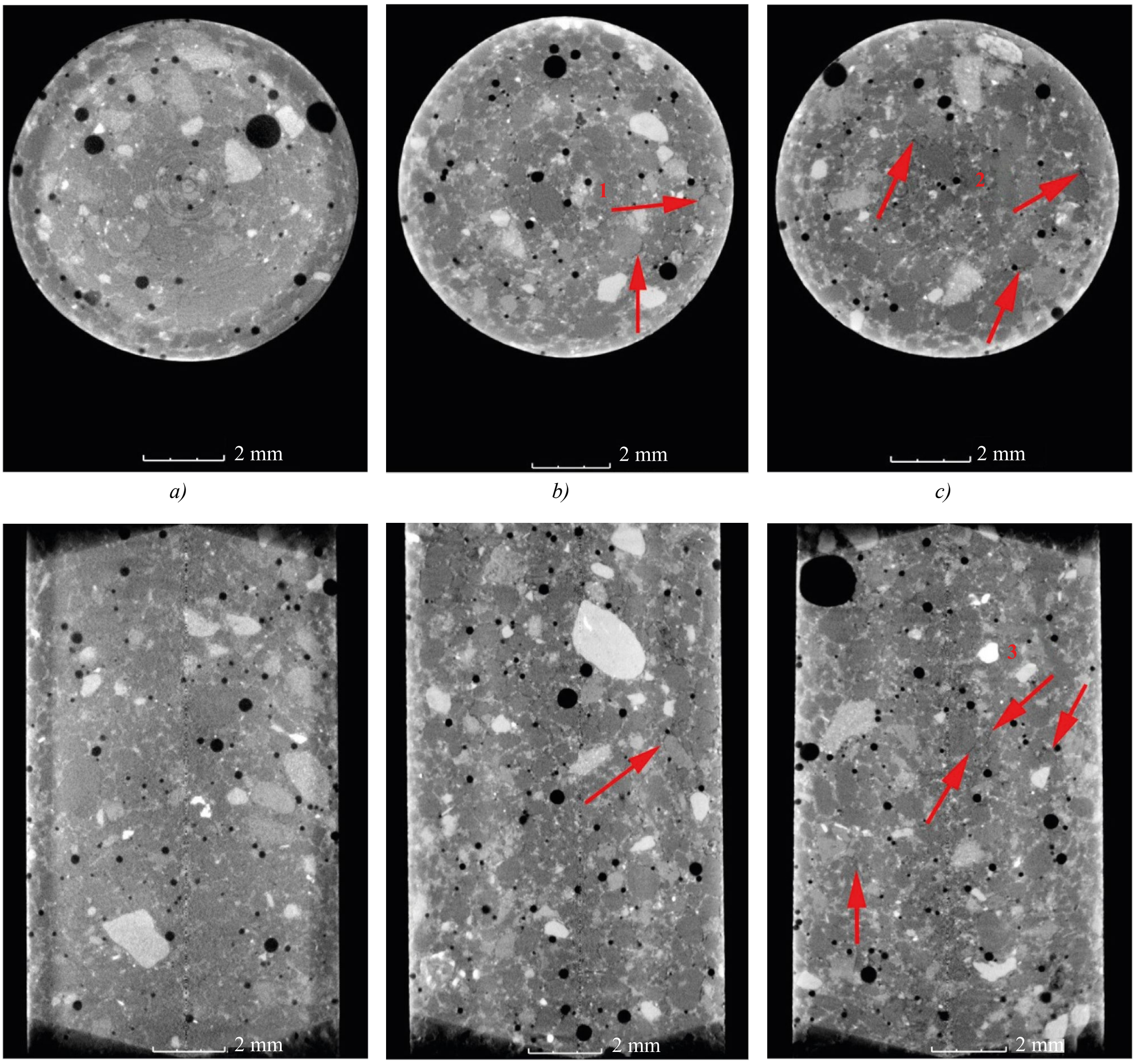

a) *b)* *c)* *d)* *e)* *f)*

Fig. 3. Internal structure of sample No. 2 (polyfraction sand): *a, d* — immediately after preparation; *b, e* — at the age of 8 days; *c, f* — at the age of 51 days

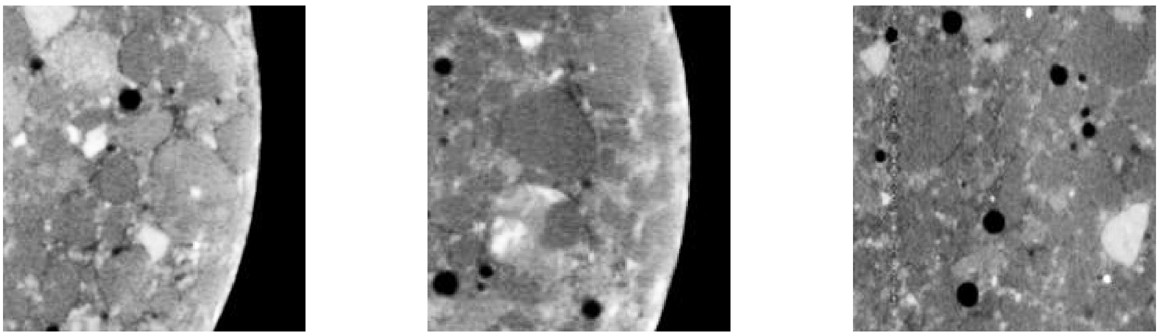

a) *b)* *c)*

Fig. 4. Enlarged fragments of Figure 3: *a* — fragment 1; *b* — fragment 2; *c* — fragment 3

The development of defects in the contact zones of samples of composition No. 2 with a polyfraction aggregate, as in composition No. 1 with a monofraction aggregate, manifested itself by the 8th day of hardening, the number of defective areas increased by the 51st day. It can be noted that the destruction of contact zones around individual large sand particles is not observed.

Images of the internal structure of samples of composition No. 3 with two-fraction sand (fractions 2.5–1.25 mm and 0.63–0.315 mm, no intermediate fraction) at the age of 0, 8, and 51 days are shown in Figure 5.

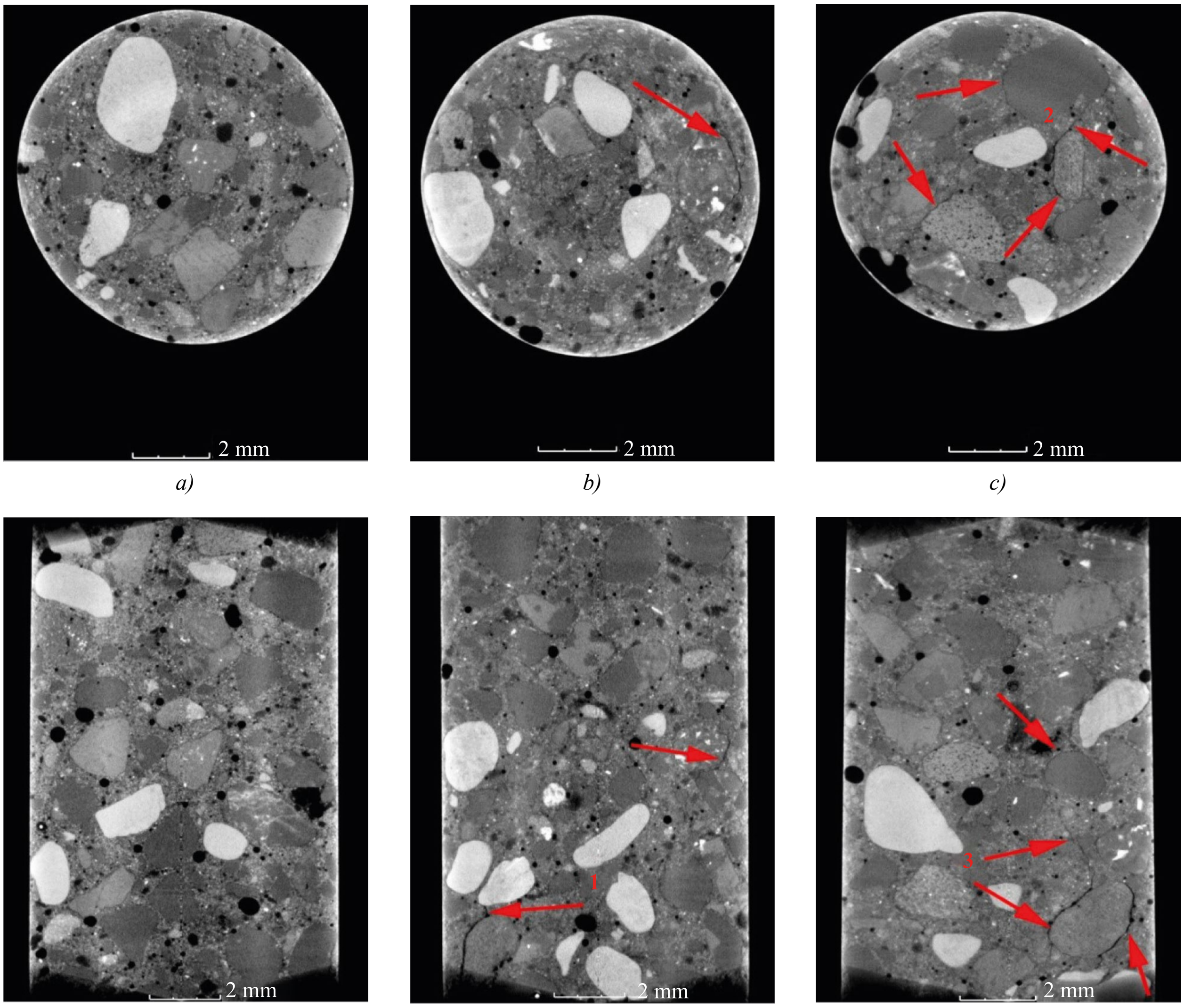

Fig. 5. Internal structure of sample No. 3 (two-fraction sand): *a, d* — immediately after preparation; *b, e* — at the age of 8 days; *c, f* — at the age of 51 days

In the images of the internal structure of the samples containing two fractions of sand, at the age of 8 and 51 days, a clear formation of cracks around large grains of sand was observed, and the main mode of the crack formation was traced when the cracks were connected to each other (Fig. 6).

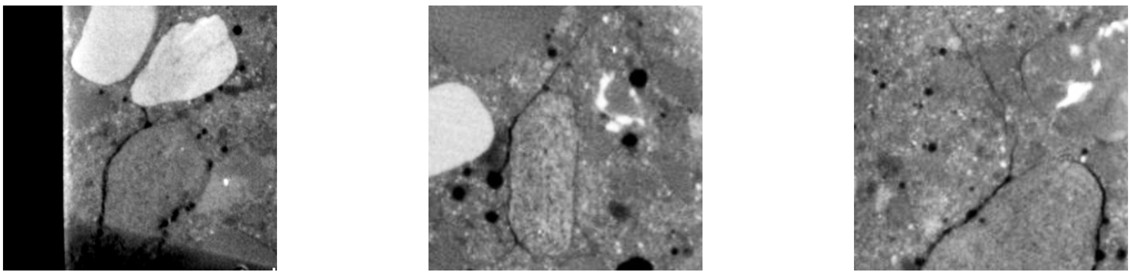

a) *b)* *c)*

Fig. 6. Enlarged fragments of Figure 5:
a — fragment 1; *b* — fragment 2; *c* — fragment 3

The formation of main cracks near coarse sand grains indicated that the contact zones around coarse aggregate particles were most stressed and susceptible to destruction during the shrinkage of the cement stone.

Based on the obtained images of the internal structure of samples with different sand sizes, it can be concluded that the development of contact zone defects due to shrinkage of the cement stone depends on the ratio of fraction sizes. In samples with mono- and polyfraction sand, the defective structure develops locally, the area of such defects is visually much smaller than in samples with two fractions of different sizes. In the presence of a coarse fraction of sand with a high-volume concentration, defects in contact zones develop near coarse grains and have the main mode.

Cube samples of composition No. 3 with two-fraction sand, modified by mechanical activation of individual components, were subjected to the application of external compressive load at the age of 3 and 7.5 hours after preparation. Images of the deformed internal structure of the samples are shown in Figure 7.

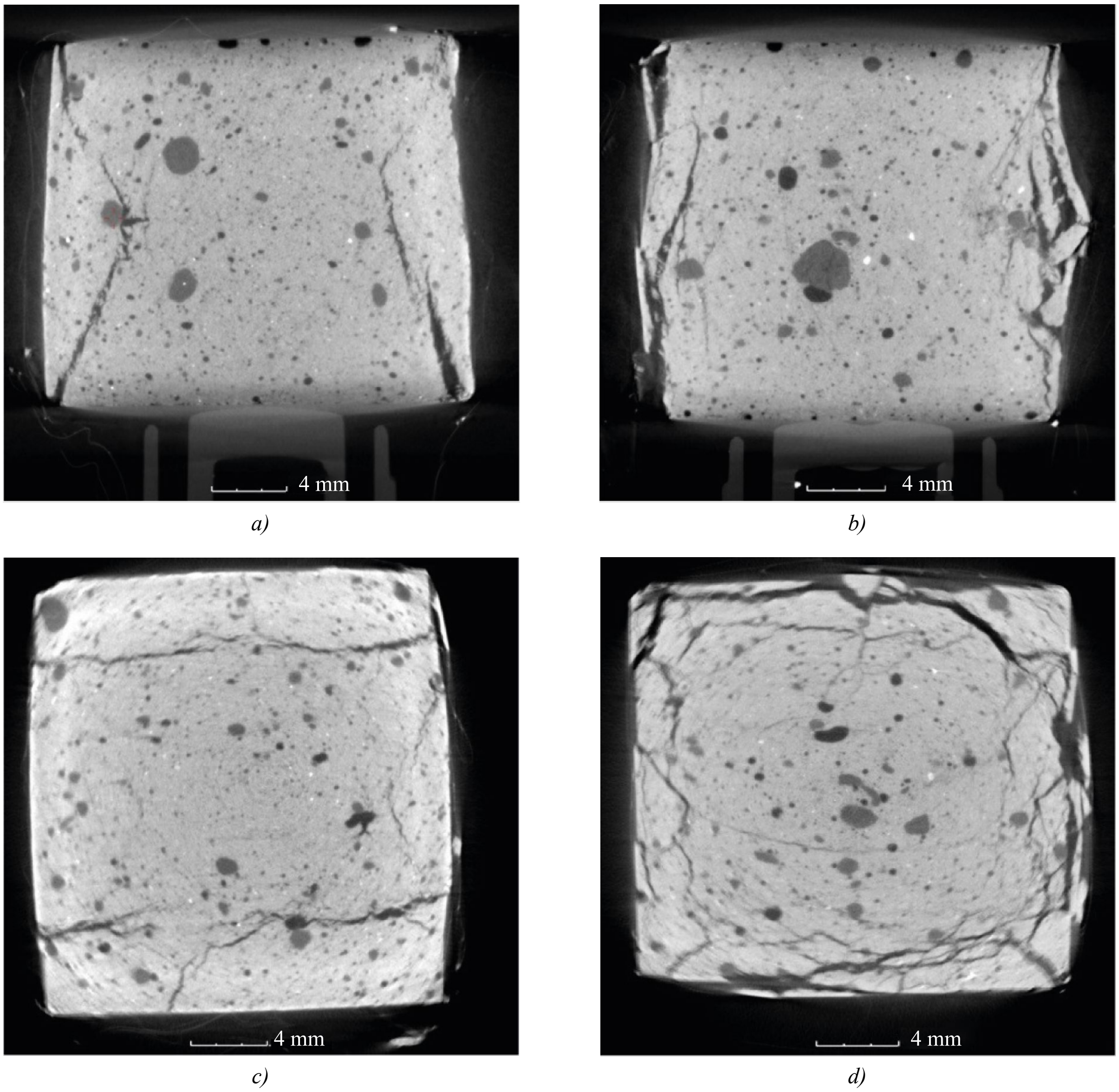

Fig. 7. Images of the internal structure of modified samples: *a* — frontal section at the age of 3 hours; *b* — frontal section at the age of 7.5 hours; *c* — horizontal section at the age of 3 hours; *d* — horizontal section at the age of 7.5 hours

The images showed the evolution of hardening concrete samples from elastic-plastic to brittle fracture. The samples tested 3 hours after production had an elastic-plastic fracture pattern, with clear cracks and chips on the sample edges. At the age of 7.5 hours, the sample edges were covered with a network of small cracks during fracture, and there were also numerous cracks and microcracks inside the sample, indicating brittle fracture.

Discussion and Conclusion. Thus, by means of mechanical tests and X-ray computed tomography, it is possible to track the processes of destruction in the structure of fine-grained concrete. The results obtained give rise to a new complex method for assessing the structural characteristics of modified fine-grained concrete at all stages of strength development.

It has been established that the destruction of contact zones depends on the ratio of fraction sizes. In the bulk of coarse sand particles in the body of concrete, the destruction of contact zones is more pronounced and has the main mode. When using fine or polyfraction sand, contact zones are destroyed locally and have a visually smaller area. This indicates that contact zones near coarse aggregate particles are most stressed and are primarily subject to destruction under the shrinkage of cement stone.

The studied dependences of the influence of the fine aggregate sizes on the mechanisms of formation and propagation of structural defects contribute to the theory of destruction processes of fine-grained concrete. The results obtained prove the prospects of using X-ray computed tomography as a method of non-destructive testing of the internal structure of fine-grained concrete, including at the early stages of strength development. Computer tomography, along with traditional methods of investigation of the structure and properties of building materials, gives rise to a new complex method that provides studying modern multicomponent concretes at all stages of strength development, the mechanisms of formation and propagation of structural defects due to natural processes of changing the state of the material and under various external loading conditions.

References

1. Dmitrieva MA, Kogai AD, Leitsin VN, Tovpinets AO, Shinyaeva MV. An Experimental and Theoretical Approach to Assessing the Structure of Fine-Grained Modified Concretes. *Vestnik MGSU*. 2023;18(1):70–81. doi.org/10.22227/1997-0935.2023.1.70-81

2. Dmitrieva MA, Sharanova AV, Leitsin VN, Shinyaeva MV. Experimental Studies of the Evolution of Structural and Mechanical Characteristics of Cement Stone in the Process of Hydration. In: *Proc. III International Conference "Advanced Building Materials and Technologies"*. Kaliningrad: IKBFU Publ.; 2021. P. 7–13. (In Russ.)

3. Mingzhong Zhang, Jivkov AP. Micromechanical Modelling of Deformation and Fracture of Hydrating Cement Paste Using X-ray Computed Tomography Characterization. *Composites Part B: Engineering*. 2016;88:64–72. https://doi.org/10.1016/j.compositesb.2015.11.007

4. Lavrov A, Panduro EAC, Torsæter M. Synchrotron Study of Cement Hydration: Towards Computed Tomography Analysis of Interfacial Transition Zone. *Energy Procedia*. 2017;114:5109–5117. https://doi.org/10.1016/j.egypro.2017.03.1666

5. Inozemtsev AS. Average Density and Porosity of High-Strength Lightweight Concrete. *Magazine of Civil Engineering*. 2014;51(7):31–37. (In Russ.) https://doi.org/10.5862/MCE.51.4

6. Osipov SP, Prishchepa IA, Kudyakov AI, Batranin AV, Osipov OS. Computer Tomography of Foam Concrete. *Systems. Methods. Technologies.* 2018;38(2):146–152. https://doi.org/10.18324/2077-5415-2018-2-146-152

7. Tuan Nguyen, Abdallah Ghazlan, Alireza Kashani, Stćphane Bordas, Tuan Ngo. 3D Meso-Scale Modelling of Foamed Concrete Based on X-ray Computed Tomography. *Construction and Building Materials*. 2018;188:583–598. https://doi.org/10.1016/j.conbuildmat.2018.08.085

8. Haizhu Lu, Eugene Alymov, Sanjay Shah, Karl Peterson. Measurement of Air Void System in Lightweight Concrete by X-ray Computed Tomography. *Construction and Building Materials*. 2017;152:467–483. https://doi.org/10.1016/j.conbuildmat.2017.06.180

9. Khuzin AF, Rahimov RZ. The Effect of Multiwalled Carbon Nanotubes on the Porosity of the Cement Stone. *News KSUAE*. 2016;37(3):231–237.

10. Sang-Yeop Chung, Mohamed Abd Elrahman, Dietmar Stephan, Paul H Kamm. The Influence of Different Concrete Additions on the Properties of Lightweight Concrete Evaluated Using Experimental and Numerical Approaches. *Construction and Building Materials*. 2018;189:314–322. https://doi.org/10.1016/j.conbuildmat.2018.08.189

11. Yujie Huang, Zhenjun Yang, Wenyuan Ren, Guohua Liu, Chuanzeng Zhang. 3D Meso-Scale Fracture Modelling and Validation of Concrete Based on In-situ X-ray Computed Tomography Images Using Damage Plasticity Model. *International Journal of Solids and Structures*. 2015;67–68:340–352. https://doi.org/10.1016/j.ijsolstr.2015.05.002

12. Levandovskiy AN, Melnikov BE, Shamkin AA. Porous Material Modeling with Finite Element Method. *Construction of Unique Buildings and Structures.* 2017;53(2):61–77. https://doi.org/10.18720/CUBS.53.5

13. Bolshakov VI, Yelisieieva MO, Shcherbak SA. Contact Strength of Mechanoactivated Fine Concretes from Granulated Blast-Furnace Slags. *Nauka ta progres transportu*. 2014;53(5):138–149. (In Russ.)

14. Egorochkina IO, Serebryanaya IA, Shlyakhova EA, Matrosov AA, Pronina KA, Kuzina AN. Study of the Structure of the Contact Zone in Concretes with Combined Aggregates. *Engineering Journal of Don*. 2019;55(4):40.

15. Bedarev VV, Bedarev NV, Bedarev AV. The Destruction of Concrete in the Contact Layer Based on the Basic Provisions of General Theory of Adhesion and Anchoring of Periodic Profile Reinforcement in Concrete. In: *Proceedings of the International Construction Congress "Science. Innovations. Goals. Construction"*. Moscow: Research Center of Construction; 2023. P. 39–43. (In Russ.)

16. Pichugin AP, Khritankov VF, Smirnova OE, Pimenov EG. Crack Formation in Large-Porous Concrete with an Integral Arrangement of a Large Filler. *Expert: Theory and Practice*. 2020;7(4):47–52. (In Russ.)

17. Pschenichniy GN. About the Features of Cement Concrete Surface Area. *Concrete Technologies.* 2015;110–111(9–10):56–60.

18. Dmitrieva MA, Sharanova AV, Panfilova AD, Plakhtiy AA. Rheological Properties of Building Mortars Used for 3D Printing. In: *Proc. International Conference "Advanced Building Materials and Technologies"*. Kaliningrad: IKBFU Publ.; 2019. P. 18–32. (In Russ.)

19. Sharanova AV, Dmitrieva MA, Leitsin VN. Ensuring Formation of Concrete Building Constructions without Formwork by Additive Technologies. In: *Proc. II International Conference "Advanced Building Materials and Technologies"*. Kaliningrad: IKBFU Publ.; 2020. P. 15–21. (In Russ.)

20. Dvorak GJ. *Micromechanics of Composite Materials. Series: Solid Mechanics and Its Applications*. Dordrecht: Springer; 2013. 442 p. https://doi.org/10.1007/978-94-007-4101-0

21. Leitsin VN, Dmitrieva MA, Ivonin IV, PonomarevSV, Polyushko VA, Tovpinets AO, et al. Determining Factors of the Formation of the Structure of Low-Temperature Ceramics. *Physical Mesomechanics*. 2017;20(6):77-85. (In Russ.)

About the Authors:

Anastasiia V. Puzatova, Head of the Laboratory of Construction Materials, Senior Lecturer of the Education and Research Cluster, Institute of High Technology, Immanuel Kant Baltic Federal University (14, Alexander Nevsky Str., Kaliningrad, 236041, Russian Federation), SPIN-code, ORCID, ScopusID, a.v.puzatova@mail.ru

Maria A. Dmitrieva, Dr.Sci. (Phys.-Math.), Professor of the Education and Research Cluster, Institute of High Technology, Immanuel Kant Baltic Federal University (14, Alexander Nevsky Str., Kaliningrad, 236041, Russian Federation), SPIN-code, ORCID, ScopusID, dmitrieva_m@inbox.ru

Alexandr O. Tovpinets, Researcher of the Education and Research Cluster, Institute of High Technology, Immanuel Kant Baltic Federal University (14, Alexander Nevsky Str., Kaliningrad, 236041, Russian Federation), SPIN-code, ORCID, ScopusID, ATovpinets@mail.ru

Vladimir N. Leitsin, Dr.Sci. (Phys.-Math.), Professor of the Education and Research Cluster, Institute of High Technology, Immanuel Kant Baltic Federal University (14, Alexander Nevsky Str., Kaliningrad, 236041, Russian Federation), SPIN-code, ORCID, ScopusID, leitsin@mail.ru

Claimed Contributorship:

AV Puzatova: conducting experiments, interpreting the results, preparing the scientific article.

MA Dmitrieva: problem statement, scientific support.

AO Tovpinets: conducting an experiment on a tomograph, processing images, describing the theoretical part of the research.

VN Leitsin: article editing, conclusion formulation, scientific support.

Conflict of Interest Statement: **the authors declare no conflict of interest.**

All authors have read and approved the final manuscript.

Об авторах:

Анастасия Вячеславовна Пузатова, заведующий лабораторией строительных материалов, старший преподаватель образовательно-научного кластера института высоких технологий Балтийского федерального университета имени Иммануила Канта (236041, Российская Федерация, г. Калининград, ул. А. Невского, 14), SPIN-код, ORCID, ScopusID, a.v.puzatova@mail.ru

Мария Александровна Дмитриева, доктор физико-математических наук, профессор образовательно-научного кластера института высоких технологий Балтийского федерального университета имени Иммануила Канта (236041, Российская Федерация, г. Калининград, ул. А. Невского, 14), SPIN-код, ORCID, ScopusID, dmitrieva_m@inbox.ru

Александр Олегович Товпинец, научный сотрудник образовательно-научного кластера института высоких технологий Балтийского федерального университета имени Иммануила Канта (236041, Российская Федерация, г. Калининград, ул. А. Невского, 14), SPIN-код, ORCID, ScopusID, ATovpinets@mail.ru

Владимир Нояхович Лейцин, доктор физико-математических наук, профессор образовательно-научного кластера Институт высоких технологий Балтийского федерального университета имени Иммануила Канта (236041, Российская Федерация, г. Калининград, ул. А. Невского, 14), SPIN-код, ORCID, ScopusID, leitsin@mail.ru

Заявленный вклад авторов:

А.В. Пузатова: проведение экспериментов, интерпретация результатов, оформление научной статьи.

М.А. Дмитриева: постановка задачи, научное сопровождение.

А.О. Товпинец: проведение эксперимента на томографе, обработка изображений, описание теоретической части исследований.

В.Н. Лейцин: редактирование статьи, формулировка выводов, научное сопровождение.

Конфликт интересов: **авторы заявляют об отсутствии конфликта интересов.**

Все авторы прочитали и одобрили окончательный вариант рукописи.

Received / Поступила в редакцию 07.06.2024
Reviewed / Поступила после рецензирования 02.07.2024
Accepted / Принята к публикации 10.07.2024

MACHINE BUILDING AND MACHINE SCIENCE
МАШИНОСТРОЕНИЕ И МАШИНОВЕДЕНИЕ

UDC 62-4; 622.23.05
https://doi.org/10.23947/2687-1653-2024-24-3-238-245

Original Empirical Research

EDN: EWVFBZ

On Self-Positioning and Self-Fixation of Parts Made of Alloys with Shape Memory Effect under Component Assembling

Balaev Etibar Yusif Ogly
Kuban State Technological University, Krasnodar, Russian Federation
✉ balaev1122@mail.ru

Abstract

Introduction Violation of mutual positioning and fixation of parts worsens the operation of the equipment. Traditional approaches to solving the problem under consideration have been sufficiently studied: interchangeability of parts and the use of special equipment. Both methods involve a significant number of additional elements and assembly operations. Fixation is often provided by means of force fitting and welding. Disadvantages of these methods include assembly, residual and other stresses, engineering constraints, etc. To solve these problems, alloys with thermoelastic phase transformations are used, which provide shape memory effects (SME) to manifest themselves. This article describes, for the first time, self-positioning and self-fixation using the example of parts specially made from an alloy with SME.

Materials and Methods. The pin element under pressing mandrels the blind hole of the cup and enters the seat. The alloy with SME was Ti-55.7wt%Ni. The temperature of the onset of its austenitic transformation was A_s = 95°C ± 5°C. The elemental composition was determined by a Shimadzu EDX-8000 X-ray fluorescence spectrometer, the phase composition — by a Shimadzu XRD-7000 diffractometer. The temperature was specified through differential scanning calorimetry. The range was 20–300°C, the heating rate was 5 deg/min. A Guide T120 thermal imager and a RangeVision DIY 3D scanner with structured illumination were used. After pressing the pin into the cup at different angles, the alignment and deviations between the axes of the cup and the pin were examined. Then, the cup was heated to 110–120°C, cooled, and control measurements were taken.

Results. Values of the deflection angle after pressing were 0.2–11°. With a rigid structure and an installation angle of 0°, the pin deflected in the mounting hole by 0.2–0.5°. The axes shifted and did not intersect. The pin was not always completely pressed in. This indicated uneven deformation of the metal and different stress values around the hole. Such a unit would soon fail. The pin took the required position after heating the cup to 110–120°C (this temperature was higher than at the end of the reverse martensitic transformation). The angular deviation of the axes was noted to be 0.03–0.1°. The maximum misalignment (0.04 mm) corresponded to high positioning accuracy. Heating during the reverse martensitic transformation created internal stresses that returned the initial geometry of the cup. They also formed the forces that positioned and fixed the pin in the hole. That is, it is the parts that provide positioning and fixation (this is self-positioning and self-fixation).

Discussion and Conclusion. For self-positioning and self-fixation of parts due to the shape memory effect, it is necessary to avoid sharp transition lines between the surfaces of parts during design, select rounded corners or fillets, and get a clean surface without burrs. Self-fixation and self-positioning reduce defects and inaccuracies during assembly. The use of certain alloys increases the profitability of equipment production.

Keywords: shape memory effect, thermoelastic phase transformation, self-positioning of a part, self-fixation of a part, mutual positioning of parts, shape restoration due to return stresses

Acknowledgements. The author would like to thank N.A. Shostak, Cand.Sci. (Engineering), Associate Professor, and M.A. Samarin, Research Associate of the Laboratory of Advanced Design of Oil and Gas Equipment, for assistance in planning and conducting experiments. In addition, the author appreciates the Editorial team of the Journal and the reviewer for their competent expertise and valuable recommendations for improving the article.

Funding Information. The research was supported by the Russian Science Foundation Grant No. 23–29–00547 “Development of Principles for Designing Drilling Equipment Elements Using Materials with Shape Memory Effect”, https://rscf.ru/project/23-29-00547/

For Citation. Balaev EYuO. On Self-Positioning and Self-Fixation of Parts Made of Alloys with Shape Memory Effect under Component Assembling. *Advanced Engineering Research* (*Rostov-on-Don*). 2024;24(3):238–245. https://doi.org/10.23947/2687-1653-2024-24-3-238-245

Оригинальное эмпирическое исследование

Самопозиционирование и самофиксирование деталей из сплавов с эффектом памяти формы при монтаже сборочных узлов

Э.Ю.О. Балаев
Кубанский государственный технологический университет, г. Краснодар, Российская Федерация
ООО «Промышленно-инженерная компания», г. Краснодар, Российская Федерация
✉ balaev1122@mail.ru

Аннотация
Введение. Нарушение взаимного позиционирования и фиксации деталей ухудшает работу оборудования. Достаточно изучены традиционные подходы к решению рассматриваемой проблемы: взаимозаменяемость деталей и использование специальной оснастки. Оба метода предполагают значительный объем дополнительных элементов и монтажных операций. Фиксацию часто обеспечивают с помощью посадки с натягом и сварки. Недостатки этих методов: монтажные, остаточные и другие напряжения, технические ограничения и пр. Для решения указанных проблем используют сплавы с термоупругими фазовыми превращениями, которые позволяют проявляться эффектам памяти формы (ЭПФ). В данной статье впервые описаны самопозиционирование и самофиксация на примере деталей, специально изготовленных из сплава с ЭПФ.
Материалы и методы. Исследовались стаканы из сплава с ЭПФ — Ti-55,7wt%Ni при запрессовке: штыревой элемент дорнует глухое отверстие и попадает в посадочное место. Температура начала аустенитного превращения — $A_s = 95$ °C ± 5 °C. Элементный состав определяли рентгенофлуоресцентным спектрометром Shimadzu EDX-8000, фазовый — дифрактометром Shimadzu XRD-7000. Температуру определяли дифференциальной сканирующей калориметрией. Диапазон 20–300 °C, скорость нагрева — 5 °C/мин. Задействовали тепловизор Guide T120 и 3D-сканер со структурированным подсветом RangeVision DIY. После запрессовки под разными углами штыря в стакан исследовали соосность и отклонения между осями стакана и штыря. Затем стакан нагревали до 110–120 °C, охлаждали и делали контрольные замеры.
Результаты исследования. Значения угла отклонения после запрессовки — 0,2–11°. При жесткой конструкции и угле установки 0° штырь отклоняется в посадочном отверстии на 0,2–0,5°. Оси смещаются и не пересекаются. Штырь не всегда полностью запрессовывается. Это говорит о неравномерной деформации металла и о разных по значению напряжениях вокруг отверстия. Такой узел быстро выйдет из строя. Штырь занимает требуемое положение после нагрева стакана до 110–120 °C (эта температура выше, чем в конце обратного мартенситного превращения). Отметили угловое отклонение осей — 0,03–0,1°. Максимальная несоосность (0,04 мм) соответствует высокой точности позиционирования. Нагрев при обратном мартенситном превращении создает внутренние напряжения, возвращающие первоначальную геометрию стакана. Они же формируют усилия, которые располагают и фиксируют штырь в отверстии. То есть именно детали обеспечивают позиционирование и фиксацию (это самопозиционирование и самофиксация).
Обсуждение и заключение. Для самопозиционирования и самофиксации деталей за счет эффекта памяти формы при конструировании следует отказаться от резких линий переходов между поверхностями деталей, выбирать скругленные углы или галтели, добиваться чистой поверхности без заусенцев. Самофиксация и самопозиционирование сокращают брак и неточности при сборке. Использование сплавов с эффектом памяти может повышать рентабельность производства.

Ключевые слова: эффект памяти формы, термоупругое фазовое превращение, самопозиционирование детали, самофиксация детали, взаимное позиционирование деталей, восстановление формы за счет возвратных напряжений

Благодарности. Автор благодарит кандидата технических наук, доцента Н.А. Шостака и научного сотрудника лаборатории перспективного проектирования нефтегазового оборудования Кубанского государственного технологического университета М.А. Самарина за помощь в планировании и проведении экспериментов. Автор также признателен редакционной коллегии журнала и рецензенту за компетентную экспертизу и рекомендации по улучшению статьи.

Финансирование. Исследование выполнено за счет гранта Российского научного фонда № 23–29–00547 «Разработка принципов конструирования элементов бурового оборудования с применением материалов с эффектом памяти формы» https://rscf.ru/project/23-29-00547/

Для цитирования. Балаев Э.Ю.О. Самопозиционирование и самофиксирование деталей из сплавов с эффектом памяти формы при монтаже сборочных узлов. *Advanced Engineering Research* (*Rostov-on-Don*). 2024;24(3):238–245. https://doi.org/10.23947/2687-1653-2024-24-3-238-245

Introduction. Self-positioning should be understood as spatial orientation, installation and positioning of a part and elements mating with it in units and mechanisms. Self-fixation is the interface along the surfaces of structural elements with such geometric features that provide fixation of the mating parts and a given fixation force due to the shape memory effect.

The accuracy of the mutual positioning of parts determines the correctness and reliability of the mechanisms. Valid positioning can reduce the inertia of the mechanical unit, it prevents the occurrence of system backlashes not provided by the design. Failure to comply with the requirements for the mutual positioning of parts can change the operation of the products, which is unacceptable in most cases [1].

The requirements for the accuracy of assembly of units are high in all industries, specifically, in machine-tool manufacture, aircraft, and shipbuilding. For correct, tight mating of parts, the method of group interchangeability is used. Custom tooling is often used when assembling units. As a rule, it is unique for this type of assembly operation. It provides positioning accuracy during installation and meets tolerance requirements [2].

In industrial practice (notably, in construction [3] and the oil and gas industry [4]), alloys with thermoelastic phase transformations, which provide for the shape memory effect (SME), are increasingly used. The uniqueness of such alloys is in the features of phase transformations, due to which shape memory effects are manifested, as well as superelasticity (pseudoelasticity) [5].

Shape memory in alloys with thermoelastic phase transformations is used, in particular, for power drives [6]. The effect is based on return stresses that restore the shape of the part. The phenomenon corresponds to the austenitic phase state of the elements of the power drive [7]. In the oil and gas industry, coupling joints of parts are used for pipe junction [8]. The method involves restoring the shape of elements that provide the envelopment and compression of mating parts [9]. Due to the shape memory effect during assembly, it is possible to provide such processes as spatial orientation, installation, and positioning. To do this, it is advisable to use two principles mentioned above at once:

– embracing and squeezing the parts;

– restoring the shape due to return stresses causing movement.

This approach allows reducing the number of assembly stages and avoiding the use of dedicated equipment (tooling) when positioning and fixing a part made of an alloy with a thermoelastic phase transformation and for the elements of the unit mating with it.

The proposed solution opens up the possibility of replacing such fixation methods as force fitting and welding. Consequently, it is possible to avoid the disadvantages of these methods: assembly, residual and other stresses. We also note the operating restrictions associated with the strength and reliability of the fixation. In addition, it is not always technically possible to perform force fitting and welding.

It is necessary to point out another advantage of parts made of alloys with thermoelastic phase transformations. Their positioning and fixation in the assembly unit allows refusing group interchangeability of parts, from fitting parts and from additional use of control units and mechanisms in the design. This simplifies the installation and manufacture of parts with high positioning accuracy and reliable fixation of parts in the assembly unit.

The presented research article, for the first time, proposes to use thermoelastic phase transformation for positioning and subsequent fixation of parts in an assembly unit. In this case, the shape memory effect of parts ensures their self-positioning and self-fixation.

The author of this article observed the phenomenon under thermoelastic transformations, when it was required to provide fixation due to the shape memory effect of teeth. In this context, the following were considered:

– drill bit roller cutter;

– ball plug in the roller bit leg;

– roller cutter on the bit leg in the design of a roller bit without a ball plug;

– nipple and couplings of a tool joint [10];

– seats enclosed in the disc rotary valve;

– disk on the stem of a disc rotary valve.

The research is aimed at studying the possibilities of self-positioning (spatial orientation, installation, and positioning) and self-fixation during the manifestation of the shape memory effect of alloys with thermoelastic phase transformations. It is expected to find out what accuracy is provided in this case during the design and installation of assembly units, and what conditions need to be maintained during assembly (design features, techniques, requirements for the implementation of self-positioning and self-fixation).

Materials and Methods. For the experiments, two samples were made from an alloy with a thermoelastic phase transformation. In shape, these were cups with a special blind hole and a pin element made of heat-treated (hardened) 40X steel. The cup had an opening — two conical steps with a right (lead-in) and inverted (fixing) cone. Transitions — by radius and by the line of intersection of cones. The pin element had a mandrel shape, so when pressed into the cup, a blind hole was mandrelized, and the pin element got into the seat in the cup. All surfaces were clean, without corners and burrs. This provided:

– free sliding of the pressed-in pin element;

– spatial orientation and installation in the seat under the pin element in the cup;

– positioning of the pin element in the seat.

Figure 1 shows the stages of pressing a pin element into a cup made of an alloy with SME.

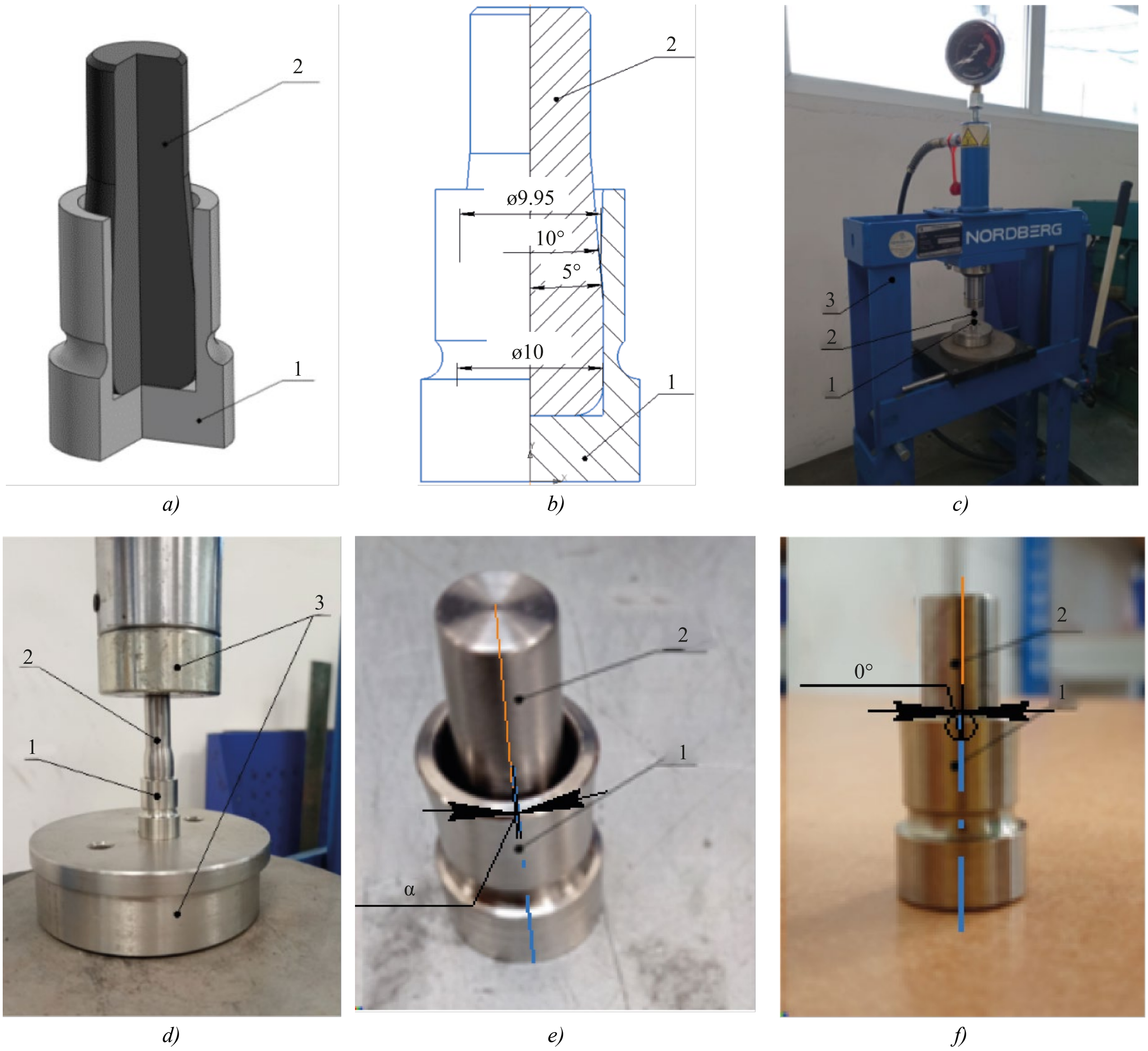

Fig. 1. Installation of pin element into seat of cup made of alloy with SME:
a — 3D model of elements assembling after installing pin element 2 into cup 1;
b — assembly drawing; *c, d* — installation of pin element 2 and cup 1 in hand press 3 before pressing the pin element into cup;
e — angle between axes of symmetry α after pressing pin element 2 into cup 1 before heating (room temperature — martensitic phase of alloy); *f* — pin element and cup at room temperature after heating to 110°C
(angle between axes of symmetry 0°, austenitic phase of the alloy)

Titanium nickelide Ti-55.7wt%Ni was selected as the alloy with SME. The temperature of the onset of its austenitic transformation was A_s = 95°C ± 5°C. Three properties listed below were determined.

1. Elemental composition. For this purpose, X-ray fluorescence analysis was performed using a Shimadzu EDX-8000 device (Japan).

2. Phase composition. X-ray phase analysis was performed using a Shimadzu XRD-7000 X-ray diffractometer (Japan). Parameters: Cu Kα — 1.54 A^0, 40 kV, 30 mA, angle range 20–90 degrees, shooting speed 1 deg/min.

3. Temperature. It was determined by differential scanning calorimetry. The range of work was 20–300°C. Heating rate — 5 deg/min.

This alloy allows for demonstration of the general principles of self-fixation and self-positioning of a pin element in the seat of the cup during the phase transition from martensite to austenite. At room temperature, the alloy is in the martensite phase.

A Nordberg manual press was used for pressing. The cup made of an alloy with SME was heated with a GHG 23–66 Bosch technical hot air gun. Temperature control provided uneven heating of the cup and maximum imitation of the assembling process at enterprises. Specifically, the worst installation conditions and operation with violations of the process were recreated.

The temperature and hot zones, as well as heating over the entire surface to the specified temperature, were monitored using a Guide T120 thermal imager. The positioning accuracy was determined by a stationary 3D scanner with structured illumination RangeVision DIY. Daheng cameras provided a measurement accuracy of 0.02 mm.

The sequence of operations for installing the pin element into the cup is described below.

1. The pin element is pressed into the blind hole of the cup. As a result, the hole is mandrelized. It deepens until the pin element enters the seating surface of the hole. The process takes place at room temperature, corresponding to the martensitic phase state of Ti-55.7wt%Ni alloy with shape memory effect.

2. The relative position of the parts is measured.

3. The cup is controllingly heated until the temperature is higher than it was at the end of the austenitic transformation. At this temperature, the initial (before deformation) shape of the cup is restored, and the force from the resulting return stresses is sufficient to shift and orient the pin element inside the blind hole of the cup. After this, the cup is cooled to room temperature.

4. A control measurement of the relative position of the parts is performed.

The pin element was pressed into the cup at different angles between the axes of symmetry of the cup and the pin element. The angle sizes were from 0 to 12 degrees. The step was 3 degrees. The alignment and the angle of deviation between the axes were determined. Then the cup was heated to 110–120°C and cooled in various ways — from free cooling in air to forced cooling (by lowering into water). Then, a control measurement of the alignment and the angle of deviation between the axes was made.

Research Results. After pressing, the angle of deviation between the axes of the cup and the pin element had values in the range from 0.2° to 11° (angle α in Fig. 2 *a*). This indicates that with the rigidity of the structure and the installation angle of 0°, some displacement of the pin element in the mounting hole still occurs (from 0.2° to 0.5°).

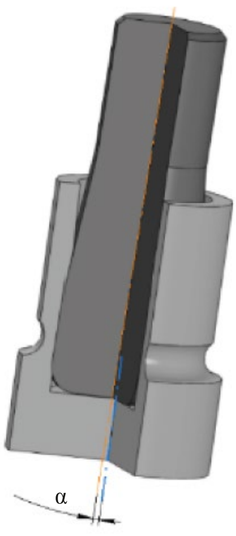

a)

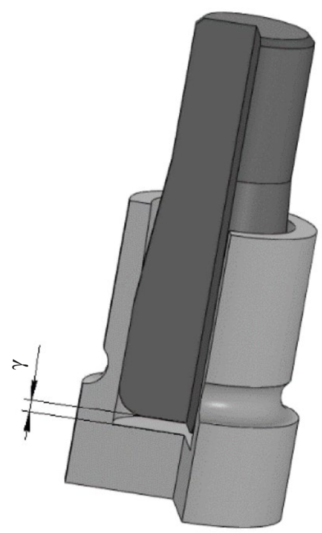

b)

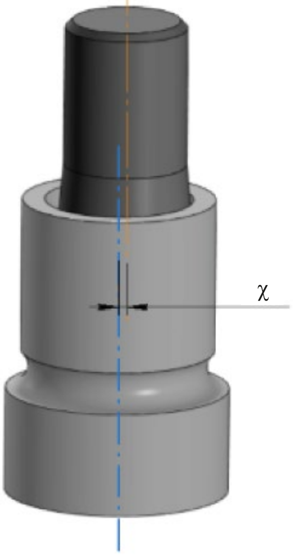

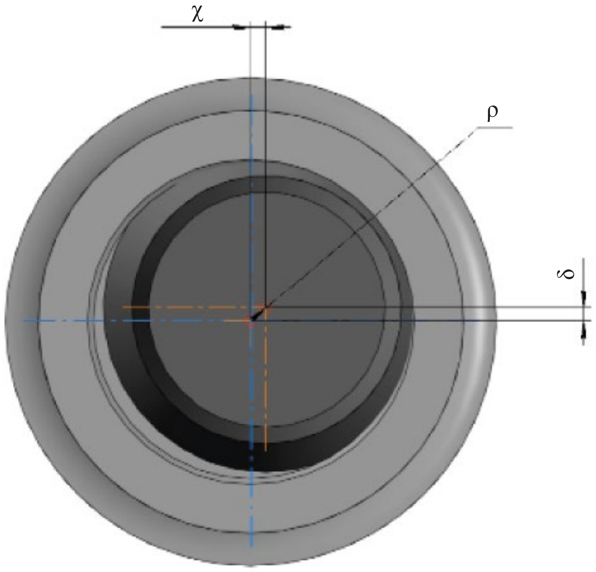

Fig. 2. Deviations arising during installation of pin element in cup mounting hole:
a — angle between the axes of symmetry; *b* — displacement as a result of underpressing;
c, d — displacement of the axes of symmetry in the section plane perpendicular
to the axes of symmetry of the pin element and the cup

The axes were offset and did not have an intersection point, as shown in Figure 2 *c* and 2 *d*. If we take the axis of the cup (reference point) as the center, the offset of the axis of the pin element will be ρ = 0.2–0.8 mm (Fig. 2 *d*), i.e., the pin element in the cup will have an offset mounting position. In a number of cases, the pin element was not completely pressed into the cup (Fig. 2 *b*). Firstly, this caused uneven deformation of the metal around the hole. Secondly, it indicated that as a result of pressing, different stress values arose along the circumference of the hole. Such a unit will quickly fail when used.

The pin element occupies the required position in the cup hole and relative to the hole seat after heating the cup to 110–120°C, i.e., at a temperature higher than at the end of the reverse martensitic transformation.

The positioning accuracy of the pin element in the cup was studied using a stationary 3D scanner with structured illumination RangeVision DIY and Daheng cameras. The angular deviation of the axes was recorded in the range of 0.03–0.1°. The maximum value of the misalignment was 0.04 mm, which corresponded to high positioning accuracy for assembly units.

It should be noted that there is a similarity between the two mechanisms that provide:

– occupation of the structurally required position of the pin element in the cup hole;

– action of the working element made of an alloy with SME of the power engine.

The specified shape of the part made of an alloy with shape memory effect of the cup in the austenitic state corresponds to the shape in which the pin element exactly occupies the position required by the design of the unit. At a temperature corresponding to the martensitic phase state, the mechanical characteristics of the alloy are lower than at a temperature corresponding to austenite. In this case, it is possible to specify a shape into which the pin element can be easily mounted. With such installation, the positioning of the pin element does not correspond to the required.

Subsequent heating of the glass as a result of the reverse martensitic transformation creates internal stresses that allow the original shape to be restored. They can be conventionally called return stresses. In this case:

– the cup takes on a shape that corresponds to the operational geometric characteristics;

– the forces arising as a result of the action of return stresses are sufficient to move, orient, install and position the pin element in the seat of the cup (it is located and fixed in the hole).

Evidently, it is the parts that provide self-positioning and self-fixation. No special equipment or special assembly techniques are needed.

There is a process similar to the one described above. To operate the satellite antenna deployment mechanism, the power drive uses the force developed by the return stresses during the reverse martensitic transformation of the working element made of an alloy with SME.

Discussion and Conclusion. The displacement of the pin element inside the cup mounting hole is provided by design features that can be applied to all mating parts under self-positioning and self-fixation due to the shape memory effect of alloys with thermoelastic phase transformations. Techniques that allow maintaining the required design features are listed below:

– rejection of sharp transition lines between surfaces of parts in favor of smoother ones;
– selection of rounded or variable radius chamfers and external corners;
– replacement of internal corners with fillets or curves with variable radius;
– high-quality surface cleaning, elimination of burrs.

These requirements should be taken into account when designing. This will provide the desired mutual displacements of parts with significantly less force. In this case, the force is compared to that given by the return stresses during the reverse martensitic transformation of the alloy with thermoelastic phase transformations (the cup is made of such material).

Self-fixation and self-positioning can maintain assembly accuracy, eliminate mounting and engineering inaccuracies during installation work, and reduce defects. The use of some alloys has economic substance, i.e., it works for the profitability of the final product [11]. These and other advantages of the approach described in the article can be implemented in machine tool manufacturing. The method seems useful for developing oil and gas, precision and other equipment with high requirements for the geometric accuracy of parts.

References

1. Nazaryev AV, Bochkarev PYu. Improving the Principles of Identifying Critical Requirements for the Assembly of High-Precision Products. *Advanced Engineering Research (Rostov-on-Don)*. 2024;24(1):66–77. https://doi.org/10.23947/2687-1653-2024-24-1-66-77

2. Anur'ev VI. *Handbook of a Mechanical Designer.* In 3 vol. Vol. 1. 8th ed. Moscow: Mashinostroenie; 2001. 920 p. (In Russ.) URL: https://www.prugini-spb.ru/anuriev/Anuriev_T1.pdf (accessed: 06.06.2024).

3. Malinin V, Moussaoui Yu, Burdin Yu. The Application of Shape Memory Alloys for Civil Structures Reinforcement. *Building and Reconstruction.* 2017;70(2):23–31.

4. Aghiney RV, Nekuchaev VO, Semitkina EV, Terentyeva MV. Opportunities for Using Innovative Shape Memory Effect Materials in Oil Industry. *Petroleum Engineering.* 2020;18(1):39–47. http://doi.org/10.17122/ngdelo-2020-1-39-47

5. Duerig TW, Pelton AR, Bhattacharya K. The Measurement and Interpretation of Transformation Temperatures in Nitinol. *Shape Memory and Superplasticity.* 2017;3:485–498. http://doi.org/10.1007/s40830-017-0133-0

6. Shishkin SV, Makhutov NA. *Calculation and Design of Power Structures on Alloys with Shape Memory Effect.* Izhevsk: RDE "Regulyarnaya i khaoticheskaya dinamika", Institute of Computer Research; 2019. 411 p. (In Russ).

7. Barvinok VA, Bogdanovich VI, Groshev AA, Plotnikov AN, Lomovsky OV. Design Method of Power Drives from Material Shape Memory Effect for Rocket and Space Technology. *Proceedings of the Samara Scientific Center of the Russian Academy of Science.* 2013;15(6):272–277.

8. Andronov IN, Semitkina EV. Use of a Variable-Diameter Coupling Manufactured from Some Material with Memory as a Connecting Element on Fields Flowlines. *Onshore and Offshore Oil and Gas Well Construction.* 2017;(11):20–27.

9. Lomovskoy OV, Vashukov YuA, Belashevskiy GE, Bogdanovich VI, Barvinok VA. Assembly of Pipeline Elements Using Technological Equipment with a Power Drive Made of Alloy with Shape Memory Effect. *Assembling in Mechanical Engineering and Instrument-Making.* 2003;(3):4. (In Russ.)

10. Ruban DA, Cherkesov TA, Balaev EYuO, Gerasimov DV. Use of Materials with Shape Memory Effect to Improve the Performance Properties of Parts of Drill String. *IOP Conference Series: Materials Science and Engineering. International Conference on Civil, Architectural and Environmental Sciences and Technologies.* 2019;775:102–112. https://doi.org/10.1088/1757-899X/775/1/012122

11. Terekhin AG. About Materials with a Memory Effect and Features of Their Application. *Innovations and Investments*. 2020;(6):222–223.

About the Author:

Etibar Yusif Ogly Balaev, Senior Research Fellow of the Department of Oil and Gas Engineering named after Prof. G.T. Vartumyan, Kuban State Technological University (2, Moskovskaya Str., Krasnodar, 350072, Russian Federation), Invention and Patent Engineer, Industrial-Engineering Company LLC (144, Uralskaya Str., Krasnodar, 350080, Russian Federation), SPIN-code, ORCID, ScopusID, balaev1122@mail.ru

Conflict of Interest Statement: **the author declares no conflict of interest.**

The author has read and approved the final version of manuscript.

Об авторе:

Эътибар Юсиф Оглы Балаев, старший научный сотрудник кафедры нефтегазового дела имени профессора Г.Т. Вартумяна Кубанского государственного технологического университета (350072, Российская Федерация, г. Краснодар, ул. Московская, 2), инженер по изобретательской и патентной деятельности ООО «Промышленно-инженерная компания» (350080, Российская Федерация, г. Краснодар, ул. Уральская, 144), SPIN-код, ORCID, ScopusID, balaev1122@mail.ru

Конфликт интересов: **автор заявляет об отсутствии конфликта интересов.**

Автор прочитал и одобрил окончательный вариант рукописи.

Received / Поступила в редакцию 25.06.2024
Reviewed / Поступила после рецензирования 18.07.2024
Accepted / Принята к публикации 01.08.2024

MACHINE BUILDING AND MACHINE SCIENCE
МАШИНОСТРОЕНИЕ И МАШИНОВЕДЕНИЕ

UDC 681.5:622.24
https://doi.org/10.23947/2687-1653-2024-24-3-246-254

Original Theoretical Research

Mathematical Model of Drilling Mud Movement along a Shale Shaker Screen

I.Yu. Kichkar
Kuban State Technological University, Krasnodar, Russian Federation
✉ kichkar@ya.ru

EDN: IULDLM

Abstract

Introduction. When drilling oil or gas wells, rock from the bottomhole is brought to the surface by drilling mud, which is cleaned of sludge by shale shakers at the first stage. Shale shakers are equipped with such a screen and create such trajectories of vibration of the frame in order to solve a dual problem: on the one hand, to provide the cleaning of the drilling mud coming from the well mouth, and on the other hand — to maintain the proper degree of cleaning. To correctly select the nomenclature of screens, it is necessary to reliably determine the throughput capacity of a shale shaker in the real-time setting. This will allow you to pre-order the required number of screens with the required cell size. Previously, studies were conducted by sieving a mixture of calibrated granules on a standard shaker or by straining mineral oil through a fixed screen. However, this does not fully correspond to the actual conditions of drilling mud screening. The objective of this article was to simulate the throughput of a drilling shale shaker under real conditions by calculating the movement of drilling mud along a vibrating screen using its previously obtained specific throughput capacity.

Materials and Methods. When creating a mathematical model of the full throughput capacity of a shale shaker, a previously known mathematical model of fluid flow in an open channel and a finite-dimensional approximation in the form of a sequence of sections of concentrated containers connected by hydraulic conductivities (by analogy with the approximation of long electrical lines and extended gas pipelines by the finite element method) were used. The fluid flow rate over the screen was determined according to Chézy law. In this case, the cross-sectional area of the flow above the screen for a specific section was specified as the arithmetic mean between the initial and final values of the drilling mud height in the corresponding section.

Results. A chain calculation scheme for sieving drilling mud was compiled. Based on the material balance, mathematical models were developed for determining the throughput and height of drilling mud above the screen:
– for the first section of the screen and the first nodal point of the screen;
– for subsequent screen sections and subsequent screen nodal points;
– for the last section of the screen and the last nodal point of the screen.

A mathematical model of the drilling mud movement along the shale shaker screen has been obtained, which, due to the finite-dimensional representation of this flow along n sections of the screen length, is a system of n integral equations describing concentrated tanks, and n – 1 algebraic equations describing the flow of drilling mud between tanks.

Discussion and Conclusion. The movement of drilling mud along the length of the shale shaker screen corresponds to the movement of a steady uneven flow in an open channel. However, in the first case, the volume flow along the length is variable (decreasing to zero), and in the second case, it is constant along the length. Therefore, the use of only one differential equation for steady uneven flow in an open channel is not sufficient in this case. The resulting mathematical model of the drilling mud movement along the shale shaker screen is a mathematical basis for the development of a modeling program to determine the throughput of the shale shaker for real operating conditions, i.e., for a specific drilling mud, a given screen or a given drive system of the shale shaker.

Keywords: shale shaker, vibrating screen, height of the mortar layer, material balance, throughput capacity, edge condition, nodal points

Acknowledgements. The author appreciates the Production Automation Department, KubSTU, for assistance in preparing the article. The author would like to thank the reviewers for their criticism and suggestions, which contributed to a significant improvement in the quality of the article.

For Citation. Kichkar IYu. Mathematical Model of Drilling Mud Movement along a Shale Shaker Screen. *Advanced Engineering Research (Rostov-on-Don)*. 2024;24(3):246–254. https://doi.org/10.23947/2687-1653-2024-24-3-246-254

Оригинальное теоретическое исследование

Математическая модель движения бурового раствора по сетке вибросита

И.Ю. Кичкарь

Кубанский государственный технологический университет, г. Краснодар, Российская Федерация

✉ kichkar@ya.ru

Аннотация

Введение. При бурении нефтяных или газовых скважин порода из забоя выносится на поверхность буровым раствором, который очищается от шлама на первой стадии виброситами. Вибросита оснащаются такой сеткой и создают такие траектории виброколебаний рамы, чтобы с одной стороны — обеспечивать очистку поступающего из устья скважины бурового раствора, а с другой — обеспечивать должную степень очистки. Для корректного подбора номенклатуры сеток нужно надежно определять пропускную способность вибросита в реальных условиях. Это позволит заранее заказать требуемое количество сеток с нужным размером ячеек. Ранее исследования проводились путем просеивания смеси калиброванных гранул на стандартном вибростенде или процеживанием минерального масла через неподвижную сетку. Однако это не в полной мере соответствует реальным условиям просеивания бурового раствора. Целью данной работы было моделирование пропускной способности бурового вибросита в реальных условиях путем расчета движения бурового раствора по вибрирующей сетке с использованием её ранее полученной удельной пропускной способности.

Материалы и методы. При создании математической модели полной пропускной способности бурового вибросита использовалась известная ранее математическая модель течения жидкости в открытом канале и конечномерная аппроксимация в виде последовательности участков из сосредоточенных емкостей, соединенных гидравлическими проводимостями (по аналогии с аппроксимацией электрических длинных линий и протяженных газопроводов методом конечных элементов). Расход течения жидкости над сеткой определялся по закону Шези. При этом площадь сечения потока над сеткой для конкретного участка определялась как среднее арифметическое между начальным и конечным значением высоты бурового раствора на соответствующем участке.

Результаты исследования. Составлена цепная расчетная схема просеивания бурового раствора. На основании материального баланса разработаны математические модели определения пропускной способности и высоты бурового раствора над сеткой:

- для первого участка сетки и первой узловой точки сетки;
- для последующих участков сетки и последующих узловых точек сетки;
- для последнего участка сетки и крайней узловой точки сетки.

Получена математическая модель движения бурового раствора по сетке вибросита, которая вследствие конечномерного представления этого потока по n участкам длины сетки представляет собой систему из n интегральных уравнений, описывающих сосредоточенные емкости, и n – 1 алгебраических уравнений, описывающие перетоки бурового раствора между емкостями.

Обсуждение и заключение. Движение бурового раствора по длине сетки вибросита соответствует движению установившегося неравномерного потока в открытом русле. Однако в первом случае — объемный расход по длине переменный (убывающий до нуля), а во втором случае — постоянный по длине. Поэтому использование только одного дифференциального уравнения установившегося неравномерного потока в открытом русле в данном случае недостаточно.

Полученная математическая модель движения бурового раствора по сетке вибросита является математическим обоснованием для разработки моделирующей программы по определению пропускной способности вибросита для реальных условий его работы, то есть для конкретного бурового раствора, данной сетки или заданной системы приводов вибросита.

Ключевые слова: буровое вибросито, вибрирующая сетка, высота слоя раствора, материальный баланс, пропускная способность, граничные условия, узловые точки

Благодарности. Автор выражает признательность кафедре «Автоматизации производственных процессов» ФГБОУ ВО «КубГТУ» за помощь в подготовке статьи.

Для цитирования. Кичкарь И.Ю. Математическая модель движения бурового раствора по сетке вибросита. *Advanced Engineering Research (Rostov-on-Don)*. 2024;24(3):246–254. https://doi.org/10.23947/2687-1653-2024-24-3-246-254

Introduction. The capacity of the drilling mud cleaning unit of the rig circulation system is limited by the flow rate of the circulating drilling mud, which must be cleaned properly [1]. The capacity is the volume of drilling mud sieved through the screen, and the flow rate is the volume of drilling mud that flows without sieving. The shale shaker is the first processing vessel in this unit, and it performs primary purification. Therefore, its throughput mainly determines the capacity of the entire cleaning system.

The capacity of the cleaning unit of the circulation system (CS) of a standard drilling rig should exceed the throughput of the drilling pump and be about 30-80 l/s. Insufficient capacity of the CS limits the rate of penetration [2].

The circulating drilling mud is fed to the shale shaker directly from the well mouth via a chute. There are no intermediate tanks; therefore, even if its consumption briefly exceeds the shale shaker's capacity, the drilling mud will flow through the screen into the tank waste, which will result in its loss. If the driller's assistant opens the gate valve, the raw mud will flow past the vibrating screen into the tank. This is an extremely undesirable case, since the sludge settles in the tank, preventing it from being pumped into the desander. This dramatically reduces the degree of drilling mud purification, which leads to increased drilling costs and even complications in the well [2].

The throughput of a particular shale shaker is largely determined by the size of the screen cell with which it is equipped. With a decrease in the cell size, the throughput of the shale shaker decreases significantly, but the degree of cleaning of the drilling mud increases. In practice, to prevent the solution from passing by the shale shaker, a screen with a larger cell with a large but unknown margin of throughput is installed on it [1].

The actual measurement of the throughput of the shale shaker is difficult, because after sieving through the screen, the mud flows into the tank under the shale shaker by gravity, without passing through the pipeline. Therefore, the throughput of the shale shaker was determined by indirect methods.

In [2], based on production experience, the parameters that change the throughput are indicated: an increase in the length of the screen, a decrease in the flow rate, a decrease in the angle of inclination of the screen, a change in the direction of particle movement, a decrease in the amplitude of screen vibrations, the simultaneous use of two consecutive or parallel screens. However, the authors do not provide quantitative indicators of these parameters. In [3], values of the shale shaker throughput when working with various drilling fluids are given, but the general formula is not given. In[1], only the formula for calculating the change in capacity is indicated. The problem of selecting a screen for a specific case

[1] *American Association of Drilling Engineers Shale Shakers and Drilling Fluid System.* Houston: Gulf Publishing Company; 1999. 335 p.

is solved in a review by a team of American engineers[2]. It consists of selecting a screen with the smallest cell, at which the shale shaker would have a throughput greater than the specified one. Several methods have been developed for testing screens, but all of them are far from the operating conditions of shale shakers on drilling rigs. Thus, in the API Recommended practice 13C standard, screens are tested either by sieving a mixture of calibrated granules on a standard shaking table or by filtering mineral oil through a stationary screen. In [4], an attempt was made to analytically describe the movement of the drilling mud flow through the screen and the process of sieving it through the screen based on the Navier-Stokes equation. The simulation results do not take into account the dynamic parameters of the screening machine. These parameters are taken into account in [5], but as a parameter in question not for the drilling fluid, but for coal sludge. The amount of all the sludge removed from the total mass is relatively small [6]. Such a concentration of sludge does not have a noticeable effect on the rheology of the drilling mud [3]. Accordingly, the separation of the dewatering process given in [7] is inappropriate. A high concentration of sludge is observed in the drilling mud leaving the desanders and desilters, which is cleaned on the second shale shaker[3].

From all has been said it follows that it has not yet been possible to determine the value of the drilling shale shaker capacity using theoretical studies. Therefore, the objective of this work was to model the full throughput capacity of the shale shaker based on previously conducted laboratory experiments to determine the specific capacity.

Specific throughput capacity

Previously, the team with the participation of the author developed a methodology [7], technical and software support for the experimental determination of a mathematical model of the specific throughput of a specified screen of the first shale shaker for a real drilling mud for a special shale shaker, and experimental studies were performed [8]. If all the points of the support frame located along the screen line have the same vibration trajectories, or, as they say in vibration engineering, “the orbits are homogeneous”, then it is enough to conduct one experiment. If the trajectories are nonhomogeneous, then it is enough to conduct three experiments with trajectories at the edges and in the center of the screen. In any case, the vibration trajectory parameters of the frame points of the production shale shaker must be known and implemented in the experiments.

Experimental benches of other scientists are known, e.g., in [9], a bench that creates polyharmonic trajectories of vibrations is described. This is achieved by the corresponding arrangement of the multi-speed drive system. During the experiments, even Lissajous figures were obtained [10]. The resulting best design may work less efficiently due to external actions. At the same time, the purpose of automatic control is to compensate for the negative impact of external actions. In [11], a control method is given, in [12] — the dynamic parameters of the shale shaker under control, and in [13], an example of step-by-step optimization using the Adams and Nastran modeling units is given.

The experiments performed on sieving a bentonite-water solution with a density of 1.19 g/cm^3 through a screen sample with square cells measuring 0.4×0.4 mm allowed us to obtain the following mathematical model of the specific capacity of the screen [9]:

$$q\left(h, Ay\right) = 0.0088 \cdot h^{1.62} \cdot Ay^{1.59}, \quad (1)$$

where $q(h, Ay)$ — specific throughput capacity of the screen, m^3/m^{2}s; h — height of the rubble mortar layer on the screen, m; Ay — amplitude of vertical vibration acceleration, m/s^2.

Boundary conditions of the sieving process

A mathematical model of specific throughput is not enough to determine the throughput capacity of a drilling shale shaker. It is also necessary to know the distribution of the height of the drilling mud layer along the length of the screen $h(x)$ at a known flow rate of the solution entering the screen $Q(0)$. It is not possible to take a linear distribution of height along the length of the screen as a first approximation, since the boundary condition at the end of the sieving process $h(0)$ is unknown. The boundary condition for the beginning of the sieving process, as described earlier, is known and has the form $h(0.8 \cdot L) = 0$, where L — length of the screen, m.

[2] Ibid. P. 3–335.
[3] Ibid. P. 3–335.

In classical hydraulics, a mathematical model is known for the distribution of the height of the liquid layer along the length of the flow with a non-pressure steady uneven flow of liquid in an open channel [14]. However, the flow rate of the liquid in this case is constant along the length of the flow, and in our case, the flow rate decreases due to the sieving of part of the drilling mud. Therefore, the steady motion of the drilling mud flow along the shale shaker screen is an object with variables $h(x)$ and $Q(x)$ distributed along the length of the screen.

Analysis techniques for distributed objects

The search for engineering solutions to such problems has shown that in electrical engineering, long electric lines are replaced by a chain of concentrated resistances, capacitances and inductances [15]. Extended gas pipelines are replaced by a chain of alternating tanks and hydraulic resistances to simulate their operation [16]. This approach is especially often used in machine dynamics, where chain calculation schemes are built according to general drawings, consisting of alternating concentrated masses or moments of inertia and concentrated pliability for vibrating machines [17] and control systems [18]. This is essentially a finite element approximation of distributed objects.

Construction of a mathematical model of the full throughput capacity of a shale shaker

Let us construct a calculation scheme of the drilling mud flow from concentrated capacities and concentrated hydraulic conductivities, shown in Figure 1. To do this, we divide the length of the shale shaker screen by nodal points into equal sections of length $\Delta x = L/m$, where m — number of sections. Nodal points must be at the beginning and end of the screen. We place concentrated capacities in the nodal points. The initial and final capacities correspond to a section of the flow of length $0.5 \cdot \Delta x$, and the remaining capacities correspond to Δx.

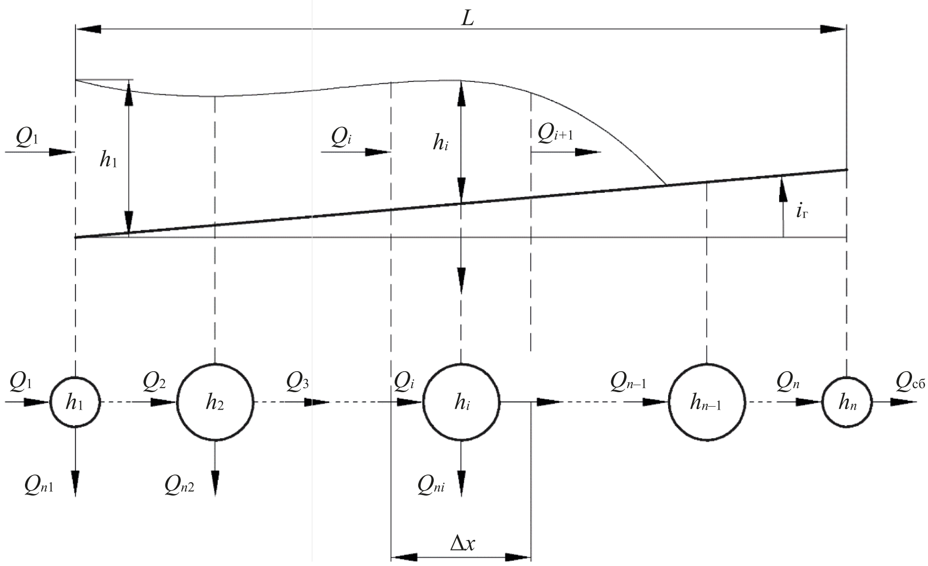

Fig. 1. Chain calculation scheme of the hydraulic system of drilling mud flow along the screen

The material balance equation for the first container in Figure 1 has the form:

$$\left(Q_1(t) - Q_2(t) - Q_{n1}(t)\right) \cdot dt = \frac{\Delta x}{2} \cdot b \cdot dh_1(t), \tag{2}$$

where $Q_1(t)$ — flow rate of the drilling mud entering the shale shaker, m^3/s; $Q_2(t)$ — flow rate of the drilling mud flowing out of the screen from the tank of the 1st nodal point to the tank of the 2nd nodal point, m^3/s; $Q_{n1}(t)$ — flow rate of the drilling mud sieved in the first section, m^3/s; $h_1(t)$ — height of the mud layer at the first nodal point, m; b — screen width, m.

The sieved flow rate at the first nodal point, taking into account the specific throughput, is equal to:

$$Q_{n1}(t) = q\left(h_1(t), Ay_1\right) \cdot \frac{\Delta x}{2} \cdot b, \tag{3}$$

where Ay_1 — vibration acceleration amplitude at the first nodal point.

Substituting expression (3) into (2) and transforming the equation, we obtain the expression for $h_1(t)$:

$$h_1(t) = \int \left[\frac{2}{\Delta x \cdot b} Q_1(t) - Q_2(t) - q\left(h_1(t), Ay_1\right) \right] \cdot dt. \tag{4}$$

The material balance equation for the capacities of all intermediate nodal points in Figure 1 has the form:

$$\left(Q_i(t) - Q_{i+1}(t) - Q_{ni}(t)\right) \cdot dt = \Delta x \cdot b \cdot dh_i(t), \tag{5}$$

where $Q_i(t)$ — flow rate of drilling mud flowing into the tank of the i-th nodal point, m^3/s; $Q_{i+1}(t)$ — flow rate of drilling mud flowing along the screen from the tank of the i-th nodal point to the tank of $i + 1$st nodal point, m^3/s; $Q_{ni}(t) = q(h_i(t), Ay) \cdot \Delta x \cdot b$ — flow rate of drilling mud flowing along the screen from the tank of the i-th nodal point to the tank of i+1st nodal point, m^3/s; $h_i(t)$ — height of the solution layer at the i-th nodal point, m.

By transforming equation (5), we obtain the expression for all intermediate nodal points:

$$h_i(t) = \int \left[\frac{1}{\Delta x \cdot b} \left(Q_i(t) - Q_{i+1}(t)\right) - q\left(h_i(t), Ay_i\right) \right] \cdot dt. \tag{6}$$

At the last nodal point, based on physical considerations, we take the height of the solution layer to be zero (C), for not to support the flow in the event of its flow into the tank waste. This is essentially the right boundary condition for the height of the solution layer. The flow rate of the drilling mud entering the shale shaker is assumed to be constant in this mathematical model and equal to the specified value $Q_1(t) = Q_{1\ \text{зад}}$. This is an indirect assignment of the left boundary condition for the height of the solution layer.

All intermediate costs in Figure 1 are determined by the difference in heights of the solution layer $h_{i-1}(t) - h_i(t)$ and the concentrated hydraulic resistance of the screen section. Drilling mud is a non-Newtonian fluid, but with the turbulent flow of clay solutions, it is possible to proceed from the usual formulas of hydraulics [19].

To determine the flow rate $Q_i(t)$, we do not specify the value of the hydraulic resistance of a section of the screen with a length of Δx, but we use the well-known differential equation for a steady-state non-uniform flow of constant flow rate [20], but for a raised screen:

$$\frac{dh(x)}{dx} = -\frac{i_\text{г} + \dfrac{Q^2}{F^2 \cdot C^2 \cdot R}}{1 - \dfrac{\alpha}{g} \cdot \dfrac{Q^2}{F^2} \cdot b}, \tag{7}$$

where $i_\text{г}$ — geometric slope of the flow channel, in Figure 1 $i_\text{г} > 0\, i_г > 0$; F — cross-sectional area of the flow, m^2; C — Chézy coefficient; R — hydraulic radius of the flow cross-section, m; α — Coriolis coefficient, α = 1.10 – 1.15 [21]; g — gravitational acceleration.

Let us express the derivative in differential equation (7) by finite differences and use the variables from the calculation scheme in Figure 1 in it:

$$\frac{h_{i-1}(t) - h_i(t)}{\Delta x} = -\frac{i_\text{г} + \dfrac{Q_i^2(t)}{F_i^2 \cdot C^2 \cdot R_i}}{1 - \dfrac{\alpha}{g} \cdot \dfrac{Q_i^2(t)}{F_i^3} \cdot b}, \tag{8}$$

where F_i — cross-sectional area of the flow in the section from the i – 1st nodal point to the i-th nodal point.

Here, it should be clarified that $Q_i(t)$ — flow rate in the section from the i – 1st nodal point to the i-th nodal point. The cross-sectional area of the flow in this section varies from $h_{i-1}(t)\, b$ to $h_i(t)\, b$. Therefore, we define value F_i as the average value of these areas:

$$F_i = b \cdot \frac{h_{i-1}(t) + h_i(t)}{2}. \tag{9}$$

Value of the hydraulic radius of the flow is equal to the ratio [15]:

$$R_i = \frac{F_i}{A_i} = b \cdot \frac{h_{i-1}(t) + h_i(t)}{2} \cdot \frac{1}{b + 2 \cdot \frac{h_{i-1}(t) + h_i(t)}{2}}, \tag{10}$$

where A_i — length of the wet perimeter of the flow in the section from the i – 1st nodal point to the i-th nodal point, m.

The width of the industrial shale shaker screen is from 1 meter, the thickness of the solution layer on the screen is several centimeters [4]. Therefore, from expression (10), it follows that $R_i \approx (h_{i-1}(t) + h_i(t))/2$. Substituting this value and value F_i from expression (9), we obtain:

$$\frac{h_{i-1}(t) - h_i(t)}{\Delta x} = -\frac{i_\Gamma + \dfrac{Q_i^2(t)}{\left(0.5 \cdot \left(h_{i-1}(t) + h_i(t)\right)\right)^3 \cdot b^2 \cdot C^2}}{1 - \dfrac{\alpha}{g} \cdot \dfrac{Q_i^2(t)}{\left(0.5 \cdot \left(h_{i-1}(t) + h_i(t)\right)\right)^3 \cdot b^2}}. \tag{11}$$

We solve equation (11) with respect to $Q_i(t)$ for $i > 1$:

$$Q_i(t) = \sqrt{\frac{\dfrac{h_{i-1}(t) - h_i(t)}{\Delta x} + i_\Gamma}{\left[\dfrac{h_{i-1}(t) - h_i(t)}{\Delta x} \cdot \dfrac{\alpha}{g} - \dfrac{1}{C^2}\right]} \cdot \left[0.5 \cdot \left(h_{i-1}(t) + h_i(t)\right)\right]^3 \cdot b^2}. \tag{12}$$

Discussion and Conclusion. The mathematical model of the flow of drilling mud through the shale shaker screen is a system of n equations (6) and n – 1equations (12).

The initial conditions for variables $h_i(0)$ cannot be taken as zero, since this will lead to division by zero in equations (12). Therefore, it is recommended to take these conditions as non-zero, but sufficiently small, e.g., $h_i(0) = 0.0001$.

Modeling of the system of equations (6) and (12) can be performed in simulating environments, such as MATLAB with the Simulink or SimInTech application. In any case, it is required to determine the number of nodal points of the chain calculation scheme in Figure 1. The throughput capacity of a shale shaker equipped with a particular screen is equal to the flow rate $Q_{1\ \text{зад}}$, at which the last 20–25% of the screen length would be free of drilling mud and used to dewater the sludge[4]. Therefore, the penultimate nodal point with a minimum number of these points should be at the same distance from the edge of the screen. This implies $\Delta x \approx 0.15 \cdot L$, what the seven nodal points correspond to.

In this work, the task was to determine the steady-state flow of the drilling mud, or more precisely, its profile. The author was forced to use the transient process of this flow, since it was impossible to establish the left boundary condition $h_1(\infty)$, instead of which an indirect assignment of this boundary condition $Q_1(t) = Q_{1\ \text{зад}}$ was used. The final number of nodal points is determined only in the process of modeling based on the accuracy of the drilling mud profile. For this purpose, the simulation of mathematical models (6) and (12) with n and n + 1 nodal points is performed. If the greatest difference in the flow profiles exceeds, e.g., 5% of the value of the mud layer height at this point, then the number of nodal points is increased by one to n + 2 [22]. Then, a simulation is performed with n + 2-nd node points and the flow profiles of this simulation are compared to the result of the previous simulation with n + 1 points. Upon reaching the specified error, the mathematical model with the latest value of the number of node points is used in the future.

The obtained mathematical model of the drilling mud flow along the shaker screen, together with the previously obtained mathematical model of the specific throughput capacity of the screen for specific drilling mud [8], makes it possible to reasonably recommend the installation of a screen with certain cell sizes for various costs of drilling mud flowing from the well mouth.

[4] *American Association of Drilling Engineers Shale Shakers and Drilling Fluid System.* Houston: Gulf Publishing Company; 1999. 335 p.

References

1. Pletnev NS, Semenov NV. Analysis of Standard Designs of Vibrating Screens and Features of Their Operation. In: *Proc. All-Russian Conference with International Participation with Elements of a Scientific School "Modern Problems of Hydrogeology, Engineering Geology and Hydrogeoecology of Eurasia"*. Tomsk: TPU Publ.; 2015. P. 632-635. (In Russ.) URL: https://earchive.tpu.ru/bitstream/11683/18336/1/conference_tpu-2015-C109-118.pdf (accessed: 29.04.2024).

2. Bulatov AI, Proselkov YuM, Shamanov SA. *Drilling Technique and Engineering of Oil and Gas Wells*. Moscow: Nedra; 2003. 1007 p. (In Russ.) URL: https://www.geokniga.org/bookfiles/geokniga-bulatov-ai-proselkov-yum-shamanov-sa-tehnika-i-tehnologiya-bureniya-neftyanyh-i-.pdf (accessed: 20.05.2024).

3. Ryazanov AYa. *Encyclopedia of Drilling Fluids*. Orenburg: Letopis'; 2004. 664 p. (In Russ.) https://search.rsl.ru/ru/record/01002873248 (accessed: 20.05.2024).

4. Sansiev VG. Hydrodynamic Principles of the Drilling Mud Screening Process. *Oil and Gas Studies.* 2009;75(3):41–46.

5. Sansiev VG. Modeling of Coal Sludge Classification and Dehydration Processes on Screen. *Mining Informational and Analytical Bulletin.* 2013;(7):325–335.

6. Golovin MV, Dobik AA, Kortunov AV, Mishchenko VI. Modern Development Trends of Shale Shakers for Drilling Mud Cleaning. *Drilling and Oil*. 2014;(3):50–52. URL: https://burneft.ru/archive/issues/2014-03/14 (accessed: 20.05.2024).

7. Kichkar YuE, Kichkar IYu, Miller AS. *Estimation of Vibration Screens Nets Specific through Capacity*. RF Patent No. 2379127 C 1. 2010. 8 p. URL: https://patents.s3.yandex.net/RU2379127C1_20100120.pdf (accessed: 20.05.2024).

8. Kichkar YuE, Kichkar IYu. A Study of the Frame Vibration Parameters Influence on a Vibrating Screen Specific Capacity. *Automation, Telemechanization and Communication in Oil Industry.* 2017;(8):37–40.

9. Penagos HP, Gantiva ME, López JAA. Detection of Failures in the Operation of Shale Shaker Machines for the Separation of Solids In: *Proc. 3rd International Conference on Electrical, Computer, Communications and Mechatronics Engineering (ICECCME)*. New York City: IEEE; 2023. P. 1–6. https://doi.org/10.1109/ICECCME57830.2023.10253357

10. Zhipeng Lyu, Sizhu Zhou. Design of Spatial Lissajous Trajectory Vibrating Screen. In book: Jianrong Tan (ed). *Advances in Mechanical Design*. Singapore: Springer; 2020. P. 493–498. https://doi.org/10.1007/978-981-32-9941-2_40

11. Kichkar YuE, Kichkar IYu, Posmitnaya LA. *Method of Vibrating Sieve Drives System Control.* RF Patent No. 2649203. 2018. 14 p. URL: https://patents.s3.yandex.net/RU2649203C1_20180330.pdf (accessed: 20.05.2024).

12. Osadolor AO, Bashir ME, Osifo TI. Development and Evaluation of a Small-Scale Shale Screening Machine. *Nigerian Journal of Scientific Research.* 2022;21(1):72–78.

13. Korostelkin AA, Filintsev AA, Novokshonov VV, Nikitin AV. On Shale Shaker's Structural Optimization and Performance Improvement. *IOP Conference Series: Materials Science and Engineering.* 2020;986(1):012058. https://doi.org/10.1088/1757-899X/986/1/012058

14. Kalinin AV. Dependence of the Chézy Coefficient from Froud Number. *Journal of Science and Education of North-West of Russia*. 2019;5(3):38–56.

15. Vasileva TN, Aronov LV. The Mathematical Model of the Long-Distance Transmission Circuits Operating Regimes. *Herald of Ryazan State Agrotechnological University Named after P.A. Kostychev.* 2012;14(2):51–54. URL: https://vestnik.rgatu.ru/archive/2_2012.pdf?ysclid=lwz0apyfjj690751007 (accessed: 20.05.2024).

16. Meshalkin VP, Chionov AM. Computer Modeling of the Long Multilayer-Insulated High-Pressure Subsea Gas Pipeline. *Matematicheskoe modelirovanie*. 2017;29(8):110–122. URL: https://www.mathnet.ru/php/archive.phtml?wshow=paper&jrnid=mm&paperid=3880&option_lang=eng (accessed: 20.05.2024).

17. Blekhman II. *Theory of Vibration Processes and Devices. Vibration Mechanics and Vibration Engineering*. St. Petersburg: Publ. House "Ruda i metally"; 2013. 640 p. (In Russ.)

18. Kulikov VO, Breido IV. Skipping Resonant Frequencies of Vibrating Screen Using Mitsubishi Electric FR A800 Series Frequency Converter. *Science: Present and Future*. 2019;1:222–226. (In Russ.) URL: http://elib.kstu.kz/fulltext/temat/2019/elibrary_41177383_25140206.pdf

19. Bulatov AI. System Analysis of Current Research Visco-Plastic Liquid – Clay and Cement Mortars (Part 1). *Drilling and Oil*. 2016;(3):18–23. URL: https://burneft.ru/archive/issues/2016-03/18 (accessed: 20.05.2024).

20. Baigaliev BE, Gortyshov YuF, Samoilenko A. Investigation of the Slope Influence on Hydraulic Resistances of Trapezoidal Channels. *Vestnik of Tupolev KNRTU*. 2012;(2):35–43.

21. Abdyukova RYa, Habibullin MYa. Calculation of Geometric Dimensions of a Mud Pump Valve and Determination of the Plate Lifting Height. *Equipment and Technologies for Oil and Gas Complex*. 2015;(5):15–18.

22. Meretukov ZA, Zaslavets AA, Koshevoi EP, Kosachev VS. Methods of Solving Differential Equations of Hydrodynamics. *New Technologies*. 2012;(1):36–41.

About the Author:

Ilia Yu. Kichkar, Cand.Sci. (Eng.), Associate Professor of the Production Automation Department, Institute of Computer Systems and Information Security, Kuban State Technological University (2, Moskovskaya Str., Krasnodar, 350072, Russian Federation), SPIN-code, ORCID, ResearcherID, kichkar@ya.ru

Conflict of Interest Statement: **the author claimed no conflict of interest.**

The author has read and approved the final version of manuscript.

Об авторе:

Илья Юрьевич Кичкарь, кандидат технических наук, доцент кафедры автоматизации производственных процессов института компьютерных систем и информационной безопасности Кубанского государственного технологического университета (350072, Российская Федерация, г. Краснодар, ул. Московская, 2), SPIN-код, ORCID, ResearcherID, kichkar@ya.ru

Конфликт интересов: **автор заявляет об отсутствии конфликта интересов.**

Автор прочитал и одобрил окончательный вариант рукописи.

Received / Поступила в редакцию 27.05.2024
Reviewed / Поступила после рецензирования 19.06.2024
Accepted / Принята к публикации 28.06.2024

INFORMATION TECHNOLOGY, COMPUTER SCIENCE AND MANAGEMENT
ИНФОРМАТИКА, ВЫЧИСЛИТЕЛЬНАЯ ТЕХНИКА И УПРАВЛЕНИЕ

Check for updates

UDC 004.05
https://doi.org/10.23947/2687-1653-2024-24-3-255-263

Original Theoretical Research

Quality Management in Software Development

Martin D. Birulia
EPAM Systems Sp z o.o., Kraków, Republic of Poland
✉ martinbirulia@gmail.com

EDN: JBGRGQ

Abstract

Introduction. The scientific literature examines various approaches to quality management in information technology (IT). The issues of identifying and correcting defects are worked out, and the possibilities for minimizing them are shown. There are materials on quality management in complex engineering processes. At the same time, there is no detailed description of quality management at each stage of the IT product life cycle, including testing. It should be noted that the coordination of software releases is closely related to quality management, but this process is rarely or fragmentarily considered in the literature. Additionally, the interprocess communication is not taken into account; therefore, there is no comprehensive understanding of quality management in the creation, testing and refinement of software. This study is designed to fill these gaps. The research is aimed at presenting a comprehensive approach that links the theory, practice and methods of software quality management.

Materials and Methods. Theoretical and applied literature on the subject were studied, analyzed, and reviewed. The author's professional experience in managing the quality of IT products was used. The practices of global suppliers of digital goods and services were taken into account. The author has used these materials and methods to study in detail the issues of software testing and code deployment.

Results. A comprehensive model of quality management in software development is elaborated, described and presented in the form of a diagram. Its interconnections with the project management model and the product life cycle, namely: analysis, design, development, testing, deployment, and support, are identified. Principles of quality management at each of these stages are specified. The processes and checks during code deployment are systematized and presented in the form of a diagram. Their features are shown in three environments: during development, testing, and production. The algorithm allows quality experts to build the sequence of actions to eliminate detected defects in the future, understand the situation when it is possible (or impossible) to deploy code and determine the moment when the software should be transferred to the user. In addition, the proposed scheme can be the basis for automating code deployment. The solution will reduce development time. As a result, the product will enter the market faster, which will speed up the payback of costs.

Discussion and Conclusion. The implementation of the model created within the framework of this scientific work into the production practice of IT companies presupposes strategic changes. Their implementation requires significant time and other resources; therefore, the overall transformation process should be divided into parts. The proposed approach is adaptable to the needs of different organizations and products. You can work with individual components to create an optimal plan for achieving quality management goals.

Keywords: code deployment, quality management in IT, IT product life cycle, IT product testing, software release

Acknowledgments. The author appreciates the leading software development organizations, such as EPAM Systems, Amazon, and Google, for their practices, which were analyzed under the preparation of this article. Special thanks to Project Management Institute for updating approaches to project management.

For Citation. Birulia MD. Quality Management in Software Development. *Advanced Engineering Research (Rostov-on-Don).* 2024;24(3):255–263. https://doi.org/10.23947/2687-1653-2024-24-3-255-263

Оригинальное теоретическое исследование

Управление качеством при разработке программного обеспечения

М.Д. Бируля
EPAM Systems, г. Краков, Республика Польша
✉ martinbirulia@gmail.com

Аннотация

Введение. В научной литературе рассматриваются разные подходы к менеджменту качества в сфере информационных технологий (ИТ). Проработаны вопросы выявления и исправления дефектов, показаны возможности их минимизации. Есть материалы об управлении качеством в сложных технологических процессах. Доказано, что работа с качеством цифровых продуктов требует в числе прочего прояснения вопросов качества кода. При этом нет детального описания управления качеством на каждом этапе жизненного цикла ИТ-продукта, включая тестирование. Отметим, что координация релизов (выпусков) программного обеспечения тесно связана с управлением качеством, однако данный процесс редко или фрагментарно рассматривается в литературе. К тому же не учитывается взаимодействие процессов, поэтому нет комплексного представления об управлении качеством при создании, тестировании и доработке программного обеспечения (ПО). Данное исследование призвано восполнить указанные пробелы. Его цель — представить комплексный подход, связывающий теорию, практику и методы управления качеством ПО.

Материалы и методы. Исследована, проанализирована и отреферирована профильная теоретическая и прикладная литература. Задействован профессиональный опыт автора в управлении качеством ИТ-продуктов. Учтены практики глобальных поставщиков цифровых товаров и услуг. Автор использовал эти материалы и методы для детальной проработки вопросов тестирования ПО и развертывания кода.

Результаты исследования. Сформирована, описана и представлена в виде схемы комплексная модель управления качеством при создании ПО. Выявлены ее взаимосвязи с моделью менеджмента проектов и жизненным циклом продукта, а именно: анализом, дизайном, разработкой, тестированием, развертыванием и поддержкой. Указаны принципы управления качеством на каждой из этих стадий. Систематизированы и представлены в виде схемы процессы и проверки при развертывании кода. Показаны их особенности в трех средах: при разработке, тестировании и производстве.

Обсуждение и заключение. Алгоритм позволяет специалистам по качеству выстроить последовательность действий для исключения в будущем выявленных дефектов, понимания ситуации, когда можно (или нельзя) развертывать код и определения момента, когда следует передать ПО пользователю. Кроме того, предложенная схема может быть базой для автоматизации развертывания кода. Решение позволит сократить время на разработку. Как следствие, продукт быстрее выйдет на рынок, что ускорит окупаемость затрат. Внедрение в производственную практику ИТ-компаний модели, созданной в рамках данной научной работы, предполагает стратегические изменения. Их реализация требует значительных затрат времени и других ресурсов, поэтому общий процесс трансформаций следует разбить на части. Предложенный подход адаптируется под нужды различных организаций и продуктов. Можно работать с отдельными компонентами, чтобы создать оптимальный план для достижения целей по управлению качеством.

Ключевые слова: развертывание кода, управление качеством в ИТ-сфере, жизненный цикл ИТ-продукта, тестирование ИТ-продукта, релиз программного обеспечения

Благодарности. Автор выражает благодарность ведущим организациям в сфере разработки программного обеспечения — EPAM Systems, Amazon и Google за их практики, которые анализировались при подготовке статьи. Особая благодарность компании Project Management Institute за обновление подходов к управлению проектами.

Для цитирования. Бируля М.Д. Управление качеством при разработке программного обеспечения. *Advanced Engineering Research (Rostov-on-Don)*. 2024;24(3):255–263. https://doi.org/10.23947/2687-1653-2024-24-3-255-263

Introduction. Within the conditions of high competition on the software market, users focus not only on the marketing but also on the product utility, pay attention to the user-friendly interface, efficiency, and operational stability. All this should be taken into account by manufacturers and divisions of software companies that work with quality. There are enough theoretical and applied publications devoted to quality management and automation of these processes in open access. The authors consider innovations in this sphere, compare them with traditional practices.

Defect handling (specifically, their early detection and analysis) allows preventing errors at the software development stage. This approach reduces time, money and other resources spent on fixing logical, syntactic, compilation and other software errors. The quality of the product is improved, and its value in terms of reliability, ease of maintenance, and cost-effectiveness is increased [1]. In [2], quality management in complex processes is described. The author shows how to identify the relationship between technology and quality. According to his assumption, there is an information correspondence between probabilistic models of technology and quality. It is known from [3] that in the information technology (IT) sector, a 49% increase in budget leads to the creation of new quality management models. As an example, we can mention the ISO/IEC standards [4]. In [5], it is shown how quality management affects manufacturing processes.

An important and complex task is to automate the control of processes on which quality depends. The key form of control is statistical. It works with indicators that are critical to quality of the endproduct. These indicators are monitored and compared to target values. As a result, a conclusion about the statistical controllability or uncontrollability of the process is obtained [6].

Software development lifecycle analysis is covered in numerous sources, but there is no detailed description of managing each stage of the lifecycle, including testing [7].

A separate line of research is the relationship between the basic quality management tools and their impact on the operational, financial and market performance of the manufacturing company. At the same time, integrated use and management of such tools is an urgent task [8].

In [9], it is shown how different quality management practices affect innovation in ISO 9001 certified companies. Some studies focus on the incorporation of practice guidelines in product life cycle development. It is known from [10] that 60–80% of potential errors in innovative product development are related to misunderstood requirements. The authors of [11] argue that when discussing product quality, the issues of code quality, cost of achieving a given quality, and time to enter the retail market should be clarified. Continuous integration (or continuous delivery) of program code plays a special role in quality automation [12]. This is the process that provides continuous updating of the code during the development of a software product. In [13], recommendations are given on how to take into account the level of competition in the industry when releasing new versions of a product sequentially.

Each of these papers considers different elements of quality management. At the same time, the system and structural interprocess communication is overlooked. As a result, there is no comprehensive view of quality management in software development, testing and revision. This study is aimed at filling this gap. It describes an integrated approach linking theory, practice and methods of quality management in the IT project. It should also be noted that due to the flexibility of the proposed model it can be adapted to the needs of a particular manufacturer.

Role of Quality Management in Software Development. Quality is a complex category that can be considered from different standpoints: philosophical, social, engineering, economic, legal [1]. In this article, quality is discussed as a set of properties of a product or service that can, to one degree or another, satisfy the needs of the target audience [3]. The product is considered as the total result of different types of activities, and each has its own input data (parameters), which, upon the production process, turn into output (value). The product is a set of values. It is designed to meet needs that are determined in advance, during the marketing development of a product or service. The quality of the product is judged by how much the actual consumer satisfaction coincides with the planned one.

In the information technology, two groups of product requirements (user needs) are considered the basic ones: functional and non-functional. As on any market, in the retail sale of IT solutions, precisely structured work with value provides loyalty of the target audience, and therefore, increases the profitability of the release of software, applications and similar products.

Defective goods sold spoil the image of the manufacturer [8]. Negative feedback is spread online and in messengers. The loss of users leads to a deterioration in financial indicators. A quality crisis can result in the bankruptcy of the manufacturer.

In [6], it is shown that quality management through process management is associated with all five types of innovation. Let us list the factors that form them:

– new equipment and technologies;
– products with new properties;
– new raw materials;
– new production organization;
– new market channels.

Materials and Methods. The scientific research, whose results are summarized in the presented article, was based on the global practice of production and sale of software products and services. In addition, the literature devoted to the creation and promotion of IT solutions was studied. The theory has been correlated with the practice of the largest software developers. The theoretical part gives an idea of the specifics of different quality management methods. Examples of their practical use in product life cycle management are given. From this point of view, some approaches to project management are considered — flexible, cascade (second name — waterfall), and hybrid.

The organization and coordination of software releases is studied. It is closely related to quality management, but is rarely or fragmentarily considered in the literature.

The practice of implementing large projects is related to a well-studied theory of quality management. This allows us to determine precisely how large organizations use the theoretical basis to provide quality of the information products (and ultimately, their commercial success).

It should be noted that the author of this article is experienced in software products management, and his professional expertise was also used as research materials.

Types of software testing. As shown in [7], on the market (i.e., outside the manufacturing company), the perception of quality (as an element of competitive advantage) is determined in the process of product design, statistical control and feedback. The perception of quality within the company depends on what percentage of products pass all tests and ultimately do not require revision. This indicator is associated primarily with process management, and not with statistical control and feedback.

It is important that the elements of the system that affect quality are supported by senior management and aligned with human resource management. In addition, quality practices and indicators should be taken into account when setting up internal corporate relations, interaction with suppliers and other contractors.

Testing is performed to determine the quality of future and end products; therefore, it is important to understand what exactly is the object of tests. In this case, it is not enough to say: "product". This is too general a concept, it should be specified. Often, certain functional and non-functional requirements are imposed on the product. In the first case, we are talking about a set of functions that the system must perform in a certain way. Let us say, when typing an address, the corresponding page should appear in the browser bar. Selecting certain menu items on this page should lead to known results in advance. At the same time, there may be several website interaction scenarios — for example, for registered and unregistered users. Thus, most online resources, when registering, open up the opportunity to comment on posts, receive collections of materials, etc.

As the name implies, non-functional requirements are not related to the functions available to the user. However, they often provide the consumer with more significant benefits than functional ones. This could be a certain level of data protection, integrated analytics collection, compliance with legislation (e.g., on personal data protection).

Product compliance with functional and non-functional requirements is verified differently.

Figure 1 shows the functional requirements testing pyramid. Test types are ranked by importance, speed, cost, and success rate.

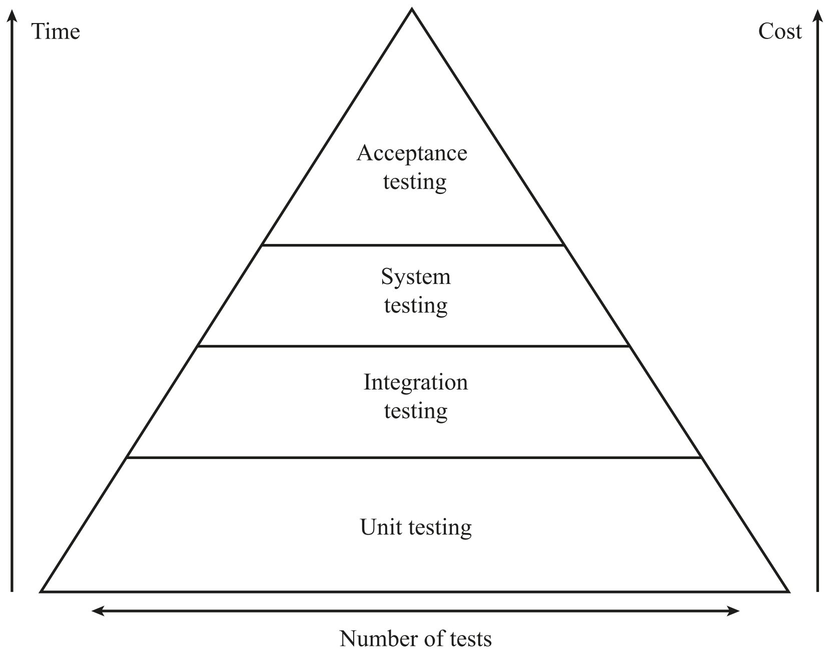

Fig. 1. Types of testing [14]

Unit testing, or modular testing, is a check of the correctness of individual modules of the program source code, individual functions of the application or service. This establishes whether the code is operational, whether it gives correct results with different inputs, and whether the logic matches the expected one. An example of such a test: when adding two numbers, their sum should be obtained — invariably. The input values required for testing are entered into the function. The unit test is passed if the expected result of the function is equal to the one actually obtained. The metric is calculated by comparing the number of lines of code that passed the test to the total number of lines of code in the repository. The best indicator is considered to be 80%. It shows that the logic of any function matches the expected one by 80% even before the next stage of testing starts. This means that problems are identified quite early and solved much cheaper and faster. Therefore, a unit test is the first step in the functional testing pyramid. Its absence (like any other type of testing) creates gaps, whose accumulation causes an unjustified increase in the cost of the project [15].

Integration testing. The next stage is testing the interaction of the components of the future application. The integration of modules is checked. These tests are more complex than unit testing, since the ability to perform sequential actions in various components is checked. Example: the user logs in — is redirected to the main page — places an ad. That is, several modules are tested at once. The basic options for integration testing are listed below.

"Big Bang". All components are assembled and tested together. This allows testing to be performed once after development. However, with a large number of modules, some may be overlooked, and this is the weak point of the method. In addition, the feedback loop increases, since ready-made solutions are tested when the development is complete. We should also note the difficulties with error localization. They are explained by the fact that it is necessary to analyze the entire development process (scenario) to find out the cause of the problem. This means that testing time will increase. The method is definitely convenient for small systems.

Incremental approach. Unlike the "big bang", this testing can start even if only two modules are ready for it, and add the rest as they are developed. In this case, it is easier to localize the initial errors, the feedback loop is shortened. There is no need to wait until all services are ready. This means that the testing will start and finish earlier. Removing defects will be cheaper. Incremental testing can be done in two ways: bottom-up and top-down.

Bottom-up integration. The least critical modules are tested first, then — the more important ones, and finally — the basic ones. Therefore, the upper components cannot be tested until there is data on the quality of the lower-level elements. This increases the time between the development and the start of testing.

Top-down integration. Testing starts with the most significant application layers. In this case, the testing of lower-level modules may not be completely adequate. However, even if this turns into problems later, they will be uncritical.

Hybrid integration. Modules of different levels are tested together. The success of such testing is determined by whether the developer understands the application architecture and can determine the optimal approach for a specific product [12].

System testing. All components of the program are tested as a single application. The specialist must ensure that the product correctly handles various scenarios and situations. This option may include testing non-functional requirements. This approach is based on requirements or on use cases. Whatever choices are made, the result will be test cases. Their successful completion confirms that the system works exactly as expected.

System testing requires considerable time, because as the product evolves, the number of possible use cases grows. Therefore, the software needs to be updated in a timely manner. This is done by the support service. With each product update, it is necessary to check whether the previously tested functions work. This process is called regression testing. If the tests worked before, but stopped working after the introduction of a new function, then there is a problem. The procedure of such checking sometimes takes up a huge amount of operation-use time for testing engineers, and they do not have time to write new tests. This explains the importance of automating tests that are performed manually. With this approach, testing is optimized to a simple analysis of the results of automatic checks. The best option is 100% automation. It is not always possible to achieve this figure, since some tests cannot be automated due to their complexity [16].

Acceptance testing. At the last stage, the product is tested by key specialists and customers. They check in real time to what extent their expectations and requirements have been met. It is determined if the functions work as intended, the interface is convenient, how likely errors and incorrect operations are, what problems the future user will face. As a result, the project is accepted or not accepted. Acceptance is the final stage of testing.

Fixing any bugs or defects found at this stage will be especially costly, since solving the problem will require going through the entire process from the very beginning, from development and unit testing to full system verification. Therefore, every effort should be made to avoid this situation at earlier stages. Non-functional testing checks the application for:

– performance;
– reliability;
– compatibility;
– security;
– utility;
– scalability.

More than 15 types of testing are used to check these properties. The most common ones are listed below.

Performance testing. The speed and efficiency of an application or system is assessed. The focus is on the speed of response to a user request. As an example, testing may include evaluating the loading time of the main page of a website. Performance targets are defined, and actual results are compared to them.

Load testing. This determines the maximum load a system can handle without failure or significant degradation in performance. Specifically, for a website, this means determining how many users can interact with the platform simultaneously before crashes or failures occur.

Fault tolerance testing. The ability of a system or application to remain operational during failures or unexpected situations is tested. The purpose of such testing is to detect vulnerabilities and develop measures to maintain continuous operation.

Compatibility testing. Compatibility of an application or system with other software, with different operating systems, browsers and devices is checked.

Security testing. The level of protection of a system or application from attacks and potential security threats is assessed. It is determined whether there are vulnerabilities. Protective mechanisms and the effectiveness of security measures are analyzed.

Disaster recovery testing. The ability of a system or application to recover from failures, crashes, or other emergencies is determined. The goal is to verify the effectiveness of recovery procedures and minimize downtime in the event of a disaster.

Research Results. Within the framework of the presented research, a comprehensive model of quality management in software development was formed. Its interrelations with the development life cycle, releases, costs, and the project management model (agile, waterfall or hybrid) were described.

Quality management process in the software development life cycle. Standard digital product development consists of six production processes, or stages. Each of them should contribute to quality assurance (Fig. 2).

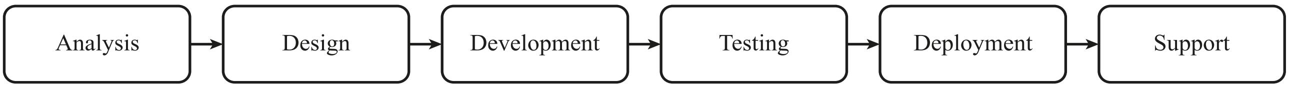

Fig. 2. Software Development Life Cycle [17]

Analysis and determination of product requirements. Problems are investigated, solutions are proposed taking into account the stated requirements. This process sets the key indicators for checking the endproduct. Depending on the development model, the strategy, approaches and testing tools are described and agreed upon. One of the documents is called “Product Vision and Capabilities”. It records the identified problems, notes the links with the business plan, describes the market situation, lists the main functional and non-functional requirements. The document is approved by the partner parties (i.e., representatives of the contractor and the customer). If necessary, adjustments are made to the text. At this stage, it is important to involve security and application architecture specialists who will help to accurately define non-functional requirements that are important for future testing.

Design of architectural and visual solution. Taking into account the requirements identified at the previous stage, an architectural solution is developed to provide their implementation, and the design of the user interface. All this is a guideline for the development team, who will test and, if required, adjust the product.

Development. Code is created to solve the tasks and problems of future users. Unit tests are written to check the logic of individual functions. The main goal is to achieve the required code coverage rate (at least 80%). However, other practices are also widely used, such as code reviews. In this case, the code is reviewed by other team members, and errors, shortcomings, omissions, and vulnerabilities are identified early in the development process. Reviewers can leave comments on specific lines of code, indicating the need for refactoring. In terms of product quality, the ideal scenario is dual code review, where at least two specialists unrelated to the author review and comment on the code.

In addition to unit testing and code review, it is necessary to use linters. These are automated tools that analyze code in real time, detect shortcomings, errors, and suggest ways to fix them. Other types of testing can be used depending on the strategy and requirements for the product.

Testing. Test engineers develop test scripts that are adequate to the tasks. As a rule, they are written manually, which slows down the implementation of this stage. It is advisable to automate the process, but this is not always possible. At this stage, specialists check and, if necessary, re-check the results of manual and automated tests. Particular attention is paid to cases where automated tests detect errors. The detected defects are ranked according to their importance to the system or users, and then are passed on to the developers for correction. After the defects are fixed, it is useful to perform a root-cause analysis (RCA) of the problem using the RCA method. This provides developing measures to prevent problems in the future, add new unit or integration tests. To fully understand the causes of the problem, it is recommended to use the “5 Why’s” technique. The method scheme looks like this: the problem is formulated and the question is asked: “Why did this happen?”. It is followed by an answer describing a certain fact or situation. The question is asked again: “Why did this happen?” And this is repeated five times. Five answers allow you to get closer to understanding the causes of the problem.

Testing is a large-scale process. The major stages are listed below.
1. Setting up and configuring the testing environment.
2. Writing and executing manual test scripts.
3. Automating previously written manual test scripts.
4. Checking the results of automated tests.
5. Maintaining up-to-date automated test scripts and fixing errors.
6. Recording defects.
7. Documenting defects.
8. Analyzing the causes of defects.
9. Developing steps to prevent future defects.

Deploying the application code. Software requires various environments for deployment. It is important to have a good understanding of how continuous integration and continuous deployment (CI/CD) maintain stable software quality with minimal effort. This is facilitated primarily by the automation of code deployment — the transfer of its changes from one environment to another. The process is divided into stages that depend on the product, organization, and accepted standards.

The degree of automation, the number and rigor of checks determine the expected quality of the product before the code is released to end users. Figure 3 shows a possible code deployment scheme. With a high level of automation, labor costs will be minimal, and only a few manual checks will have to be performed.

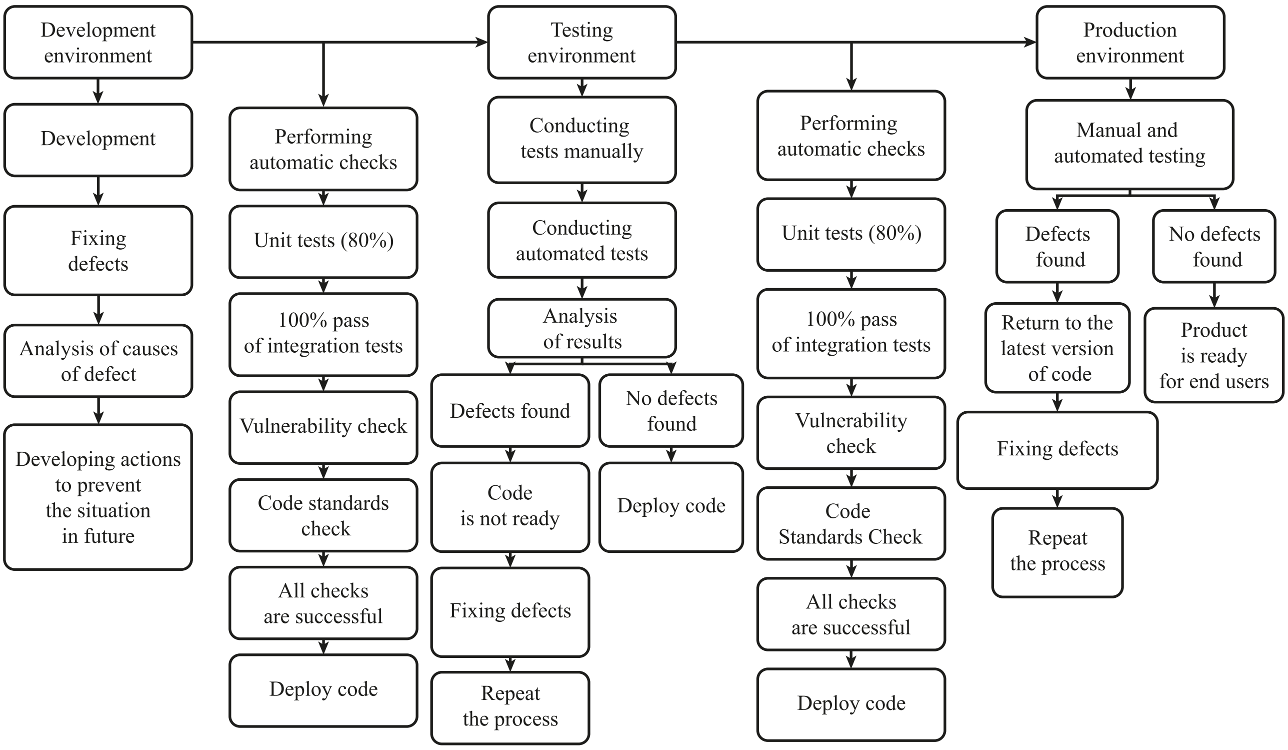

Fig. 3. Code Deployment Process and Checklist Diagram

Following the presented scheme, you can control the quality and automate the deployment of the code. This will reduce the development time, which means the product will enter the market faster.

Product support. At this stage, it is necessary to build feedback with users: conduct surveys, collect and analyze metrics. All this will be the basis for tasks and ideas for improving the software. Assumptions should be confirmed by A/B tests, i.e., comparison of product options. It is also important to provide feedback to the support team, which directly contacts users. These are the specialists who share valuable observations, convey wishes of the target audience, on the basis of which analysis is performed and new strategies are formed. Evidently, the process does not end even if the product is completely ready. New data appears for analysis, collection of requirements, and development of a digital product or service.

Discussion and Conclusion. The quality management model presented in this article can be adapted to the needs of various organizations and products. Its components can be further studied to create an optimal plan for achieving quality management goals. However, it is important to keep in mind the key factors for commercial software success: developers and testers must think critically, establish collaboration, and continuously improve processes.

The proposed model involves strategic changes, whose implementation requires a significant amount of time; therefore, the overall transformation process should be broken down into parts.

The presented material will be useful for management that administrates quality issues related to the company's overall strategy and optimization of individual processes.

It should be noted that achieving significant results requires a high degree of testing automation, a developed engineering culture, and significant costs for creating and maintaining infrastructure.

References

1. Suma V, Gopalakrishnan Nair TR. Defect Management Strategies in Software Development. In book: *Recent Advances in Technologies*. Vienna: Intec Web Publishers; 2009. P. 379–404. https://doi.org/10.48550/arXiv.1209.5573

2. Kuznetsov LA. Quality Management in Complex Processes. *Control Sciences.* 2007;(3):47–53.

3. Munoz M, Mejia J, Ibarra S. Tools and Practices to Software Quality Assurance: A Systematic Literature Review. In: *Proc. 13th Liberian Conference on Information Systems and Technologies* (*CISTI*). New York City: IEEE; 2018. P. 1–6. https://doi.org/10.23919/CISTI.2018.8399334

4. Carrozza G, Pietrantuono R, Russo S. A Software Quality Framework for Large-Scale Mission-Critical Systems Engineering. *Information and Software Technology.* 2018;102(3):100–116. https://doi.org/10.1016/j.infsof.2018.05.009

5. Vallabhaneni RS. Corporate Management, Governance, and Ethics Best Practices. Ch. 7. In book: *Quality-Management Best Practices*. Hoboken, NJ: Wiley; 2008. 456 p. https://doi.org/10.1002/9781119196662.ch7

6. Razmochayeva NV, Semenov VP, Bezrukov AA. Investigation of Statistical Process Control in Process Automation Tasks. In: *Proc. XII International Conference on Soft Computing and Measurements.* 2019;1:355–358. (In Russ.) URL: https://scm.etu.ru/assets/files/2019/scm2019/papers/7/355.pdf (accessed: 20.06.2024).

7. Nevlyudov ISh, Andrushevich AA, Evseyev VV. Software Development Life Cycle Analysis for Enterprise Information Systems. *Eastern European Journal of Enterprise Technologies.* 2010;6(8):25–27. (In Russ.)

8. Kaynak H. The Relationship between Total Quality Management Practices and Their Effects on Firm Performance. *Journal of Operations Management.* 2003;21(4):405–435. https://doi.org/10.1016/S0272-6963(03)00004-4

9. Dong-Young Kim, Vinod Kumar, Uma Kumar. Relationship between Quality Management Practices and Innovation. *Journal of Operations Management*. 2012;30(4):295–315. https://doi.org/10.1016/j.jom.2012.02.003

10. Ramasubbu N, Kemerer CF. Integrating Technical Debt Management and Software Quality Management Processes: A Normative Framework and Field Tests. *IEEE Transactions of Software Engineering*. 2019;45(3):285–300. https://doi.org/10.1109/TSE.2017.2774832

11. Alhassan A, Alzahrani W, AbdulAziz A. Total Quality Management for Software Development. *International Journal of Computer Applications.* 2017;158(5):38–44. URL: https://www.ijcaonline.org/archives/volume158/number5/alhassan-2017-ijca-912850.pdf (accessed: 20.06.2024).

12. Mohamed SI. Software Release Management Evolution — Comparative Analysis across Agile and DevOps Continuous Delivery. *International Journal of Advanced Engineering Research and Science*. 2016;3(6):52–59. URL: https://ijaers.com/detail/software-release-management-evolution-comparative-analysis-across-agile-and-devops-continuous-delivery/ (accessed: 20.06.2024).

13. Adelman D, Mancini A. Dynamic Release Management: A Market Intensity Approach. *Chicago Booth Research Paper*. 2016;(16–19):42. http://doi.org/10.2139/ssrn.2847264

14. Radziwill N, Freeman G. Reframing the Test Pyramid for Digitally Transformed Organizations. *Semantic Scholar*. URL: https://www.semanticscholar.org/reader/62a5c71b33437bc40e146a13a6fb95371b866262 (accessed: 22.06.2024).

15. Alves NSR, Mendes TS, Mendonca MG, Spinola RO, Shull F, Seaman C. Identification and Management of Technical Debt: A Systematic Mapping Study. *Information and Software Technology.* 2016;70(2):100–121. https://doi.org/10.1016/j.infsof.2015.10.008

16. Concas G, Marchesi M, Murgia A, Tonelli R, Turnu I. On the Distribution of Bugs in the Eclipse System. *IEEE Transactions on Software Engineering*. 2011;37(6):872–877. http://doi.org/10.1109/TSE.2011.54

17. Lemke G. The Software Development Life Cycle and Its Application. *Senior Honors Theses and Projects*. 589. Ypsilanti, MI: Eastern Michigan University; 2018. URL: https://commons.emich.edu/cgi/viewcontent.cgi?article=1588&context=honors (accessed: 22.06.2024).

About the Author:

Martin D. Birulia, project manager, EPAM Systems Sp z o.o. (114, Opolska Str., Krakow, 31–553, Poland), SPIN-code, ORCID, martinbirulia@gmail.com

***Conflict of Interest Statement:* the author claimed no conflict of interest.**

The author has read and approved the final manuscript.

Об авторе:

Мартин Дмитриевич Бируля, менеджер проектов EPAM Systems Sp z o.o. (Польша, 31–553, г. Краков, ул. Опольска, 114), SPIN-код, ORCID, martinbirulia@gmail.com

Конфликт интересов: **автор заявляет об отсутствии конфликта интересов.**

Автор прочитал и одобрил окончательный вариант рукописи.

Received / **Поступила в редакцию** 30.06.2024
Reviewed / Поступила после рецензирования 20.07.2024
Accepted / Принята к публикации 27.07.2024

INFORMATION TECHNOLOGY, COMPUTER SCIENCE AND MANAGEMENT
ИНФОРМАТИКА, ВЫЧИСЛИТЕЛЬНАЯ ТЕХНИКА И УПРАВЛЕНИЕ

UDC 004.032.26, 531.3
https://doi.org/10.23947/2687-1653-2024-24-3-264-273

Original Empirical Research

Determination of Dynamic Stresses and Displacements under the Action of an Impact Load on a Two-Layer Structure during the Indentation Process

EDN: VVRPYB

Natalia E. Babushkina ✉, **Alexandr A. Lyapin**
Don State Technical University, Rostov-on-Don, Russian Federation
✉ copybird@yandex.ru

Abstract

Introduction. Numerous researchers of the reliability of building structures pay attention to hardness, an important characteristic of the structural material. It is determined by indentation — pressing the tip of the tool into the surface. The advantages of dynamic indentation methods and the distribution of stress intensity on the surface and inside the sample are investigated. However, the condition of layered materials on impact has been poorly studied. The objective of the presented work is to consider indentation for a two-layer sample and determine the sensitivity of the top layer to the strength of the substrate. This will allow us to identify significant characteristics of the strength properties of homogeneous and heterogeneous structures.

Materials and Methods. An elastoplastic model of material behavior and a shock indentation scheme were used, which took into account the masses of the indenter and the striker coupled by linear springs. The surface of the indenter was conical, the opening angle was 120°. The impact was simulated in the MATLAB system. Finite element model in Ansys APDL was used to verify the data and analyze the results of the experiment. Traditional models of elasticity theory were used for calculations. The behavior of the material in the zone of plastic deformation was described using the options of multilinear isotropic hardening and the von Mises plasticity criterion.

Results. The results of comparing three versions of varying the level of yield strength in the bottom layer are presented: when the yield strength in the bottom layer is half as high as the top one, equal to it, and twice as high. Displacements at different observation points for samples with a top layer of 2 mm and 1 mm were analyzed. In the first case, under horizontal shear, the displacement indices inside the sample did not change if the yield strength level was twice lower or higher than in the top one. If these indicators were equal, the difference became noticeable. In the second case (layer 1 mm), the difference in displacement was visible at all observation points. Thus, it can be reasonably concluded that a structure with a smaller top layer is more sensitive to impact. In the course of the research, it became known that vibrations associated with the transition to the plasticity zone occurred in the 2 mm zone, and elastic damping vibrations occurred below this zone. We solved the classification problem for the top layer of the material with changing characteristics of the base. The indicator for comparison was the Brinell hardness (HB) in the range of 200–600. The results were processed using a neural network and visualized in the form of graphs. The accuracy of its calculations was 98%.

Discussion and Conclusion. To determine the strength properties of homogeneous structures, it is sufficient to characterize the speed of displacement inside the sample. For an inhomogeneous structure, additional parameters should be introduced — displacements on the surface and inside the sample at fixed observation points. An integrated approach to determining the strength properties of an inhomogeneous structure improves the accuracy of calculations, and the use of neural networks increases their speed.

Keywords: multilayer structure, layered material on impact, yield strength level, Brinell hardness, strength of heterogeneous structure

Acknowledgements. The authors would like to thank the Editorial board and the reviewers for their attentive attitude to the article and for the specified comments that improved the quality of the article.

For Citation. Babushkina NE, Lyapin AA. Determination of Dynamic Stresses and Displacements under the Action of an Impact Load on a Two-Layer Structure during the Indentation Process. *Advanced Engineering Research* (*Rostov-on-Don*). 2024;24(3):264–273. https://doi.org/10.23947/2687-1653-2024-24-3-264-273

Оригинальное эмпирическое исследование

Определение динамических напряжений и перемещений при действии ударной нагрузки на двухслойную конструкцию в процессе индентирования

Н.Е. Бабушкина ✉, **А.А. Ляпин**
Донской государственный технический университет, г. Ростов-на-Дону, Российская Федерация
✉ copybird@yandex.ru

Аннотация
Введение. Многие исследователи надежности строительных конструкций уделяют внимание твердости — важной характеристике конструкционного материала. Ее определяют индентированием — вдавливанием наконечника инструмента в поверхность. Исследуются преимущества методов динамического индентирования, распределение интенсивности напряжений на поверхности и внутри образца. Однако мало изучено состояние слоистых материалов при ударе. Цели представленной работы — рассмотреть индентирование для двухслойного образца и определить чувствительность верхнего слоя к прочности подложки. Это позволит выявить значимые характеристики прочностных свойств однородных и неоднородных конструкций.
Материалы и методы. Использовали упруго-пластическую модель поведения материала и схему ударного индентирования, которая учитывает массы индентора и ударника, сцепленных линейными пружинами. Поверхность индентора — коническая, угол раскрытия — 120°. Удар моделировали в системе Matlab. Конечноэлементную модель в Ansys APDL применили для верификации данных и анализа результатов эксперимента. Для расчетов взяли традиционные модели теории упругости. Поведение материала в области пластического деформирования описали с помощью опций мультилинейного изотропного упрочнения и критерия пластичности Мизеса.
Результаты исследования. Приводятся итоги сопоставления трех вариантов варьирования уровня предела текучести в нижнем слое: когда предел текучести в нижнем слое вдвое меньше верхнего, равен ему и вдвое больше. Проанализированы перемещения в разных точках наблюдения для образцов с верхним слоем 2 мм и 1 мм. В первом случае при горизонтальном сдвиге не меняются показатели перемещений внутри образца, если уровень предела текучести вдвое ниже или выше, чем в верхнем. При равенстве этих показателей разница становится заметной. Во втором случае (слой 1 мм) разница перемещений видна во всех точках наблюдения. Так можно обоснованно заключить, что конструкция с меньшим верхним слоем более чувствительна к ударному воздействию. В ходе изысканий стало известно, что в зоне 2 мм совершаются колебания, связанные с переходом в зону пластичности, ниже этой зоны — упругие затухающие колебания. Решили задачу классификации для верхнего слоя материала с меняющимися характеристиками основания. Показатель для сравнения — твердость по Бринеллю (HB) в диапазоне 200–600. Результаты визуализировали в виде графиков и обработали с помощью нейросети. Точность ее вычислений составила 98 %.
Обсуждение и заключение. Для определения прочностных свойств однородных конструкций достаточно характеристики скорости перемещения внутри образца. Для неоднородной структуры необходимо вводить дополнительные параметры — перемещения на поверхности и внутри образца в фиксированных точках наблюдений. Комплексный подход к определению прочностных свойств неоднородной конструкции повышает точность расчетов, а использование нейросетей — их скорость.

Ключевые слова: многослойная конструкция, слоистый материал при ударе, уровень предела текучести, твердость по Бринеллю, прочность неоднородной конструкции

Благодарности. Авторы выражают благодарность редакции и рецензентам за внимательное отношение к статье и замечания, которые позволили повысить ее качество.

Для цитирования. Бабушкина Н.Е., Ляпин А.А. Определение динамических напряжений и перемещений при действии ударной нагрузки на двухслойную конструкцию в процессе индентирования. *Advanced Engineering Research* (*Rostov-on-Don*). 2024;24(3):264–273. https://doi.org/10.23947/2687-1653-2024-24-3-264-273

Introduction. When designing and operating building structures, strict requirements are specified to their strength and reliability [1]. The literature discusses the issues of reliability of the structure [2], as well as the preservation of its operational properties throughout its entire service life [3].

From an engineering point of view, hardness is one of the important material specifications. It is associated with mechanical properties, such as yield strength, tensile strength, endurance, etc. Hardness of the material is determined by pressing the tip of the tool into the surface. There is a distinction between static and dynamic indentation. The static indentation test involves the indentation of a solid indenter into a flat and smooth surface of a soft material (target), whose mechanical properties are determined by the measured dependence of the applied load on the depth of penetration. Static methods do not allow us to evaluate the physicomathematical characteristics of the material under dynamic loading conditions [4]. Dynamic indentation methods are used for this purpose [5].

GOST R 56474–2015[1] presents dynamic indentation as the introduction of an indenter into material under the action of a single shock pulse created by a special acceleration device or gravity. This approach applies to non-destructive testing methods. Their basic principle is safe inspection, determination of the integrity, and basic working properties of the object [6]. The primary advantage is the ease of use.

Indentation testing is a complex process that includes contact mechanics, material nonlinearity, and fracture mechanics. For general cases, it is very difficult to obtain analytical solutions. Therefore, the understanding of the processes under consideration is based mainly on experiments and finite element modeling.

Elastic contact was first studied by G. Hertz [7] at the end of the XIX century. He tried to find an accurate definition of hardness using an elastic process. Later, J.V. Boussinesq developed a method based on potential theory for calculating stresses and displacements in an elastic body loaded with any rigid axisymmetric indenter. As for the depressions associated with plastic deformation, early research focused on yield strength and tensile strength.

Publications pay attention to the methods of dynamic indentation to determine the strength properties of structures. Thus, N.N. Avtonomov and A.V. Tololo considered the problem of pressing a spherical indenter into an elastoplastic material [8]. The authors analyzed the distribution of stress intensity on the surface and inside the sample. Thus, it became known that the zones of maximum intensity are located at a short distance from the contact zone of the indenter and the sample, and expand with increasing load.

Foreign authors [9] have developed a method of dynamic indentation, which consists in measuring the depth and reaction to the load of the sample during the indentation process. To determine the depth, a displacement measurement method based on moire interferometry was used. The load was measured with a quartz sensor. The results of numerical simulation by the finite element method indicated that this approach was in good agreement with the values obtained using traditional methods for determining the strain rate.

Scientists considered strength properties of materials in the indentation process. Many papers are devoted to this, for example [10]. The study of the behavior of the "target" under the mechanical loads plays a key role in the development of new materials, structures and products [11]. Comprehensive research makes it possible to solve the problems of optimizing operating procedures, providing the reliability of structures, and preventing failures in their operation.

The solutions obtained open up the possibility of creating more efficient and sustainable structures [12], which determines the relevance of research in this direction. At the same time, the issue of the state of layered structures under impact is still insufficiently studied.

The work is aimed at analyzing stresses and displacements in a two-layer structure and identifying the sensitivity level of the top layer of the sample to the strength of the substrate. The study will allow us to establish significant characteristics for determining the strength properties of homogeneous and heterogeneous structures.

Materials and Methods. The diagram of the impact indentation device is shown in Figure 1.

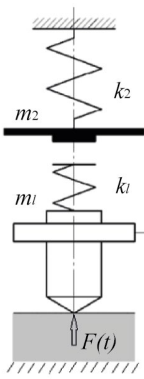

Fig. 1. Diagram of the impact indentation device

[1] GOST R 56474–2015. Space Systems. Non-destructive Testing of Physical and Mechanical Properties of Space Technique's Materials and Coatings by Dynamic Indentation. General Requirements. *Electronic Fund of Legal and Regulatory Documents*. URL: https://docs.cntd.ru/document/1200122009 (accessed: 14.05.2024).

The system of differential equations corresponding to the dynamics of the mechanical elements of the shock indentation device has the form:

$$m_1\ddot{x}_1 = k_1\left(x_2 - x_1\right) - F\left(t\right),$$
$$m_2\ddot{x}_2 = -k_2x_2 - k_1\left(x_2 - x_1\right). \qquad (1)$$

This is how the oscillatory process of a dynamic system with two masses is described: m_1 — mass of the indenter; m_2 — mass of the striker. The masses are coupled by linear springs with stiffness k_1 and k_2, respectively [13]. The values of vertical displacements $x_1(t)$, $x_2(t)$ as degrees of freedom of massive elements are unknown in time. The striker was cocked to height ***h*.** After descending, at the moment of contact with the indenter, he reached the speed

$$v_{20} = \sqrt{2gh + \frac{k_2h^2}{m_2}}.$$

Thus, the initial conditions should be added to the system (1):

$$x_1\left(0\right) = 0, \dot{x}_1\left(0\right) = 0, x_2\left(0\right) = 0, \dot{x}_2\left(0\right) = v_{20}. \qquad (2)$$

Value $F(t)$ of the resistance force from the injected material is unknown.

We assume that the surface of the indenter is conical with opening angle α = 120 degrees. Therefore, it is required to use an elastic-plastic model of the behavior of the test material. At the apex of the cone, the onset of impact and plastic deformation coincides.

The impact process was modeled in the MATLAB system. This made it possible to select the mechanical parameters of the installation. A finite element model in the Ansys APDL environment was used to verify the data and analyze the results of the experiment. A two-layer construction was considered. Its displacements and stresses arising in a two-layer sample under the action of a dynamic load were analyzed. Traditional models of elasticity theory were used in the calculations. To describe the behavior of the material in the zone of plastic deformation, the options of multilinear isotropic hardening and the von Mises plasticity criterion were used:

$$f\left(\sigma, \sigma_y\right) = \sigma_e - \sigma_y = 0. \qquad (3)$$

where σ_e — von Mises equivalent stress, $\sigma_e = \sqrt{\frac{3}{2}\left(\sigma : \sigma - \frac{1}{3}tr\left(\sigma\right)^2\right)}$, σ_y — uniaxial yield strength.

To control the convergence accuracy, a finite element grid was pre-selected. When studying the parameters of a two-layer structure, we considered three options for varying the level of yield strength in the bottom layer in three cases — when the yield strength in the bottom layer is half as high as the top one, equal to it, and twice as high (Table 1).

Table 1

Structure and Parameters of the Studied Structures

No.	Level of yield strength in the bottom layer relative to the top one (strength coefficient K)	Level, mm	
		top	bottom
1	1/2	1	9
2	1		
3	2		
4	1/2	2	8
5	1		
6	2		

A detailed analysis of the displacements at different observation points clearly shows the difference in the nature of displacements in the zone of plastic deformations. To study the displacements, the following scheme was selected (Fig. 2). The top layer of the structure was highlighted in a darker gray color for clarity.

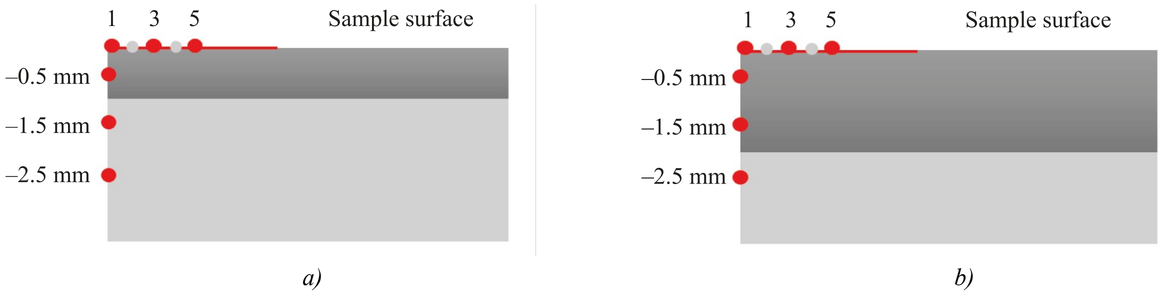

Fig. 2. Determination of points for measuring vertical and horizontal displacements: *a* — construction with a top layer of 1 mm; *b* — construction with a top layer of 2 mm. Numbers 1, 3 and 5 indicate the level of yield strength in the bottom layer relative to the top one in accordance with Table 1

Research Results. Figure 3 shows a comparative characteristic of the displacement level on the sample surface with a horizontal shear of the observation point from the impact point.

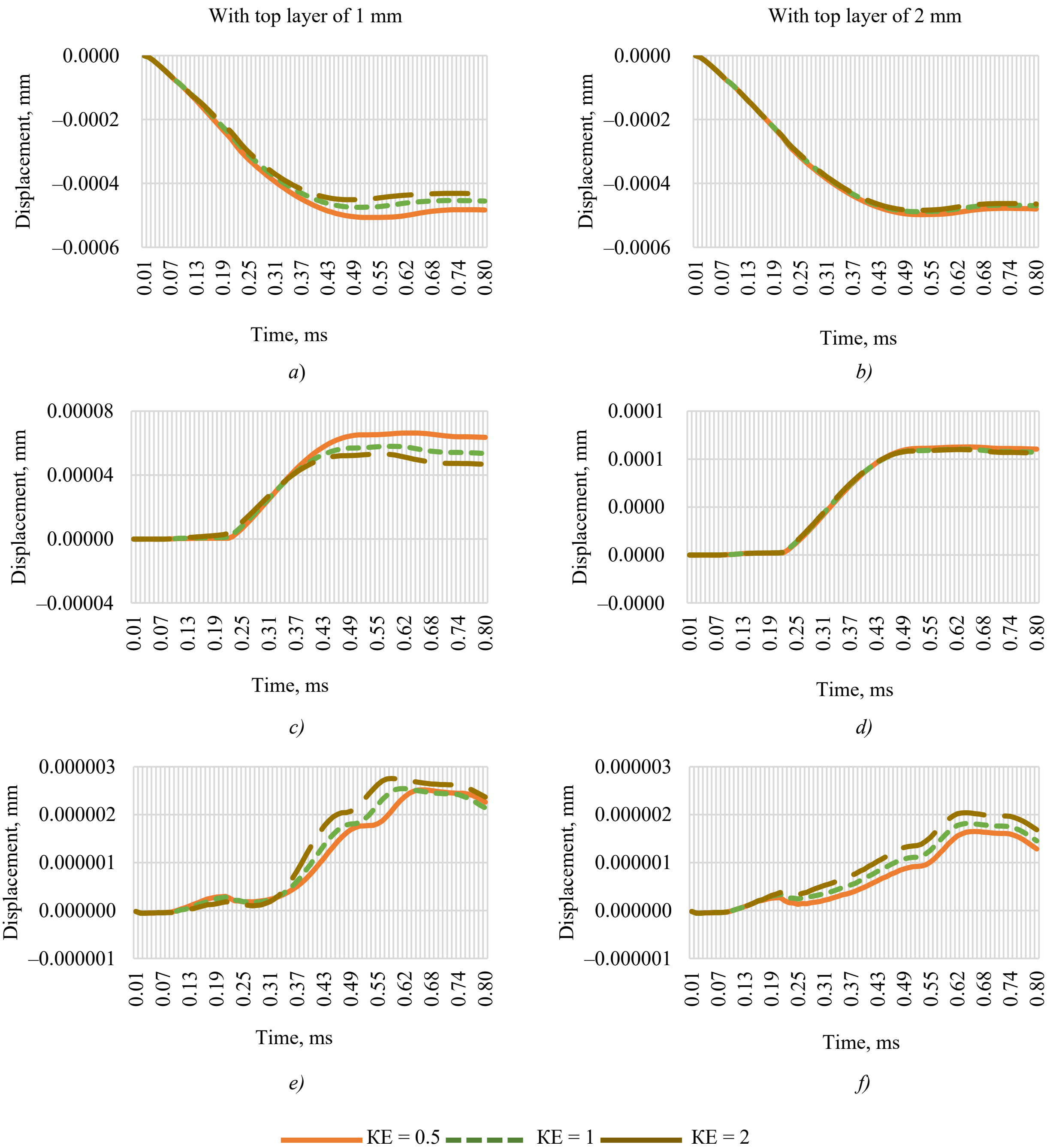

Fig. 3. Displacements on the sample surface at various contact points: *a*, *b* — at the 1st contact point; *c*, *d* — at the 3rd point on the surface; *e*, *f*, — at the 5th point on the surface

Evidently, for a two-layer structure with a top layer of 2 mm, a change in the yield level at the 1st and 3rd contact points during horizontal shear does not affect the displacement parameters inside the sample. At the 5th point, the difference becomes noticeable. For a structure with a top layer of 1 mm, the difference in the level of displacement is noticeable at all observation points. It can be concluded that a structure with a smaller top layer is more sensitive to impact.

Figure 4 shows the distribution of stress intensity at different levels of the top coating. These data suggest that fluctuations associated with the transition to the plasticity zone occur in the 2 mm zone, and elastic vibrations that fade over time occur below this zone.

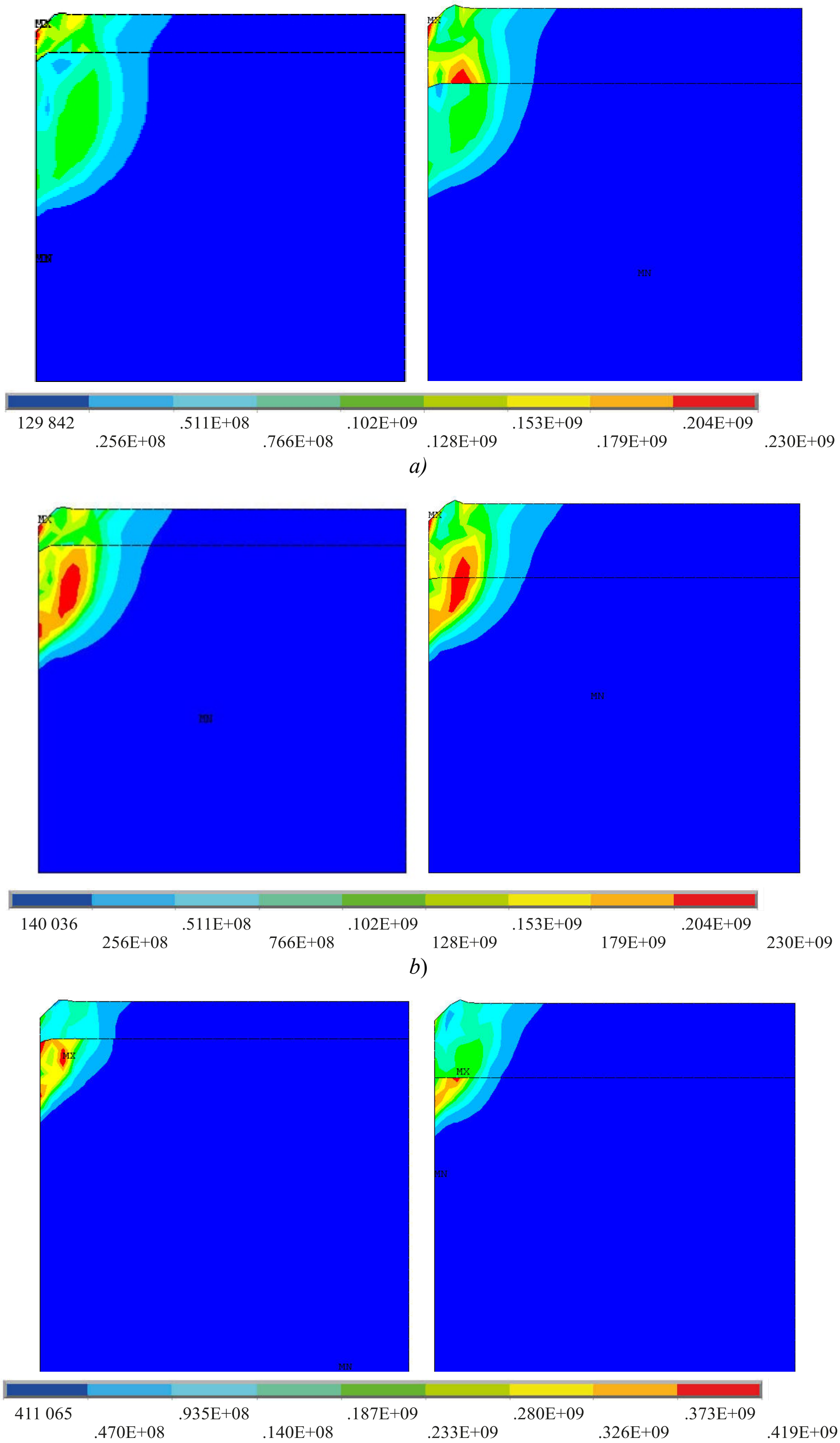

Fig. 4. Stress intensity at different values of strength coefficient K, MPa: *a* — K = 0.5; *b* — K = 1; *c*— K = 2

Figure 5 shows graphs of stresses on the surface at various observation points.

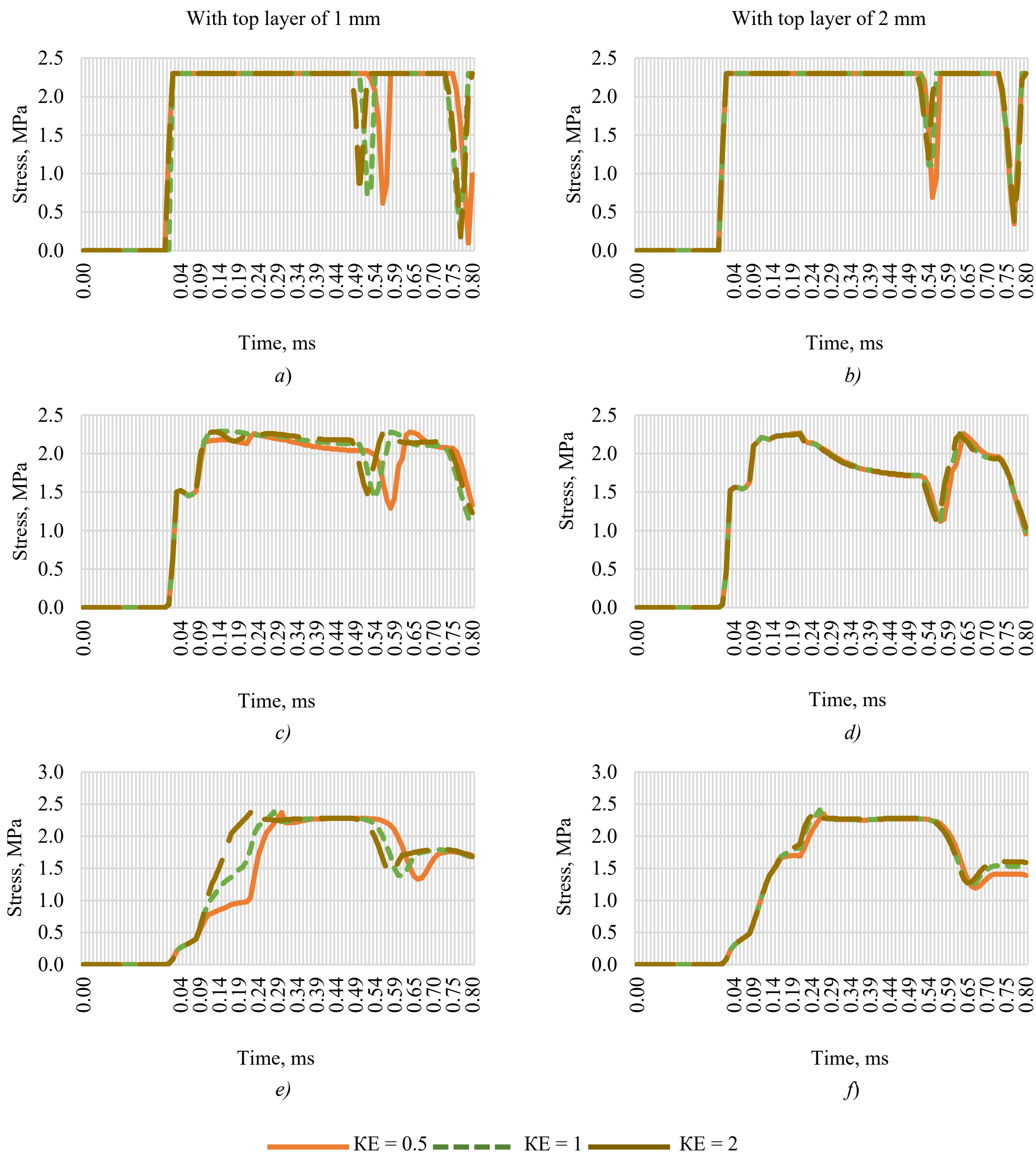

Fig. 5. Stresses on the sample surface at various contact points: *a*, *b* — at the contact point; *c*, *d* — at the 3rd point on the surface; *e*, *f*, — at the 5th point on the surface

To analyze the influence of the base on the strength properties of the sample, the problem of classification [13] by the value of Brinell hardness (HB) of the top layer of the material with varying characteristics of the base was solved. Within the framework of the study, five classification groups were identified (Table 2).

Table 2

Classification Groups

No.	Group	Value of HB
1	I	200
2	II	300
3	III	400
4	IV	500
5	V	600

The calculated values obtained using a mathematical model were fed to the input of a neural network. Figure 6 shows the values of speeds and displacements for the selected hardness groups.

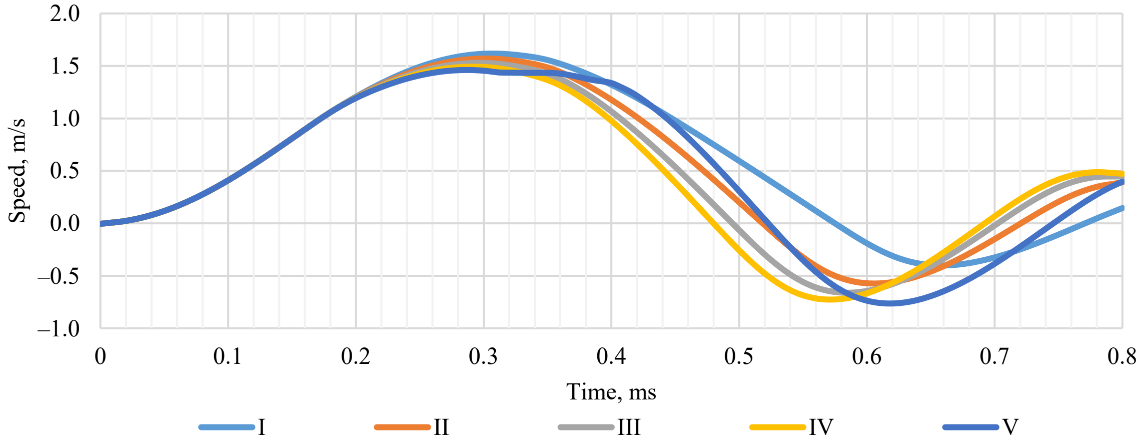

a)

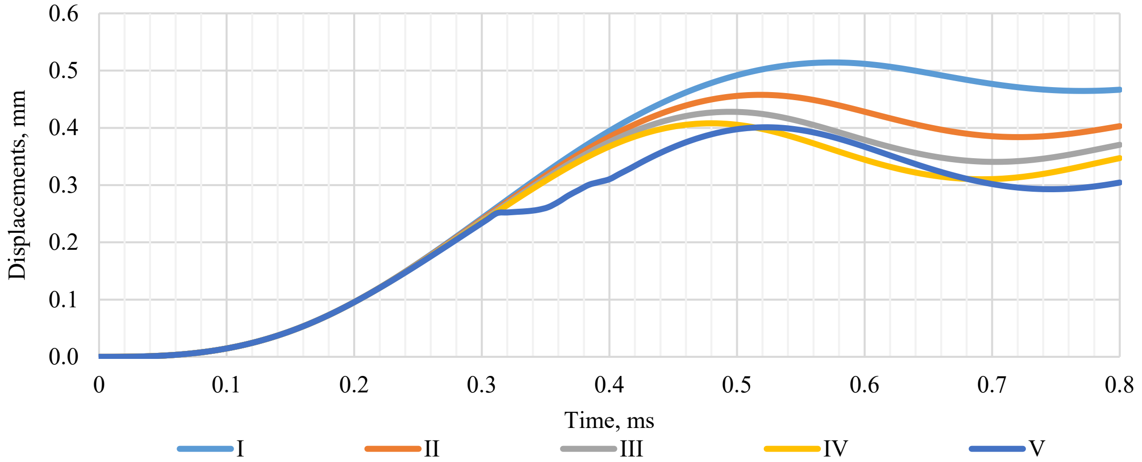

b)

Fig 6. Calculated values for classification groups:
a — rate of indenter introduction; *b* — displacements

For further data processing, a created and trained neural network with a fully-connected structure was used [14]. It is worth noting that neural networks have extensive capabilities in solving this type of tasks [15], in particular, in the sphere of construction [16]. Neural networks are often used for qualitative assessment, forecasting and monitoring of the condition of building structures [17], as well as for parametric identification of objects [18]. The increase in computing power of neural networks directly affects the development of their functionality [19].

The accuracy of neural network calculations was 98%. Therefore, the neural network correctly analyzes the experimental data and is able to adequately take into account the behavior of the material under shock loading.

Discussion and Conclusion. Thus, the analysis of the distribution of displacements and stresses in the sample allows us to draw a number of conclusions.

1. Level of vertical displacements in the wave process is much higher than in the horizontal one.
2. Level of stiffness of the substrate affects the distribution of displacements and stresses.
3. In the more solid bottom layer, the displacement is noticeably less than in the soft one.
4. Top layer is sensitive to the strength of the substrate if its height does not exceed 1 mm.
5. With distance from the indentation site, the deformations become elastic, the stress does not go out into the zone of plastic deformations.

Based on the research results, it can be argued that to determine the strength properties of homogeneous structures, one value characterizing the speed of displacement inside the sample is sufficient. For an inhomogeneous structure, it is required to introduce additional parameters, such as displacements on the surface and inside the sample at fixed observation points. An integrated approach to determining the strength properties of an inhomogeneous structure will improve the accuracy of calculations. And the use of neural network technologies to solve this type of problem opens up the possibility of faster calculations.

References

1. Lyapin A, Beskopylny A, Meskhi B. Structural Monitoring of Underground Structures in Multi-Layer Media by Dynamic Methods. *Sensors*. 2020;20(18):5241. https://doi.org/10.3390/s20185241

2. Chesnokov AV, Mikhailov VV, Dolmatov IV. Damage Detection in the Soft Shell of the Fabric Roof Construction of Buildings by means of Artificial Neural Network. *Structural Mechanics and Structures.* 2022;33(2):98–109.

3. Kuklina MV, Leber AI, Makhakova AM. The Use of Neural Network Technology in a Construction Organization. *Bulletin of the Altai Academy of Economics and Law.* 2022;(5–3):362–368. https://doi.org/10.17513/vaael.2219

4. Kuzmichev MV, Egorov RA. Modeling and Algorithmic Provision of Dynamic Indentation Process. *Scientific and Technical Journal of Information Technologies, Mechanics and Optics.* 2018;18(5):794–800. https://doi.org/10.17586/2226-1494-2018-18-5-794-800

5. Matlin MM, Kazankin VA, Kazankina EN. Prediction of the Technical Condition of Parts by Indenting in Different Loading Conditions. *Herald of Tver State University. Series: Technical Sciences.* 2022;13(1):22–27.

6. Rudnitsky VA, Kren AP, Lantsman GA. Evaluation of Metallic Materials Plasticity by Dynamic Indentation Method. *Litiyo i Metallurgiya = Foundry Production and Metallurgy*. 2017;(2):81-87. (In Russ.) https://doi.org/10.21122/1683-6065-2017-2-81-87

7. Oliver WC, Pharr GM. An Improved Technique for Determining Hardness and Elastic Modulus Using Load and Displacement Sensing Indentation Experiments. *Journal of Materials Research*. 1992;7:1564–1583. http://dx.doi.org/10.1557/JMR.1992.1564

8. Avtonomov NN, Tololo AV. Exploration of the Stress Distribution in the Specimen during Indentation of the Indenter Ball. *Actual Problems of Aviation and Cosmonautics*. 2018;14(1):245–247.

9. Jun Lu, Subra Suresh, Guruswami Ravichandran. Dynamic Indentation for Determining the Strain Rate Sensitivity of Metals. *Journal of the Mechanics and Physics of Solids.* 2003;51(11-12):1923–1938. https://doi.org/10.1016/j.jmps.2003.09.007

10. Matyunin VM, Nuha Abusaif, Marchenkov AYu. Analysis of the Indentation Size Effect on the Hardness Measurements of Materials. *Journal of Physics: Conference Series*. 2019;1399(4):044016. https://doi.org/10.1088/1742-6596/1399/4/044016

11. Varghese J, Radig GF, Herkommer D, Dasgupta A. Hybrid Experimental and Computational Approach for Rate Dependent Mechanical Properties Using Indentation Techniques. In: *EuroSimE 2005. Proc. 6th International Conference on Thermal, Mechanical and Multi-Physics Simulation and Experiments in Micro-Electronics and Micro-Systems*. New York City: IEEE; 2005. P. 510–514. https://doi.org/510-514. 10.1109/ESIME.2005.1502858

12. Kubenko V. Nonstationary Displacements in an Axisymmetric Problem for an Elastic Half-Space Under Mixed Boundary Conditions. *International Applied Mechanics*. 2021;57:148–159. https://doi.org/10.1007/s10778-021-01069-3

13. Beskopylny AN, Veremeenko AA, Kopylov FS, Krymskiy VS. The Problem for Static Conical Indentation into the Surface Hardened Area. *Engineering Journal of Don.* 2018;49(2):214–218.

14. Zesheng Lin, Hongxia Ye, Bin Zhan, Xiaofeng Huang. An Efficient Network for Surface Defect Detection. *Applied Sciences*. 2020;10(17):6085. https://doi.org/10.3390/app10176085

15. Babushkina N, Lyapin A, Kovaleva A. Analysis of Neural Network Results Based on Experimental Data during Indentation. In: *Topical Problems of Agriculture, Civil and Environmental Engineering. E3S Web of Conferences* (*TPACEE*). 2020;224:01018. https://doi.org/10.1051/e3sconf/202022401018

16. Elfaki AO, Alatawi S, Abushandi E. Using Intelligent Techniques in Construction Project Cost Estimation: 10-Year Survey. *Advances in Civil Engineering*. 2014;2014:107926. https://doi.org/10.1155/2014/107926

17. Patel DA, Jha KN. Evaluation of Construction Projects Based on the Safe Work Behavior of Co-employees through a Neural Network Model. *Safety Science*. 2016;89:240–248. https://doi.org/10.1016/J.SSCI.2016.06.020

18. Poroshin IE, Titov MA. Using Artificial Neural Networks for Parametric Identification of Objects. *Young Scientist.* 2020;316(26):39–42. (In Russ.)

19. Alferev DA. Usage of Artificial Neural Networks in Modern Society. *Social Area*. 2020;6(3):6. https://doi.org/10.15838/sa.2020.3.25.6

About the Authors:

Natalia E. Babushkina, Teaching assistant of the Computer Engineering and Programming Department, Don State Technical University (1, Gagarin sq., Rostov-on-Don, 344003, Russian Federation), SPIN-code, ORCID, ScopusID, ResearcherID, copybird@yandex.ru

Alexandr A. Lyapin, Dr.Sci. (Phys.-Math.), Professor, Head of the Information Systems in Construction Department, Don State Technical University (1, Gagarin sq., Rostov-on-Don, 344003, Russian Federation), SPIN-code, ORCID, ScopusID, ResearcherID, lyapin.rnd@yandex.ru

Claimed Contributorship:

NE Babushkina: description of the theoretical part of the study, calculations, creation of a neural network, formulation of conclusions, design of the scientific article.

AA Lyapin: setting research objective and tasks, analysis of the study results, revision of the text, correction of the conclusions.

Conflict of Interest Statement: **the authors declare no conflict of interest.**

All authors have read and approved the final manuscript.

Об авторах:

Наталья Евгеньевна Бабушкина, ассистент кафедры вычислительной техники и программирования Донского государственного технического университета (344003, Российская Федерация, г. Ростов-на-Дону, пл. Гагарина, 1), SPIN-код, ORCID, ScopusID, ResearcherID, copybird@yandex.ru

Александр Александрович Ляпин, доктор физико-математических наук, профессор, заведующий кафедрой информационных систем в строительстве Донского государственного технического университета (344003, Российская Федерация, г. Ростов-на-Дону, пл. Гагарина, 1), SPIN-код, ORCID, ScopusID, ResearcherID, lyapin.rnd@yandex.ru

Заявленный вклад авторов:

Н.Е. Бабушкина: описание теоретической части исследования, проведение расчетов, создание нейронной сети, формирование выводов, оформление научной статьи.

А.А. Ляпин: постановка цели и задач исследования, анализ результатов исследования, доработка текста, корректировка выводов.

Конфликт интересов**: авторы заявляют об отсутствии конфликта интересов.**

Все авторы прочитали и одобрили окончательный вариант рукописи.

Received / Поступила в редакцию 28.05.2024
Reviewed / Поступила после рецензирования Received 25.06.2024
Accepted / Принята к публикации 27.06.2024

INFORMATION TECHNOLOGY, COMPUTER SCIENCE AND MANAGEMENT
ИНФОРМАТИКА, ВЫЧИСЛИТЕЛЬНАЯ ТЕХНИКА И УПРАВЛЕНИЕ

UDC 004.75:005.8
https://doi.org/10.23947/2687-1653-2024-24-3-274-282

Original Empirical Research

Typification of Projects for the Transition to Cloud Services

Anna G. Voronova
Luhansk Vladimir Dahl State University, Luhansk, Luhansk People's Republic
✉ annaec@ya.ru

EDN: XYZSQL

Abstract

Introduction. Digital solutions make the operation of the company clearer, reduce staff costs, and provide data security. Various aspects of automation, digitalization and cloud technologies are described in the literature. The question is raised about the quality of the methodological basis for such transformations. Global and narrow technical approaches are presented. As a rule, materials are presented from the perspective of experts in the implementation of digital technologies. In this paper, for the first time, the author's scheme is proposed that can allow not only providers, but also their customers to navigate the upcoming transition to the cloud. The latter will receive systematic information on how to select a contractor and the most economically feasible option of cooperation.

Materials and Methods. The information model was based on the semantic network as a system of nodes, their characteristics and connections. Management of the cloud migration project and the migration itself were visualized. The contraction practice between providers and their customers was summarized. The specifics of the tasks of such projects were taken into account. The part of the subject area related to the implementation of a cloud service is algorithmic — a step-by-step transition to the cloud, a generalized scheme of the process taking into account the hierarchy of elements are presented.

Results. For the first time, a method of self-preparation of a company for the implementation of cloud solutions is proposed. The algorithm systematizes the cloud migration processes. The activities related to goal setting, audit, selection of cloud environment and services, calculation of the economic efficiency of the project, planning and implementation of migration, technical support and scaling of processes are described. The possibilities of determining the economic feasibility of measures for the transition to the cloud are shown. The costs of equipment, data storage and processing, software licenses, salaries, information security, etc., are taken into account. The amount received is compared to the providers' offers. For the final decision, the costs of infrastructure support are taken into account — by the customer or the outsourcer. The best option is selected. As a result, the customer gets the opportunity to work with better profitability and scale the project. Feedback is provided, and processes are adjusted, starting with IT reaudit.

Discussion and Conclusion. The proposed solution will give the customer's management a system view of the execution sequence when migrating to the cloud, the issues and tasks to discuss with a potential outsourcer. Providers can use the algorithm to typify and unify projects, which can eventually simplify the coordination of the list of services and the migration procedure with customers. In this way, the parties can free up significant resources in terms of time, labor and other costs. In addition, customers and providers can partially use the described semantic network to develop not only the organizational, but also the technical aspect of the project.

Keywords: digital transformation methodology, step-by-step transition to the cloud, cloud migration, profitability of cloud migration

Acknowledgements. The author would like to thank the Editorial board and the reviewers for their attentive attitude to the article and for the specified comments that improved the quality of the article.

For Citation. Voronova AG. Typification of Projects for the Transition to Cloud Services. *Advanced Engineering Research (Rostov-on-Don)*. 2024;24(3):274–282. https://doi.org/10.23947/2687-1653-2024-24-3-274-282

Оригинальное эмпирическое исследование

Типизация проектов перехода на облачные сервисы

А.Г. Воронова
Луганский государственный университет имени Владимира Даля, г. Луганск
✉ annaec@ya.ru

Аннотация

Введение. Цифровые решения позволяют сделать работу компании четче, сократить расходы на персонал, обеспечить безопасность данных. В литературе описаны различные аспекты автоматизации, цифровизации и облачных технологий. Ставится вопрос о качестве методологической основы таких преобразований. Представлены глобальный и узкий технический подходы. Как правило, материалы подаются с позиций специалистов по внедрению цифровых технологий. В данной работе впервые предлагается авторская схема, которая позволит ориентироваться в предстоящем переходе в облако не только провайдерам, но и их заказчикам. Последние получат систематизированные сведения о том, как выбрать подрядчика и вариант сотрудничества, наиболее целесообразный с экономической точки зрения.

Материалы и методы. Информационная модель строилась на базе семантической сети как система узлов, их характеристик и связей. Визуализированы управление проектом миграции в облачные сервисы и сама миграция. Обобщена практика заключения договоров между провайдерами и их заказчиками. Учтены особенности техзаданий таких проектов. Часть предметной области, касающаяся реализации облачного сервиса, алгоритмирована — представлен пошаговый переход в облако, обобщенная схема процесса с учетом иерархии элементов.

Результаты исследования. Впервые предложен метод самостоятельной подготовки компании к внедрению облачных решений. Алгоритм систематизирует процессы миграции в облако. Описаны мероприятия, связанные с целеполаганием, ИТ-аудитом, выбором облачной среды и сервисов, расчетом экономической эффективности проекта, планированием и реализацией миграции, техподдержкой и масштабированием процессов. Показаны возможности определения экономической целесообразности мероприятий по переходу в облако. Учитываются затраты на оборудование, хранение и обработку данных, лицензии на софт, зарплаты, обеспечение информационной безопасности и пр. Полученную сумму сравнивают с предложениями провайдеров. Для окончательного решения принимаются во внимание расходы на поддержку инфраструктуры — заказчиком или аутсорсером. Выбирается оптимальный вариант. В итоге заказчик получает возможность работать с лучшей рентабельностью и масштабировать проект. Предусмотрена отработка обратной связи и корректировка процессов, начиная с повторного ИТ-аудита.

Обсуждение и заключение. Предложенное решение даст менеджменту заказчика системное представление о том, в какой последовательности действовать при миграции в облако, какие вопросы и задачи обсуждать с потенциальным аутсорсером. Провайдеры могут применить алгоритм для типизации, унификации проектов, что в итоге упростит согласование с клиентами перечня услуг и порядка миграции. Таким образом стороны высвободят значительные ресурсы по времени, трудовым и иным затратам. К тому же заказчики и провайдеры могут отчасти задействовать описанную семантическую сеть, чтобы отработать не только организационную, но и техническую сторону проекта.

Ключевые слова: методология цифровых преобразований, пошаговый переход в облако, миграция в облако, рентабельность миграции в облако

Благодарности. Автор выражает благодарность редакции и рецензентам за внимательное отношение к статье и замечания, которые позволили повысить ее качество.

Для цитирования. Воронова А.Г. Типизация проектов перехода на облачные сервисы. *Advanced Engineering Research (Rostov-on-Don)*. 2024;24(3):274–282. https://doi.org/10.23947/2687-1653-2024-24-3-274-282

Introduction. The current socio-economic environment creates conditions for automation and digitalization of the operation of enterprises and organizations. This is due, in particular, to a shortage of personnel, new requirements for the efficiency and sustainability of production and management processes. Various aspects of automation, digitalization and cloud technologies are being investigated. In [1], a global approach to the digitalization of entrepreneurial activity is considered. Paper [2] shows the need to move to new digital business models. Stepwise digital transformation of an enterprise involves the consistent development of different levels, which are described in [3]. In [4], the reconfiguration of management processes required for digitalization is investigated.

Main stages of digitalization are as follows:

– preliminary research — goal definition and modeling of business processes;

– selection and implementation of hardware, software and hardware-software solutions.

Organizations can carry out these procedures on their own, but in practice, they often turn to IT companies.

One of the priorities of digital transformation is the development of cloud technologies and services [5]. RF President Vladimir Putin set the task to provide the operation of cloud infrastructure in the country and develop domestic cloud technologies[1].

Adequate implementation of cloud services requires a high-quality methodological framework. In [6], a methodology for decision support in the selection of cloud IT services is proposed. However, the issue of algorithmization of the cloud transition has not been sufficiently studied, specifically, for customers of cloud services who do not work in tech sector. At the same time, they can plan and implement some migration activities themselves. The presented work fills this gap. Its objective is to form a standard structure for the project of cloud transition services in the context of digital transformation. The proposed solution will be the basis for the creation and implementation of such projects. In addition, it will allow you to collect, process and use analytics on the processes being implemented.

Materials and Methods. A semantic network is selected to build an information model and display knowledge in the subject area. It contains objects (nodes and connections) and relations between them. This visual structure simplifies the understanding and interpretation of knowledge. Figure 1 shows the semantic network of project management for the transition to cloud services.

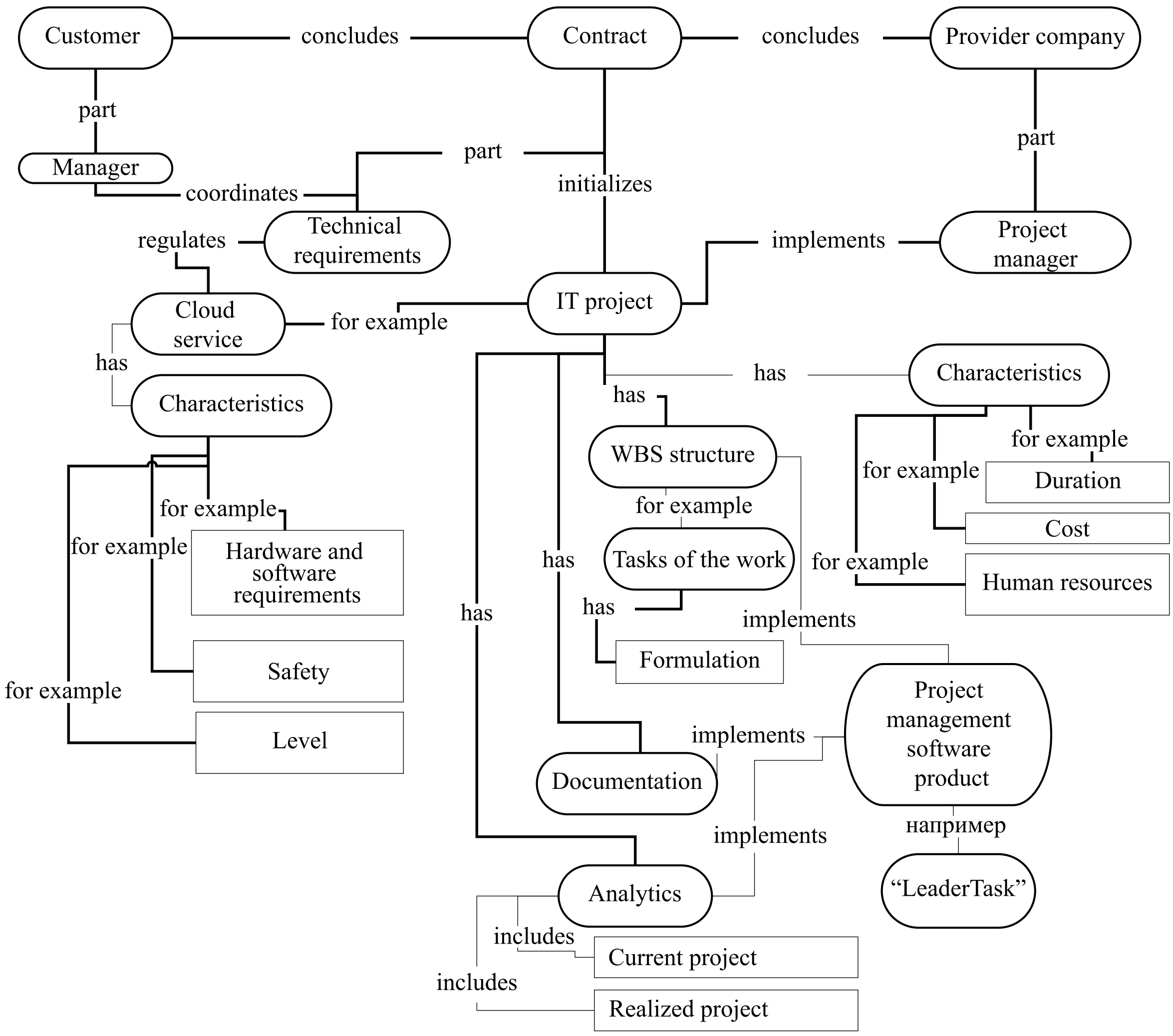

Fig. 1. Semantic network of project management for cloud transition:

— nodes; — characteristics; — connections between nodes

[1] *Putin set the task to support the development of domestic cloud technologies*. TASS. (In Russ.) URL: https://tass.ru/ekonomika/16418975 (accessed: 16.01.2024).

The provider of cloud solutions enters into an agreement with the customer. Technical requirements (TR) are drawn up, and an IT project is launched, which is managed by an expert from the provider company. TR regulate the content, composition and requirements for the service (cloud service). The cloud service has the following requirements:

– to the hardware and software (infrastructure placement, virtual resources, cloud services);

– to safety assurance;

– to technical support.

The customer's representative and the project manager from the provider determine the part that is outsourced and will be implemented within the framework of the IT project.

The part of the subject area related to the implementation of a cloud service requires more formalization. In this case, algorithmization makes it possible to describe a step-by-step cloud transition and show a generalized scheme of this process. In the algorithm:

– main processes and subprocesses of the implementation of cloud services are identified;

– sequence of transition between them is determined;

– connections that provide returning to previous stages to make other decisions are indicated.

To describe the technical specifications of the cloud transition, we have analyzed the best practices known from open sources, including scientific literature. The IT project management part is formalized using a semantic network.

The basic actions in the development of the project are taken into account:

– identification and analysis of requirements;

– clarification of the customer 's wishes;

– preparation of technical specifications.

Based on the project method, the basic tasks (jobs) that are required for the cloud transition are identified, and their hierarchy is built. The WBS structure of the project includes a list of tasks-jobs. Their duration, connections are specified, and resources are assigned for execution. When resources are loaded, it is possible to recalculate the duration of jobs. Then critical tasks are determined, whose total duration corresponds to the duration of the project as a whole.

Thus, the major features of the IT project are the following: duration, cost, labor resources. There are special software products for managing an IT project. As an example, these are "Jira" (created by the Atlassian company, Australia) [7] or the domestic analogue of "LeaderTask" (developer: Organizer LeaderTask, LLC) [8].

Note that the WBS structure is being built in the project management software product along with the tasks-jobs. The provider needs to unify the tasks-jobs. In a unified system, the provider, among other things, maintains owned project documentation. Analytics are also generated here to track the implementation of the project and its operation after going.

On the subnet "IT project has", the requirement to unify the formulation and execution of tasks-jobs is identified. A possible option is proposed in this article. Cloud services are considered from the point of view of business development, increasing its competitiveness [9].

Research Results. Thus, professional providers offer ready-made cloud services, configure them and accompany the operation. However, the company can independently create, implement a solution and supervise its performance.

The project management methodology[2] [10] assumes the following stages: initialization, development, execution, and completion [11]. Note that the same tasks can be formulated variously, especially if the projects are realized by different managers. Typification of solutions reduces labor costs for the creation of project documentation, enhances its quality, and improves analysis.

Main steps for migrating to the cloud are listed below.

1. Defining goals.
2. Selecting a provider.
3. IT-audit. At this stage, the initial IT infrastructure is evaluated (efficiency, security, etc.).
4. Selecting the type of cloud environment and cloud services.
5. Cost-effectiveness analysis of the cloud transition.
6. Migration planning (a roadmap is drawn up, priorities, stages, deadlines, resources, budget are determined).
7. Migration (application dependency scheme is drawn up, cloud infrastructure is designed, test run is conducted, data is transferred to the cloud, and service is put into operation).
8. Operation monitoring and technical support.
9. Scaling.

The transition to cloud services can be represented as an algorithm (Fig. 2).

[2] *A Guide to the Project Management Body of Knowledge. PMBOK Guide.* Newtown Square, PA: Project Management Institute, Inc.; 2017. 579 p. URL: https://prothoughts.co.in/wp-content/uploads/2022/06/a-guide-to-the-project-management-body-of-knowledge-6e.pdf (accessed: 12.04.2024).

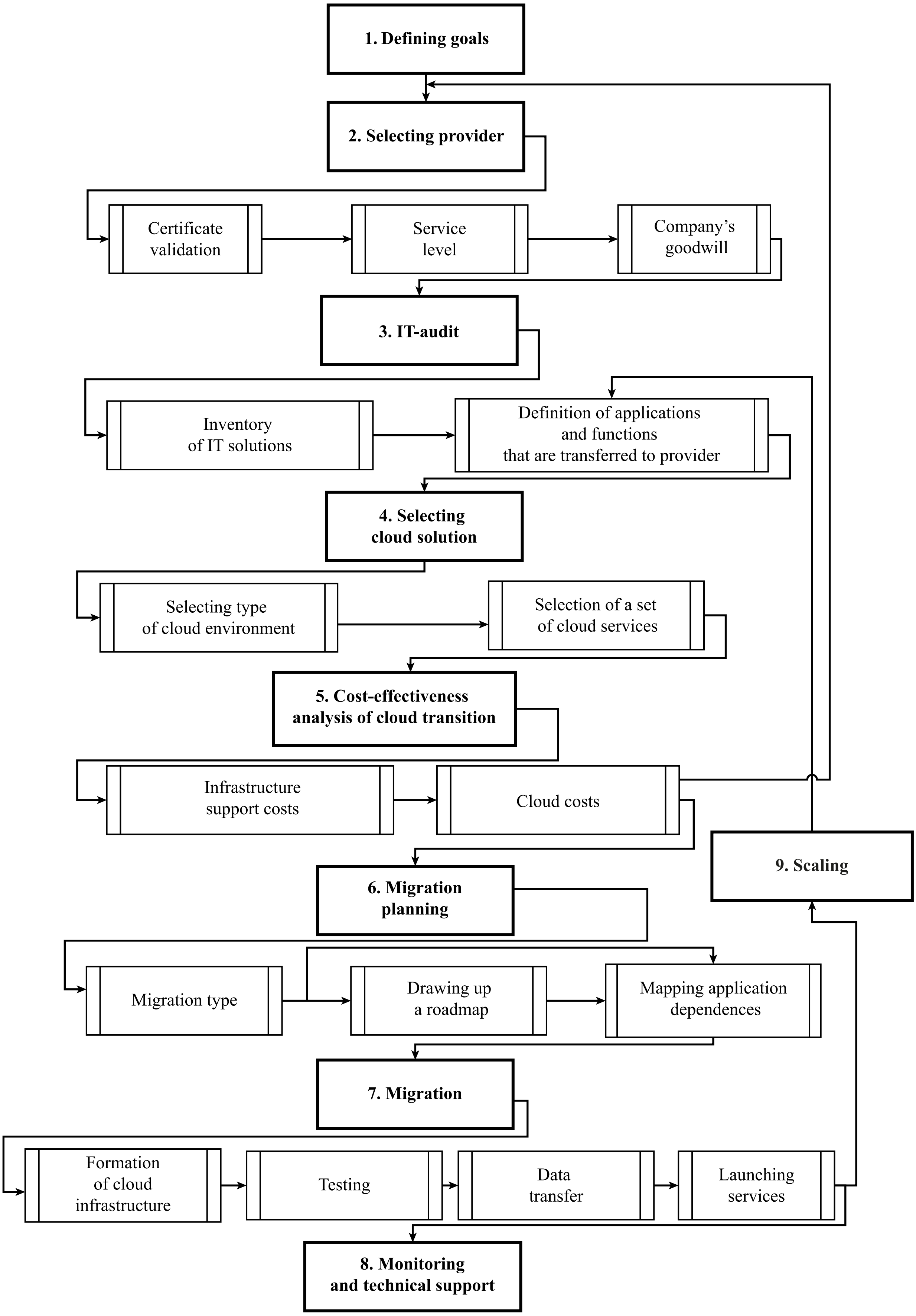

Fig. 2. Cloud transition algorithm:
— process; — subprocess; — transition to stage

We comment on the presented scheme.

1. The goal of cloud transition should be consistent with the company's business strategy. As noted above, the use of cloud services makes business more flexible and efficient.

Tasks in the project:

– negotiations with stakeholders and customers;

– formulation of the planned business result.

2. It is necessary to find out in advance whether a foreign company can be a partner in the project. In some cases, cooperation is possible only with domestic providers. Restrictions are related to the scope of the company's activities, top-secret information, processing of personal data, etc. In these cases, the provider must have a set of documents:

– license of the Federal Service for Technical and Export Control (FSTEC) for the technical protection of confidential information;

– FSTEC certificate;

– license of the Federal Security Service (FSB) for cryptography;

– FSB license to work with the national security information;

– FSTEC license for the protection of national security information;

– certificate of compliance when working with personal data.

Reference offers from cloud providers are as follows: implementation and maintenance of virtual machines, data centers, etc. However, the services of various companies differ in the nuances of settings, payment models, quality of service and user support.

If the partner's goodwill is important to the customer, he contacts an organization that is well known in the market.

At this stage, first of all, the certificate and license of the provider should be checked. Secondly, it is necessary to agree on the general characteristics of the service:

– hypervisor;

– reliability category of data centers according to the Uptime Institute standard;

– technical support terms;

– service level agreement;

– test access;

– payment model.

The above are the tasks in the project.

Hypervisor is software that is used by a cloud provider for virtualization. It allows for creating multiuser logically independent cloud environments.

The reliability of the data center infrastructure can meet the Uptime Institute standard [12] and, in some cases, it should be at least “Tier III” [13].

The service level agreement specifies the areas of responsibility of the customer and the client, and fixes guarantees for services. The terms and parameters of the test access are approved.

Various payment models for cloud services are practiced. The most common is hourly.

3. The customer's IT infrastructure, applications and their connections with the IT environment are analyzed. IT audit allows for determining which functions can be transferred to a cloud provider and which ones can be left in owned infrastructure. It is not uncommon for a customer to decide on a full transition to the cloud.

Tasks in the project include:

– conclusion of an IT audit contract;

– acquisition of information about the company's software;

– gathering information about the technical support of the enterprise;

– acquisition of information about the topology of the enterprise;

– building a business process model “as is”;

– building a business process model “as it will be”;

– compiling a list of functions that are transferred to the cloud provider;

– submission of the IT audit report.

4. A cloud solution is selected. First, you need to decide on the type of cloud environment [14]:

– IaaS (infrastructure as a service);

– PaaS (platform as a service);

– SaaS (software as a service).

Types of cloud environment differ in the elements that are transferred to the provider for maintenance (data, network, servers, operating systems, software, etc.) [15]. Elements of the environment may remain under the control of the customer's services.

Tasks in the project:

– select the type of cloud environment;

– define a set of cloud services.

5. Under the cloud transition, an enterprise needs to estimate the costs on operating a standard data center. It is about the costs of a data storage and processing system, communication equipment, software and hardware licenses, servers, salaries of IT specialists of the enterprise, information security, etc. The amount received is compared to the offers of cloud providers. They can do all these calculations.

The following costs are determined:

– for the support of the infrastructure by the client;

– for the selected type of cloud environment.

The above are the tasks of this stage of the project.

6. The selection of migration method depends on the scale, structure and IT infrastructure of the organization. Full migration is often recommended for small and medium-sized businesses, partial migration is practiced by large companies. Project deadlines range from a few weeks to a year. When switching to the cloud model, issues of supporting the access to data sources, using archiving and recovery tools, are being resolved.

There are tasks of this part of the project. You should create an application dependency map and determine the following:

– migration type;

– list of critical services;

– transfer time.

7. At the migration stage, much is determined by the individual characteristics of the customer, therefore detailed solutions are formed for specific conditions. Thus, for example, specifics of migrating physical infrastructure to a virtual environment and transferring existing virtual infrastructure depend on this.

Tasks in the project:

– transfer (installation from scratch; “hot” or “cold” backup);

– test run;

– application recycling (when required).

8. Problems are possible when using any resources. Cloud services are no exception. One of the central issues of their use is safety. As a rule, it is determined by the quality of interaction between the provider and the customer's employees. The basic task is continuous improvement and correction of shortcomings.

9. The diagram shows the scaling process separately — the development of the solution, its distribution (e.g., to other divisions of the customer). It is recommended to systematically work out the feedback. In this way, you can get information that will indicate the further direction of the project. In some cases, it is advisable to return to the previous steps of the algorithm — up to the third, i.e., IT audit.

Discussion and Conclusion. The cloud transition allows organizations to defend digital processes more flexibly and economically. The introduction of clouds can significantly reduce the cost of hardware, software, licenses, salaries, etc. The Russian cloud services market is developing. Numerous providers deliver services. The literature devoted to the study of these processes is published. Within the framework of this work, a scheme is visualized and explained. It can be the basis for starting a digital transformation of an enterprise. It gives management a systematic idea of what sequence to act in, what to pay attention to, which issues to discuss with the provider, and which issues to work out with their own specialists.

Providers can use the proposed algorithm to typify projects, coordinate the list of services with customers and the stages of transition to cloud technologies on-the-fly.

The unification of task complexes for each step of the described algorithm should provide an improvement in the quality of project documentation due to the elaboration of organizational solutions for the project. It should be noted that both customers and providers can partially take into account the presented material to design and coordinate the technical aspect of migration. Thus, organizational and management processes should be taken into account when forming approaches to data coordination and control in cloud solutions. In addition, information management technologies in cloud solutions that will enable migration between providers should be developed.

References

1. Fikhtner OA. Digitalization of Business Processes in the Global World. *Herald of Siberian Institute of Business and Information Technologies*. 2022;11(4):117–122. (In Russ.) https://doi.org/10.24412/2225-8264-2022-4-117-122

2. Veligura AV. Basic Directions of Digitalization of Economy. *Social Work: Modern Problems and Technologies*. 2020;1(1):54–62. (In Russ.)

3. Nigai EA. Business Digitalization Process: From Point-to-Point Business Process Digitization to Digital Transformation. *ETAP: Economic Theory, Analysis, Practice*. 2022;(2):134–145. (In Russ.) https://doi.org/10.24412/2071-6435-2022-2-134-145

4. Ryazantseva NA, Lofichenko AA. Analysis of the State of the Digital Transformation of the Economy of the Russian Federation. *Manager*. 2022;102(4):55–61. https://doi.org/10.5281/zenodo.7442029

5. Buryi A. Cloud Computing in the Digital Transformation of Information Technologies. *Legal Informatics*. 2021;(2):4–14. https://doi.org/10.21681/1994-1404-2021-2-04-14

6. Razumnikov SV. Methods Decision Support by Selecting Cloud IT Services for Implementation for Enterprise. *Transactions of the Free Economic Society of Russia*. 2018;212(4):339–362. URL: https://veorus.ru/upload/iblock/a6a/veo_212.pdf (accessed: 14.04.2024).

7. Chistyakova KA, Yudin VV. Practical Methods for Managing the Implementation of Innovative Projects Based on the Use of the Jira Software. *Science and Art of Management. Bulletin of the Institute of Economics, Management and Law of the Russian State University for the Humanities*. 2023;(1):80–93. (In Russ.) https://doi.org/10.28995/2782-2222-2023-1-80-93

8. Vershinin VP, Schmidt VR. Russian Project Management Systems: Characteristics and Development Trends. *Economics of Sustainable Development*. 2023;54(2):167–171. (In Russ.) https://doi.org/10.37124/20799136_2023_2_54_167

9. Tuchina AV, Voronova AG. Business Automation Based on Cloud Services Considering IT-Sector's Sustainable Technological Trends. *Vestnik. Lugansk State University named after Vladimir Dahl*. 2023;70(4):115–118. (In Russ.)

10. Kochnev MM. Analysis of Existing Project Management Methodologies and Development of a Digital Product Management Methodology. *Nauchnye issledovaniya*. 2023;37(1):23–27. (In Russ.) URL: https://scientificresearch.ru/images/PDF/2023/42/analizsushchestvuyushchikh.pdf (accessed: 14.04.2024).

11. Agbejule A, Lehtineva L. The Relationship between Traditional Project Management, Agile Project Management and Teamwork Quality on Project Success. *International Journal of Organizational Analysis*. 2022;30(7):124–136. https://doi.org/10.1108/ijoa-02-2022-3149

12. Ganzha D. Uptime Institute in Russia. *LAN. Network Solutions Magazine*. 2013;(2):4–15. (In Russ.) URL: https://www.osp.ru/lan/2013/02/13033998 (accessed: 12.06.2024).

13. Wiboonrat M. Condition-Based Maintenance for Data Center Operations Management. In book: A Petrillo, F De Felice, G Lambert-Torres, E Bonaldi (eds). *Operations Management — Emerging Trend in the Digital Era*. London: IntechOpen; 2021. P. 16–21. https://doi.org/10.5772/intechopen.93945

14. Inozemtseva SA, Abdrakhmanov AR. The Role of Cloud Technologies for Socio-Economic Systems of Business. In: *Proc. V Anniversary All-Russian Scientific and Practical Conference with International Participation "Challenges of the Digital Economy: Import Substitution and Strategic Development Priorities"*. Bryansk: BGITU Publ.; 2022. P. 720–724. (In Russ.)

15. Voronova AG, Sharenko MM. Development of University Subsystem IT-Infrastructure Modernization Project. *Vestnik. Lugansk State University named after Vladimir Dahl*. 2022;55(1):46–51. (In Russ.)

About the Author:

Anna G. Voronova, Cand.Sci. (Economics), Associate Professor of the Department of Economic Cybernetics and Applied Statistics, Luhansk Vladimir Dahl State University (20a, Molodezhnyy Block, Luhansk, 291034, Luhansk People's Republic), SPIN-code, ORCID, annaec@ya.ru

Conflict of Interest Statement: **the author declares no conflict of interest.**

The author has read and approved the final manuscript.

Об авторе:

Анна Геннадьевна Воронова, кандидат экономических наук, доцент кафедры экономической кибернетики и прикладной статистики Луганского государственного университета имени Владимира Даля (291034, г. Луганск, кв. Молодежный, 20а), SPIN-код, ORCID, annaec@ya.ru

Конфликт интересов: **автор заявляет об отсутствии конфликта интересов.**

Автор прочитал и одобрил окончательный вариант рукописи.

Received / Поступила в редакцию 17.06.2024
Reviewed / Поступила после рецензирования 12.07.2024
Accepted / Принята к публикации 22.07.2024

INFORMATION TECHNOLOGY, COMPUTER SCIENCE AND MANAGEMENT
ИНФОРМАТИКА, ВЫЧИСЛИТЕЛЬНАЯ ТЕХНИКА И УПРАВЛЕНИЕ

Check for updates

UDC 004.021
Original Empirical Research
https://doi.org/10.23947/2687-1653-2024-24-3-283-292

Development of an Algorithm for Semantic Segmentation of Earth Remote Sensing Data to Determine Phytoplankton Populations

EDN: SICESA

Yulia V. Belova, Irina F. Razveeva ✉, Elena O. Rakhimbaeva
Don State Technical University, Rostov-on-Don, Russian Federation
✉ razveevai@mail.ru

Abstract

Introduction. Computer vision is widely used for semantic segmentation of Earth remote sensing (ERS) data. The method allows monitoring ecosystems, including aquatic ones. Algorithms that maintain the quality of semantic segmentation of ERS images are in demand, specifically, to identify areas with phytoplankton, where water blooms— the cause of suffocation — are possible. The objective of the study is to create an algorithm that processes satellite data as input information for the formation and checking of mathematical models of hydrodynamics, which are used to monitor the state of water bodies. Various algorithms for semantic segmentation are described in the literature. New research focuses on enhancing the reliability of recognition — often using neural networks. This approach is modified in the presented work. To develop the direction, a new set of information from open sources and synthetic data are proposed. They are aimed at improving the generalization ability of the model. For the first time, the contour area of the phytoplankton population is compared to the database — and thus the boundary conditions are formed for the implementation of mathematical models and the construction of boundary-adaptive grids.

Materials and Methods. The set of remote sensing images was supplemented with the author's augmentation algorithm in Python. Computer vision segmented areas of phytoplankton populations in the images. The U-Net convolutional neural network (CNN) was trained on the basis of NVIDIA Tesla T4 computing accelerators.

Results. To automate the detection of phytoplankton distribution areas, a computer vision algorithm based on the U-Net CNN was developed. The model was evaluated by the calculated values of the main quality metrics related to segmentation tasks. The following metric values were obtained: Precision = 0.89, Recall = 0.88, F1 = 0.87, Dice = 0.87, and IoU = 0.79. Graphical visualization of the results of CNN learning on the training and validation sets showed good quality of model learning. This is evidenced by small changes in the loss function at the end of training. The segmentation performed by the model turned out to be close to manual marking, which indicated the high quality of the proposed solution. The area of the segmented region of the phytoplankton population was calculated by the area of one pixel. The result obtained for the original image was 51202.5 (based on information about the number of pixels related to the bloom of blue-green algae). The corresponding result of the modeling was 51312.

Discussion and Conclusion. The study expands theoretical and practical knowledge on the use of convolutional neural networks for semantic segmentation of space imagery data. Given the results of the work, it is possible to assess the potential for automating the process of semantic segmentation of remote sensing data to determine the boundaries of phytoplankton populations using artificial intelligence. The use of the proposed computer vision model to obtain contours of water bloom due to phytoplankton will provide for the creation of databases — the basis for environmental monitoring of water resources and predictive modeling of hydrobiological processes.

Keywords: environmental monitoring of water resources, phytoplankton boundaries, water bloom contour, blue-green algae bloom, space image data segmentation

Acknowledgements. The authors would like to thank the project scientist A.I. Sukhinov, Corresponding Member of the Russian Academy of Sciences, Dr.Sci. (Phys.-Math.), Professor.

Funding Information. The research was done with the financial support of the Russian Science Foundation (grant No. 22–71–10102 "Mathematical Models and Parallel Algorithms for Predicting the Dynamics of Phytoplankton Populations in Marine Systems Taking into Account the Exchange of Oxygen and Carbon Dioxide on Supercomputer Computation Systems").

For Citation. Belova YV, Razveeva IF, Rakhimbaeva EO. Development of an Algorithm for Semantic Segmentation of Earth Remote Sensing Data to Determine Phytoplankton Populations. *Advanced Engineering Research* (*Rostov-on-Don*). 2024;24(3):283–292. https://doi.org/10.23947/2687-1653-2024-24-3-283-292

Оригинальное эмпирическое исследование

Разработка алгоритма семантической сегментации данных дистанционного зондирования Земли для определения фитопланктонных популяций

Ю.В. Белова, И.Ф. Развеева ✉, Е.О. Рахимбаева

Донской государственный технический университет, г. Ростов-на-Дону, Российская Федерация

✉ razveevai@mail.ru

Аннотация

Введение. Компьютерное зрение широко используется для семантической сегментации данных дистанционного зондирования Земли (ДЗЗ). Метод позволяет контролировать экосистемы, в том числе водные. Востребованы алгоритмы, обеспечивающие качество семантической сегментации снимков ДЗЗ, в частности, для выявления областей с фитопланктоном, где возможно цветение воды — причина заморов. Цель исследования — создание алгоритма, обрабатывающего спутниковые данные как входную информацию для формирования и верификации математических моделей гидродинамики, по которым отслеживается состояние водных объектов. В литературе описаны различные алгоритмы семантической сегментации. Новые исследования сосредоточены на повышении надежности распознавания — чаще с помощью нейросетей. Этот подход совершенствуется в представленной работе. Для развития направления предлагаются новый набор сведений из открытых источников и синтетические данные для улучшения обобщающей способности модели. Впервые область контура фитопланктонной популяции сравнивается с базой данных — и так формируются граничные условия для реализации математических моделей и построения гранично-адаптивных сеток.

Материалы и методы. Набор снимков ДЗЗ дополнили с помощью авторского аугментационного алгоритма на языке Python. Компьютерное зрение сегментировало области фитопланктонных популяций на снимках. Сверточную нейронную сеть (СНС) U-Net обучили на базе ускорителей вычислений NVIDIA Tesla T4.

Результаты исследования. Для автоматизации обнаружения областей распространения фитопланктона разработан алгоритм компьютерного зрения, основанный на СНС U-Net. Модель оценили по вычисленным значениям основных метрик качества, относящихся к задачам сегментации. Получены следующие значения метрик: Precision = 0,89, Recall = 0,88, F1 = 0,87, Dice = 0,87 и IoU = 0,79. Графическая визуализация результатов обучения СНС на обучающем и валидационном наборах показала хорошее качество обучения модели. Об этом свидетельствуют малые изменения функции потерь в конце обучения. Выполненная моделью сегментация оказалась близка к ручной разметке, что говорит о высоком качестве предложенного решения. По площади одного пикселя рассчитали площадь сегментированной области фитопланктонной популяции. Полученный результат для исходного изображения — 51202,5 (по информации о количестве пикселей, относящихся к цветению сине-зеленых водорослей). Соответствующий итог моделирования — 51312.

Обсуждение и заключение. Исследование расширяет теоретические и практические знания о применении сверточных нейронных сетей для семантической сегментации данных космических снимков. Учитывая итоги работы, можно оценить потенциал автоматизации процесса семантической сегментации данных ДЗЗ для определения границ фитопланктонных популяций с помощью искусственного интеллекта. Применение предложенной модели компьютерного зрения для получения контуров цветения воды из-за фитопланктона позволит создать базы данных — основу для экологического мониторинга водных ресурсов и прогностического моделирования гидробиологических процессов.

Ключевые слова: экологический мониторинг водных ресурсов, границы фитопланктона, контур цветения воды, цветение воды из-за сине-зеленых водорослей, сегментация данных космических снимков

Благодарности. Авторы благодарят научного консультанта проекта члена-корреспондента РАН, доктора физико-математических наук, профессора А.И. Сухинова.

Финансирование. Исследование выполнено при финансовой поддержке Российского научного фонда (грант РНФ № 22–71–10102 «Математические модели и параллельные алгоритмы для прогнозирования динамики фитопланктонных популяций в морских системах с учетом обмена кислородом и углекислым газом на суперкомпьютерных вычислительных системах»).

Для цитирования. Белова Ю.В., Развеева И.Ф., Рахимбаева Е.О. Разработка алгоритма семантической сегментации данных дистанционного зондирования Земли для определения фитопланктонных популяций. *Advanced Engineering Research* (*Rostov-on-Don*)*.* 2024;24(3):283–292. https://doi.org/10.23947/2687-1653-2024-24-3-283-292

Introduction. Automated algorithms for processing information received from satellites are needed in various fields of activity. Solving fundamental and applied problems of ecology requires segmentation of regions in accordance with the focus of attention of researchers. This optimizes the process of studying and modeling hydrobiological processes. An example of such local interest is the bloom of water due to the spread of phytoplankton. The phenomenon is important for current and complex monitoring of water resources. It is clearly visible from satellites during remote sensing of the Earth (ERS).

Water bloom affects significantly its quality in surface sources used for domestic water supply systems [1]. The reaction of phytoplankton populations in the hydrological environment can reliably assess the general state of the aquatic ecosystem [2]. The negative consequences of uncontrolled algae growth are mass death of fish (suffocation), increased load on water purification plants [3], and pollution of shores and beaches [4].

Systematic measurements at automatic water quality monitors, as well as obtaining data from research expeditions, are labor-intensive and expensive activities. An additional source of information on the state of the phytoplankton community is modern satellite systems equipped with survey instruments. They allow remote recording of the state of the algae biomass, tracking its dynamics in a given time period.

A significant advantage of satellite data as a tool for monitoring water resources is the possibility of full-scale and operational control at any point on Earth. A wide view of the water area, as a rule, gives researchers a significant amount of useful information. But, despite the active development of systems based on computer vision algorithms, the problem of identifying the contours of regions of interest in remote sensing data has not yet been fully solved.

Good results are obtained by various algorithms of semantic segmentation on images. With their help, it is possible to identify and clarify the boundaries and structure of natural objects. In [5], the efficiency of the LBP method (local binary patterns) for recognizing objects consisting of curvilinear contours is shown. LBP provides high edge sharpness and detail of Earth satellite sensing data. In [6], it is noted that to increase the reliability of recognition, it is required to combine artificial intelligence algorithms and such classical methods of image edge detection as Sobel, Kirsch and Laplace operators. In [7], a comprehensive approach is proposed for semantic processing of satellite images of unlimited size using U-Net neural network models, which showed an F1-score value from 0.78 to 0.91 when detecting objects.

Paper [8] provides an overview of intelligent methods for solving the problem of semantic segmentation of data on satellite images. The authors conclude that in this case, neural network algorithms are the most effective and productive. As an example, a convolutional neural network (CNN) is given, trained on several thousand satellite images of Massachusetts (USA). The accuracy of the model was 85.31%. In [9], semantic segmentation, instance segmentation, and panoptic segmentation are considered. The advantages of using deep learning methods implemented in the architectures of such CNN as SegNet, U-Net, and DeepLab are specified. In [10], automated processing of satellite images is based on a combination of the SpaceNet dataset and progress in computer vision which are made possible by deep learning. This paper presents five approaches based on improvements to the U-Net and Mask R-Convolutional Neural Networks models. The metric values for the best models are as follows: average precision (AP) and average recall (AR) are 0.937 and 0.959, respectively. An effective application of CNN for detecting contrails on satellite images is described in [11]. It is proven that in large-scale monitoring of contrails with measurement of their impact on climate, the approach based on CNN of U-Net architecture demonstrates F1-score equal to 0.52, with an overall average detection probability of 0.51.

The 2023 models Segment Anything (SAM), Language-Segment-Anything (Lang-SAM), and HQ-SAM are of particular interest. These are dynamic deep learning tools that can predict object masks from images using input hints. Several researchers have already applied this approach to the analysis of aerial photographs and ERS data. The accuracy of identifying areas of interest has proven to be high [12]. In [13], the F1- score value reaches 86.5%±4.1%. In the future, models of similar architecture with various modifications (Polyp-SAM, Grounding DINO, etc.) will provide for both interactive (requiring user intervention) and automatic segmentation.

Intelligent technologies are increasingly being introduced to process remote sensing data. High accuracy of models is noted. Particular attention is paid to methods based on such CNN as SegNet, U-Net, DeepLab in combination with classical methods of image preprocessing. A generalized approach to segmentation is actively developing.

This paper considers the solution to a problem in the ERS data assimilation using computer vision. The application of U-Net CNN for segmentation of areas containing phytoplankton populations is shown. The algorithm created by the authors provides for the segmentation of regions of interest and calculation of their areas, which is required for further analysis when solving problems of hydrodynamics and hydrobiology.

The following four points describe the scientific novelty of the presented study.

1. A data set was formed from open sources.

2. Synthetic data were generated to improve the generalizing ability of the model. For this purpose, the authors' own augmentation algorithm was used to make the model more resistant to noise in practical use [14].

3. An intelligent model based on the U-Net CNN architecture was implemented in the high-level Python language. Its key hyperparameters were optimized using the Optuna library and checked on a test dataset.

4. The areas of the found contour containing phytoplankton populations were compared to the existing database. In this way, boundary conditions have been formed for the subsequent implementation of mathematical models and the construction of boundary-adaptive grids.

To achieve the set goal, it is required to solve a number of problems:

– to prepare an ERS database containing regions of interest segments of water bloom;

– to validate and describe the topology of the U-Ne SNS;

– to perform data augmentation to create an extended representative set;

– to implement, optimize, debug and test the CNN of U-Net architecture;

– to determine values of key metrics of the model quality for segmentation;

– to calculate the areas of the segmented contour given the scale of the original image.

The theoretical significance of the study is due to the expansion of ideas about the possibilities of using computer vision technology in the field of water resources monitoring. The practical significance consists in the development of an applied cross-platform and scalable tool for analyzing remote sensing images to record regions of interest in aquatic ecosystems.

Materials and Methods. For geospatial analysis, we use open-source software that is often applied to solve environmental problems [15].

The study is based on current satellite data. The authors focus on the state of water bodies during the bloom of blue-green algae. Analysis of this information allows:

– predicting the volume and distribution of phytoplankton in the water area [16];

– checking physical and biological processes that determine the rate of phytoplankton growth and biomass accumulation [17];

– analyzing climate change based on the forecast of the dynamics of the bloom process [18];

– studying in detail the process of CO_2 exchange between a water body and air [19].

To automate the process of detecting regions of phytoplankton populations and calculating their areas, it is proposed to develop a computer vision algorithm based on the U-Net CNN architecture.

As a training sample for the deep learning algorithm, 20 space images of water bodies such as the Black, Caspian, Azov Seas, etc., were taken. The photos were obtained at different points on the earth's surface.

The first step was to label the images to transform the information into a format that could be understood by the computer vision algorithm for performing the segmentation. There were two common approaches to providing annotations:

– creating a pixel-level mask;

– selecting polygon boundaries for the region of interest.

We have used the first option, where the pixel-level mask files represent regions of interest for the algorithm. The marked masks are files with the extension jpeg or png. The proportions correspond to the image they annotate. Figure 1 shows an example of the original image and its mask, where green indicates land, blue indicates water surface, and red indicates the region of the phytoplankton population.

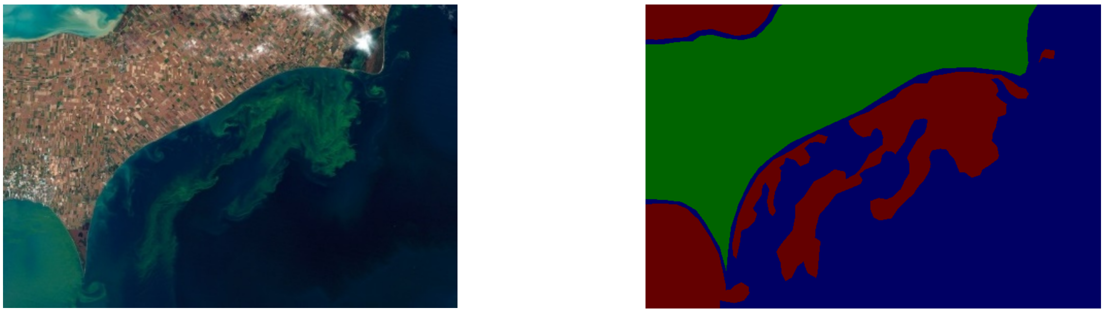

Fig. 1. Image mapping: *a* — original image; *b* — image mask

To increase the number of images in the data set, we used the authors' augmentation code, supplemented with noise effects. When creating the extended data set, we used the following modifications of the original images:

– rotation by an arbitrary angle;
– display along the OX and OY axes;
– cropping;
– scaling;
– color correction.

All changes were made taking into account the noise that may appear on real images obtained through remote sensing, and were segmented using the developed algorithm.

Let us note the advantage of the authors' algorithm for creating additional source data. Under conditions of a limited set of real images, the use of artificially created images for training will allow for a more fine-tuning of the developed model, optimizing its parameters and making it more resistant to distortion in practical application.

The U-Net CNN architecture is designed to solve the problem of biomedical data segmentation. The determining factor in its selection is the relatively small size of the initial data, with which U-Net shows satisfactory results in practice.

The U-Net CNN architecture is based on the interaction of convolution layers + pooling, which first reduce the spatial resolution of the image (encoder), and then increase it, having previously combined it with the image data and passed it through other convolution layers (decoder) (Fig. 2).

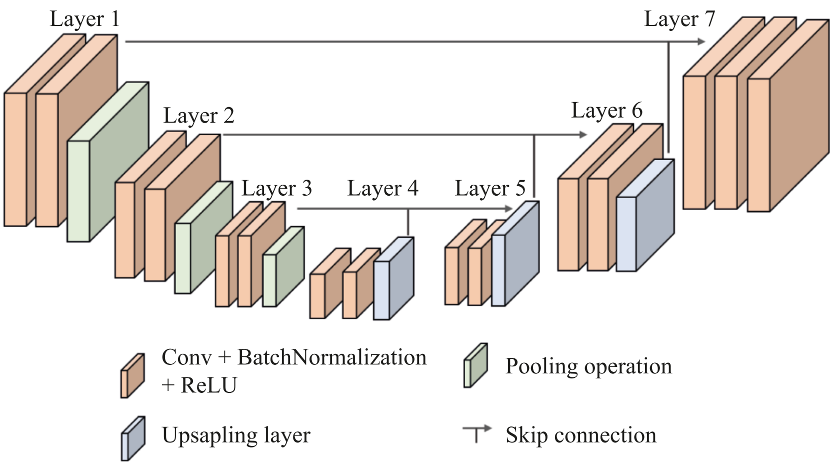

Fig. 2. Architecture of U-Net SNN

The convolutional blocks of the decoder and encoder are linked by end-to-end connections, or skip connections. This solves the problem of vanishing gradient, which is a challenge for computer vision [20]. In this study, we used the encoder from the ResNet–50 neural network, pre-trained on the ImageNet dataset.

To select the hyperparameters of the U-Net CNN that affect the architecture and training process, the Optuna library was used. This made it possible to automate the model tuning to achieve better results.

Research Results. Table 1 shows the model parameters specified under training.

Table 1

Parameters for Training the U-Net Convolutional Neural Network

No.	Parameter	Value
1	Number of images in training set	700
2	Number of images in validation set	200
3	Number of images in test sample	100
4	Batch size	10
5	Learning rate	1st-4
6	Overfitting detector	Early stopping
7	Solver	Adam

The model was trained using optimization of the Dice loss function (2) based on the Dice coefficient (1).

$$DSC = \frac{2|X \cap Y|}{|X| + |Y|}, \quad (1)$$

$$Dice\ Loss = 1 - \frac{2|X \cap Y| + Smooth}{|X| + |Y| + Smooth}. \quad (2)$$

Here, X — a set of pixels defined during the mapping as a scope of a specific class; Y — a set of pixels assigned to a specific class according to the conclusions of the developed segmentation model. The Smooth coefficient is used to smooth the calculation result in the case when the values X and Y are close to zero.

The Adam method for stochastic optimization was used to train the model. Early stopping was used as an overfitting detector. In machine learning, this is one of the most widely used regularization methods to prevent overfitting. The training process was performed on the basis of NVIDIA Tesla T4 computing accelerators, it was implemented in 100 epochs and took 55 minutes.

Figure 3 shows the graph of CNN training on the training and validation sets. The OX axis shows the training epochs, and the OY axis shows the values of the loss function. Analyzing the graph, we can conclude that the quality of model training is good, since at the end of training on the training sample, small changes in the loss function are observed.

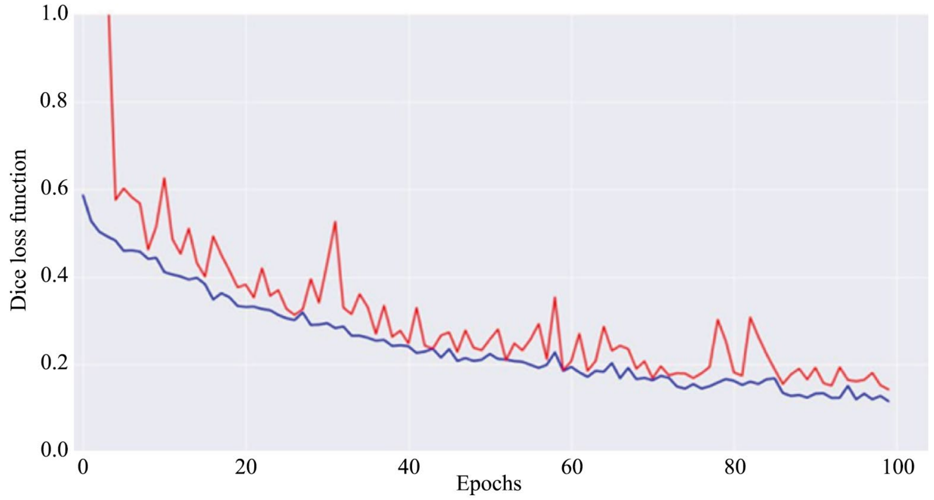

Fig. 3. Training U-Net CNN: — on training sample; — on validation sample

When assessing the quality of segmentation models, the Dice coefficient and the metric of the degree of intersection between two bounding rectangles (Intersection over Union — IoU, Jaccard index), determined form the following formula, are used:

$$IoU = \frac{X \cap Y}{X \cup Y}, \quad (2)$$

where X — a set of pixels defined under the mapping as a scope of a concrete class; Y — a set of pixels assigned to a concrete class according to the conclusions of the developed segmentation model.

Table 2 presents the values of per-pixel precision, recall, F1-score, Dice coefficient, and IoU. To obtain the final IoU value, the weighted average is calculated for the values of this metric for each class.

Table 2

Results of Model Quality Assessment on the Test Sample

Metric	Precision	Recall	F1	Dice	IoU
Average value for test sample	0.89	0.88	0.87	0.87	0.79

Figure 4 shows the results of the algorithm's work on segmenting regions of water resources, land and phytoplankton populations. The results obtained satisfy the tasks of water resource monitoring and have practical value.

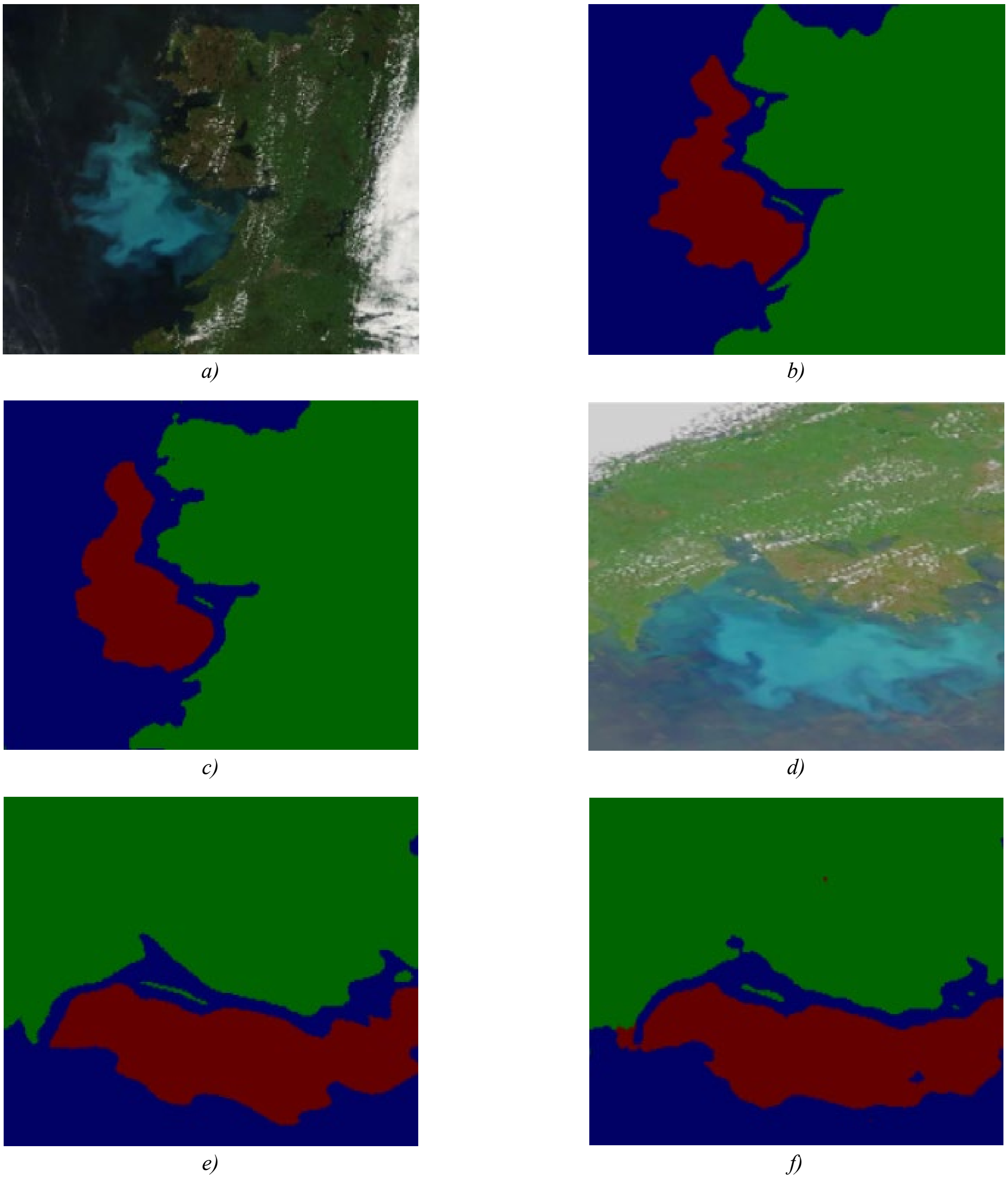

Fig. 4. Algorithm results for segmenting areas of water resources, land and phytoplankton populations:
a, *d* — original image; *b*, *e* — manual mapping; *c*, *f* — model result

The segmentation result in Figures 4 *c* and 4 *f* is visually close to manual mapping, which indicates the high quality of the model. The area of the segmented region of the phytoplankton population was calculated by estimating the area of one pixel. Each image provided has additional metadata indicating the image scale and its resolution. Based on this value, the area occupied by each pixel is calculated. In the case considered for Figure 4 *a*, the final value is 51202.5. This figure was obtained according to information on the number of pixels related to blue-green algae blooms from a set of segmented images of phytoplankton populations in coastal systems [21]. The calculation result for Figure 4 *c* is 51312.

Discussion and Conclusion. When assessing the state of water resources, computer vision and other machine learning algorithms allow specialists to become free from monotonous operations. They are performed by intelligent systems. In this case, monitoring can be carried out round-the-clock. The algorithm will adequately predict risks, model the development of situation, and support the adoption of operational decisions. Stored and replicated knowledge in the form of databases and registers can be used to create long-term sources of information that researchers can use to analyze the state of water bodies and build climate models.

Processing ERS data in the form of semantic contours will provide verifying complex mathematical models through refining boundary and initial conditions, increasing the accuracy, speed and reliability of predictive modeling of hydrobiological processes.

References

1. Yun Zhang, Wanli Gao, Yuying Li, Yeqing Jiang, Xiaonuo Chen, Yinlei Yao, et al. Characteristics of the Phytoplankton Community Structure and Water Quality Evaluation in Autumn in the Huaihe River (China). *International Journal of Environmental Research and Public Health.* 2021;18(22):12092. https://doi.org/10.3390/ijerph182212092

2. Huang Yiqiang, Shen Yucheng, Zhang Shouzhi, Li Yang, Sun Zeyu, Feng Mingming, et al. Characteristics of Phytoplankton Community Structure and Indication to Water Quality in the Lake in Agricultural Areas. *Frontiers in Environmental Science.* 2022;10:1–14. http://doi.org/10.3389/fenvs.2022.833409

3. Govorova ZhM, Govorov OB. Influence of Phytoplankton on the Formation of Water Quality and Methods of its Removal. Part 1. *Plumbing, Heating, Air Conditioning*. 2019;206(2):32–35. (In Russ.) URL: https://www.c-o-k.ru/articles/vliyanie-fitoplanktona-na-formirovanie-kachestva-vody-i-metody-ego-udaleniya-chast-1 (accessed: 04.06.2024).

4. Erina ON, Puklakov VV, Sokolov DI, Goncharov AV. Subglacial Phytoplankton Bloom in the Mozhaisk Reservoir. *Yu.A. Ovchinnikov Bulletin of Biotechnology and Physical and Chemical Biology*. 2019;15(2):49–54. (In Russ.) URL: https://biorosinfo.ru/upload/file/journal_56.pdf (accessed: 04.06.2024).

5. Panasenko ND, Poluyan AYu, Motuz NS. Algorithm for Monitoring the Plankton Population Dynamics Based on Satellite Sensing Data. *Journal of Physics: Conference Series.* 2021;2131(3):032052. https://doi.org/10.1088/1742-6596/2131/3/032052

6. Panasenko ND, Ganzhur MA, Ganzhur AP. Multichannel Satellite Image Application for Water Surface Objects Identification. *Engineering Journal of Don*. 2020;72(12):376–387. URL: http://www.ivdon.ru/uploads/article/pdf/IVD_19__11_Panasenko_Ganzhur1.pdf_244b44d819.pdf (accessed: 04.06.2024).

7. Yanakova ES, Tyurin AA. Complex Algorithm for Semantic Processing of Satellite Images. *Izvestiya TulGU*. 2020;(10):183–189.

8. Druki AA, Spitsyn VG, Bolotova YuA, Bashlykov AA. Semantic Segmentation of Earth Remote Sensing Data Using Neural Network Algorithms. *Bulletin of Tomsk Polytechnic University*. *Geo Assets Engineering*. 2018;329(1):59–68. URL: https://earchive.tpu.ru/bitstream/11683/46113/1/bulletin_tpu-2018-v329-i1-07.pdf (accessed: 04.06.2024).

9. Lukashik DV. Analysis of Modern Image Segmentation Methods. *Economics and Quality of Communication Systems.* 2022;24(2):57–65. URL: https://journal-ekss.ru/wp-content/uploads/2022/06/57-65.pdf (accessed: 04.06.2024).

10. Mohanty S, Czakon J, Kaczmarek K, Pyskir A, Tarasiewicz P, Kunwar S, et al. Deep Learning for Understanding Satellite Imagery: An Experimental Survey. *Frontiers in Artificial Intelligence.* 2020;3:534696. http://doi.org/10.3389/frai.2020.534696

11. Hoffman JP, Rahmes TF, Wimmers AJ, Feltz WF. The Application of a Convolutional Neural Network for the Detection of Contrails in Satellite Imagery. *Remote Sensing*. 2023;15(11):2854. https://doi.org/10.3390/rs15112854

12. Ren Yougui, Xiaomei Yang, Zhihua Wang, Ge Yu, Yueming Liu, Xiaoliang Liu, et al. Segment Anything Model (SAM) Assisted Remote Sensing Supervision for Mariculture — Using Liaoning Province, China as an Example. *Remote Sensing*. 2023;15(24):5781. https://doi.org/10.3390/rs15245781

13. Alagialoglou L, Manakos I, Papadopoulou S, Chadoulis R-T, Kita A. Mapping Underwater Aquatic Vegetation Using Foundation Models With Air- and Space-Borne Images: The Case of Polyphytos Lake. *Remote Sensing.* 2023;15(16):4001. https://doi.org/10.3390/rs15164001

14. Beskopylny AN, Stelmakh SA, Shcherban EM, Razveeva IF, Kozhakin AN, Beskopylny NA, et al. Image Augmentation Software. RF Patent, No. 2022685192. 2022. (In Russ.) URL: https://new.fips.ru/registers-doc-view/fips_servlet?DB=EVM&DocNumber=2022685192&TypeFile=html (accessed: 04.06.2024).

15. Cortés IM. Open-Source Software for Geospatial Analysis*. Nature Reviews Earth and Environment*. 2023;4(143):1. https://doi.org/10.1038/s43017-023-00401-4

16. Razveeva IF, Rakhimbaeva EO. Application of Artificial Intelligence Methods in the Analysis of Phytoplankton Populations on the Water Surface. In: *Proc. International Scientific Conference "Intelligent Information Technologies and Mathematical Modeling"*. Rostov-on-Don: DSTU Publ. House; 2022. P. 45-49.

17. Hopkins JE, Palmer MR, Poulton AJ, Hickman AE, Sharples J. Control of a Phytoplankton Bloom by Wind-Driven Vertical Mixing and Light Availability. *Limnology and Oceanography.* 2021;66:1926–1949. https://doi.org/10.1002/lno.11734

18. Yanhui Dai, Shangbo Yang, Dan Zhao, Chuanmin Hu, Wang Xu, Donald M Anderson, et al. Coastal Phytoplankton Blooms Expand and Intensify in the 21st Century. *Nature*. 2023;615:280–284. https://www.nature.com/articles/s41586-023-05760-y

19. Asselot R, Lunkeit F, Holden P, Hense I. Climate Pathways behind Phytoplankton-Induced Atmospheric Warming. *Biogeosciences*. 2022;19(1):223–239. http://doi.org/10.5194/bg-19-223-2022

20. Kaiming He, Xiangyu Zhang, Shaoqing Ren, Jian Sun. Deep Residual Learning for Image Recognition. In: *Proc. IEEE Conference on Computer Vision and Pattern Recognition* (*CVPR*). New York City: IEEE; 2016. P. 770–778. https://doi.org/10.48550/arXiv.1512.03385

21. Belova YuV, Razveeva IF, Rakhimbaeva EO. A Program for Delineating the Area of Phytoplankton Populations in Coastal Systems. RF Patent, No. 2022684631. 2022. (In Russ.) URL: https://new.fips.ru/registers-doc-view/fips_servlet?DB=EVM&DocNumber=2022685220&TypeFile=html (accessed: 04.06.2024).

About the Authors:

Yulia V. Belova, Cand.Sci. (Eng.), Associate Professor of the Mathematics and Computer Science Department, Don State Technical University (1, Gagarin Square, Rostov-on-Don, 344003, Russian Federation), SPIN-code, ORCID, yvbelova@yandex.ru

Irina F. Razveeva, Senior Lecturer of the Construction of Unique Buildings and Structures Department, Don State Technical University (1, Gagarin Square, Rostov-on-Don, 344003, Russian Federation), SPIN-code, ORCID, razveevai@mail.ru

Elena O. Rakhimbaeva, Postgraduate student, Teaching assistant of the Computer and Automated Systems Software Department, Don State Technical University (1, Gagarin Square, Rostov-on-Don, 344003, Russian Federation), SPIN-code, ORCID, lena_rahimbaeva@mail.ru

Claimed Contributorship:

YuV Belova: software implementation and testing of an intelligent algorithm based on deep learning for processing satellite observation data, analysis of the quality of the segmentation algorithm based on field observations.

IF Razveeva: software implementation, training and debugging of an intelligent algorithm based on deep learning for processing satellite observation data, correction of the text.

E Rakhimbaeva: collection and preprocessing of the training data set, implementation of the data augmentation process, formatting of the article.

Conflict of Interest Statement: **the authors claimed no conflict of interest.**

All authors have read and approved the final manuscript.

Об авторах:

Юлия Валериевна Белова, кандидат физико-математических наук, доцент кафедры математики и информатики Донского государственного технического университета (344003, Российская Федерация, г. Ростов-на-Дону, пл. Гагарина, 1), SPIN-код, ORCID, yvbelova@yandex.ru

Ирина Федоровна Развеева, старший преподаватель кафедры строительства уникальных зданий и сооружений Донского государственного технического университета (344003, Российская Федерация, г. Ростов-на-Дону, пл. Гагарина, 1), SPIN-код, ORCID, razveevai@mail.ru

Елена Олеговна Рахимбаева, аспирант, ассистент кафедры программного обеспечения вычислительной техники и автоматизированных систем Донского государственного технического университета (344003, Российская Федерация, г. Ростов-на-Дону, пл. Гагарина, 1), SPIN-код, ORCID, lena_rahimbaeva@mail.ru

Заявленный вклад авторов:

Ю.В. Белова: программная реализация и тестирование интеллектуального алгоритма на основе глубокого обучения для обработки данных спутниковых наблюдений, анализ качества алгоритма сегментации по данным натурных наблюдений.

И.Ф. Развеева: программная реализация, обучение и отладка интеллектуального алгоритма на основе глубокого обучения для обработки данных спутниковых наблюдений, корректировка текста статьи.

Е.О. Рахимбаева: сбор и предобработка обучающего набора данных, реализация процесса аугментации данных, оформление научной статьи.

Конфликт интересов: **авторы заявляют об отсутствии конфликта интересов.**

Все авторы прочитали и одобрили окончательный вариант рукописи.

Received / Поступила в редакцию 21.06.2024
Reviewed / Поступила после рецензирования 15.07.2024
Accepted / Принята к публикации 24.07.2024

INFORMATION TECHNOLOGY, COMPUTER SCIENCE AND MANAGEMENT
ИНФОРМАТИКА, ВЫЧИСЛИТЕЛЬНАЯ ТЕХНИКА И УПРАВЛЕНИЕ

UDC 519.688/534–16
https://doi.org/10.23947/2687-1653-2024-24-3-293-300

Original Empirical Research

EDN: PLDLKG

Algorithm for Processing X-ray Images Using Fuzzy Logic

Ali Sajae Mannaa
Southern Federal University, Rostov-on-Don, Russian Federation
mannaa@sfedu.ru

Abstract
Introduction. To improve the diagnostics of knee joint diseases, it is necessary to enhance the quality of processing radiographic images, i.e., to provide experts with more accurate information for pathology analysis. The objective of the study is to demonstrate the capabilities of fuzzy logic in improving the algorithm for determining reference lines and knee flexion angles. This requires a program that analyzes X-ray images. The methods known today, described in scientific and applied literature, are not sufficiently automated. In some cases, orthopedists and surgeons have to manually refine images and adjust lines. This gap is filled by the presented work. The algorithm developed by the author is described. It does not involve human participation and automatically identifies the lines and angles of knee flexion. Based on the result issued by the system, the doctor can, firstly, judge the presence of pathology. Secondly, the information provided by the program allows for more accurate planning, performing operations, and prescribing therapy.
Materials and Methods. Images from two X-ray machines operating in Al-Basel Hospital (Latakia, Syria) were used. The Python language was used for the software implementation of the algorithm. The solution was tested on 500 patients at Al-Basel Hospital. The results generated by the new system and previous versions of X-ray image processing programs were compared.
Results. An algorithm for constructing reference lines and angles for processing knee joint X-ray images is created, described, and implemented in practice. The capabilities of fuzzy logic in automating double threshold detection when identifying bone boundaries in images are shown. The operation of an improved Gaussian filter designed for processing X-ray images is described. The modified method of knee bone X-ray analysis includes the development of an algorithm for automatic detection of structures and anomalies in knee joints, determination and measurement of anatomical parameters, assessment of the degree of damage, etc. The method for determining the contour boundaries on radiographs combined the Canny detector, the watershed algorithm, and fuzzy logic. The program has been implemented in medical practice and shows 98% accuracy, spending less than 20 seconds to process the image.
Discussion and Conclusion. The new system provides high accuracy, acceptable efficiency, and does not require manual correction of images. Experts are now able to identify subtle indicators of disorders. In addition, the new method makes it possible to understand complex cases when several factors are combined, indicating potential pathology. Widespread implementation of the method will improve the quality of medical services in orthopedics. Scientific research in this direction should be continued to expand the set of strategies for the treatment of diseases of the musculoskeletal system. It is necessary to create solutions with absolute accuracy, higher processing efficiency, as well as methods suitable for analyzing other joints.

Keywords: reference lines in radiography, knee joint angles in radiography, Canny algorithm, improved Gaussian filter, watershed algorithm

For Citation. Mannaa AS. Algorithm for Processing X-ray Images Using Fuzzy Logic. *Advanced Engineering Research* (*Rostov-on-Don*). 2024;24(3):293–300. https://doi.org/10.23947/2687-1653-2024-24-3-293-300

Оригинальное эмпирическое исследование

Алгоритм обработки рентгеновских изображений с использованием нечеткой логики

А.С. Маннаа ✉

Южный федеральный университет, г. Ростов-на-Дону, Российская Федерация

✉ mannaa@sfedu.ru

Аннотация

Введение. Для улучшения диагностики заболеваний коленного сустава необходимо повысить качество обработки рентгенографических изображений, т.е. дать специалистам более точную информацию для анализа патологии. Цель исследования — показать возможности нечеткой логики в совершенствовании алгоритма определения опорных линий и углов сгибания колена. Для этого необходима программа, которая анализирует рентгеновские снимки. Известные на сегодня методы, описанные в научной и прикладной литературе, недостаточно автоматизированы. В ряде случаев ортопедам и хирургам приходится вручную дорабатывать изображения, корректировать линии. Этот пробел восполняет представленная работа. Описан созданный автором алгоритм, который не предполагает участия человека, автоматически идентифицирует линии и углы сгибания колена. По результату, выданному системой, врач может, во-первых, судить о наличии патологии. Во-вторых, сведения, предоставляемые программой, позволяют точнее планировать, проводить операции и назначать терапию.

Материалы и методы. Использовались снимки двух рентгеновских аппаратов, которые работают в больнице Аль-Базель (Латакия, Сирия). Для программной реализации алгоритма задействовали язык «Питон» (Python). Решение протестировали на 500 пациентах больницы Аль-Базель. Сравнивались результаты, которые сгенерировала новая система и предшествующие версии программ обработки рентгеновских снимков.

Результаты исследования. Создан, описан и реализован на практике алгоритм построения опорных линий и углов для обработки рентгеновских снимков коленного сустава. Показаны возможности нечеткой логики в автоматизации обнаружения двойного порога при выявлении границ кости на изображениях. Описана работа усовершенствованного гауссовского фильтра, предназначенного для обработки рентгенограмм.

Модифицированный метод анализа рентгеновских снимков коленных костей включает разработку алгоритма для автоматического обнаружения структур и аномалий в коленных суставах, определения и измерения анатомических параметров, оценку степени повреждения и т.д.

Метод определения границ контуров на рентгенограммах объединил детектор Кэнни, алгоритм водораздела и нечеткую логику. Программа реализована в медицинской практике и показывает точность 98 %, затрачивая на обработку снимка менее 20 секунд.

Обсуждение и заключение. Новая система дает высокую точность, приемлемую оперативность и не требует ручной корректировки снимков. Специалисты получили возможность выявить малозаметные индикаторы нарушений. Кроме того, новый метод позволяет разобраться в сложных случаях, когда сочетаются несколько факторов, указывающих на возможную патологию. Широкое внедрение метода повысит качество медицинских услуг в ортопедии. Следует продолжить научные изыскания в данном направлении для расширения набора стратегий лечения заболеваний опорно-двигательного аппарата. Предстоит создать решения с абсолютной точностью, более высокой оперативностью обработки, а также методы, подходящие для анализа других суставов.

Ключевые слова: опорные линии в рентгенографии, углы коленных суставов в рентгенографии, алгоритм Кэнни, усовершенствованный фильтр Гаусса, алгоритм водораздела

Для цитирования. Маннаа А.С. Алгоритм обработки рентгеновских изображений с использованием нечеткой логики. *Advanced Engineering Research* (*Rostov-on-Don*). 2024;24(3):293–300. https://doi.org/10.23947/2687-1653-2024-24-3-293-300

Introduction. Improving the quality of X-ray images is a critical task with direct implications for the quality of medical diagnosis and subsequent treatment, especially in cases like joint replacement surgeries. Advancements in medical imaging technologies, including X-ray imaging, are vital for providing more accurate and detailed information to healthcare professionals. There are some strategies and advancements that can help improve X-ray image quality and subsequently benefit joint replacement surgeries and other medical procedures.

Analysis of X-ray images allows identifying and evaluate various pathological conditions [1]. Algorithms for image segmentation and bone delimitation have made a significant contribution to improving the clarity and accuracy of X-ray image interpretation. However, such visualization still needs improvement, as it is not always completely defined, leaving room for different interpretations [2].

Advances in intelligent computing make it possible to use fuzzy logic to remove imprecision and ambiguity in the medical image analysis. Fuzzy logic mimics human thinking, and it is a reliable basis for creating algorithms that can efficiently process and analyze X-ray images [3].

In [4], reference lines and their relationships were studied for the purpose of correcting the shape of the legs. In [5], clinical results of treating multiaxial deformities of the lower extremities were compared to how this was reflected in X-ray images. The literature describes software products that can analyze X-ray images of bones. However, all these systems have a common drawback: sometimes they incorrectly recognize contours. If this happens, the specialist manually refines the image. This problem is solved in the presented scientific work. A new algorithm for analyzing X-ray images is proposed using fuzzy logic and improved traditional approaches. The solution eliminates the need for manual image processing. The program operates with high accuracy and ample efficiency. It allows for more accurate detection and characterization of anomalies in X-ray images, i.e., improves diagnostics.

Materials and Methods. In carrying out this scientific work, the author proceeded from the fact that the assessment of limb deformations requires an analysis of the anatomical and mechanical axes of long bones, as well as the angles between them. Figure 1 shows the initial limits of angles for healthy people of different ages. If the indicator is outside these limits, then the patient has a deformed limb and needs surgical intervention.

Fig. 1. Support angles between mechanical axes for healthy people:
a — for young people; *b* — for elderly people [4]

In orthopaedics, the concepts of mechanical and anatomical axis are crucial to understanding the arrangement and function of bones, especially in the lower extremities. The anatomical axis runs through the center of the bone shaft, through the middle of the diaphysis. The mechanical axis reflects the direction of the forces acting on it. In the lower extremities, it runs from the center of the hip joint to the center of the ankle joint.

By examining the mechanical axis, it is possible to understand the load-bearing capacity and load distribution in the bone. This is particularly important for the diagnosis and treatment of osteoarthritis, fractures, and for determining the position of implants or prostheses.

It is necessary to know the features of the anatomical axis to distinguish natural curvature from pathological curvature. This is also important under surgical interventions, since it helps surgeons understand whether the bone is positioned correctly.

Two parameters are particularly important for assessing the anatomy of the femur and tibia:

- ALDFA (axial length of the distal femoral axis);
- MPTA (medial proximal tibial angle).

They are extremely informative when it comes to identifying knee deformities. ALDFA determines the orientation of the distal femur relative to its longitudinal axis, MPTA shows the inclination of the medial surface of the tibia relative to its mechanical axis (Fig. 2).

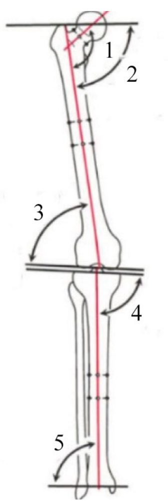

Fig. 2. Angles between femur and tibia used to assess anatomy and detect pathology:
1 — medial genu-diaphyseal angle (MGDA) = 130° (124°–136°); 2 — medial proximal femoral angle (MPFA) = 84° (80°–89°);
3 — ALDFA = 81° (79°–83°); 4 — MPTA = 87° (85°–90°); 5 — lateral distal tibial angle (LDTA) = 89° (85°–92°) [5]

The angles shown in Figure 2, in combination, demonstrate the possibilities of knee joint alignment or deformation. Orthopedists use the norm (numbers in brackets) to draw conclusions about the type, severity of deformations, and develop a treatment plan [6].

The Canny edge detection algorithm is a robust method widely used to identify boundaries in images. It builds reference lines and angles from X-ray images as follows. The first step uses an improved Gaussian filter, which smoothes the image, reduces noise [7]. Next, gradients are calculated using the Sobel or Prewitt operators. The method is often used to detect the image edges. This allows both weak and strong edges to be taken into account. This way, the algorithm determines the edges more accurately and reduces the noise level more effectively.

Despite its computational complexity, the Canny algorithm remains a fundamental part of computer vision due to its ability to cope with noise and clearly detect edges.

To correctly select the standard deviation value, the absolute values of the point $x(i, j)$ in the gray pixel are compared [8]. If $|x(i, j)| < |x(i, j)| \times |x(i, j) - \mu|$, then the standard deviation $\sigma = 1$. In this case, the point is less affected by noise. Standard deviation $\sigma = 1.6$ indicates significant noise.

To automatically detect the edges ($T1$, $T2$), Canny uses double thresholding, classifying pixels in the image by gray intensity. We calculate the average value of all pixels ($T1$), after which $T1$ is used to divide the image into two areas — object and background. Pixel values that exceed the initial threshold $T1$ are taken as objects, and the rest are taken as background. Now there are two sets of values: one for the object (ob) and one for the background (bg). For each of the two regions (object, background), a threshold value is calculated. Let us calculate $T2$. We start with the fact that:

$$T0 = \left(Tob + Tbg\right) / 2. \quad (1)$$

New value $T0$ is taken as $T1$, and the process is repeated until $T0$ ~= $T1$. Final value $T0$ is taken as $T2$.

The final step involves boundary binding to identify related boundary components in the VNSA (valgus knee shaft angle) image. This helps to combine disparate boundaries into larger structures, which improves image perception and analysis. It is advisable to integrate fuzzy logic principles and traditional software approaches to edge detection. In this case, membership functions are used that assign membership degrees to pixels based on gray intensity values, allowing for a detailed representation of edges.

Unlike the binary approach, the fuzzy method facilitates a gradual transition in the range of membership values from 0 (no membership at all) to 1 (full membership), capturing the inaccuracies of the boundaries. Fuzzification transforms crisp image data into fuzzy sets, taking into account the uncertainty. Defuzzification transforms fuzzy results into crisp ones for further analysis.

A notable advantage of the method is its adaptability to real-world scripts, specifically to those with varying degrees of noise and ambiguity. However, careful parameter tuning may be required to achieve optimal performance; therefore, finding a balance between sensitivity and specificity in edge detection applications is critical [9].

A more detailed representation of edges can be achieved by disambiguating image boundaries. This requires assigning membership degrees to pixels.

Each pixel is processed using fuzzy rules. If any of the fuzzy rules shown in Figure 3 are met, the pixel is processed as an edge, otherwise it is not taken into account. This provides highlighting the boundaries of objects that are different from noise and other image elements. The importance of this solution has been proven in relation to the analysis of the humerus from X-ray images [10].

I3 = 1 I1&&I2&&I4&&I5&&I6&&I7&&I8 = 0	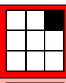	I8 = 1 I1&&I2&&I3&&I4&&I5&&I6&&I7 = 0	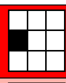
I4 = 1 I1&&I2&&I3&&I5&&I6&&I7&&I8 = 0	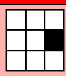	I3 = 1, I4 = 1, I5 = 1, I1&&I2&&I6&&I7&&I8 = 0	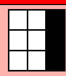
I5 = 1 I1&&I2&&I3&&I4&&I6&&I7&&I8 = 0	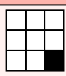	I1 = 1, I2 = 1, I3 = 1, I4&&I5&&I6&&I7&&I8 = 0	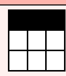
I6 = 1 I1&&I2&&I3&&I4&&I5&&I7&&I8 = 0	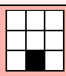	I5 = 1, I6 = 1, I7 = 1, I1&&I2&&I3&&I4&&I8 = 0	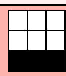
I8 = 1 I1&&I2&&I3&&I4&&I5&&I6&&I7 = 0	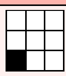	I1 = 1, I7 = 1, I8 = 1, I1&&I2&&I3&&I4&&I8 = 0	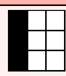

Fig. 3. Fuzzy logic rules

The watershed segmentation algorithm is used in computer vision to recognize objects. It was originally developed for cartography. And now it perceives images as a topographic landscape, where the grayscale intensity corresponds to the terrain elevation. Watershed lines outline individual objects as boundaries between drainage basins. By filling the landscape from local minima, the algorithm separates objects by the intensity of gray color.

The watershed detection algorithm is effective for some applications, but it can be sensitive to noise and may cause over-segmentation. In practice, careful preprocessing and marker-driven watershed options are used to improve performance [11].

The watershed algorithm output is shown in Figure 4.

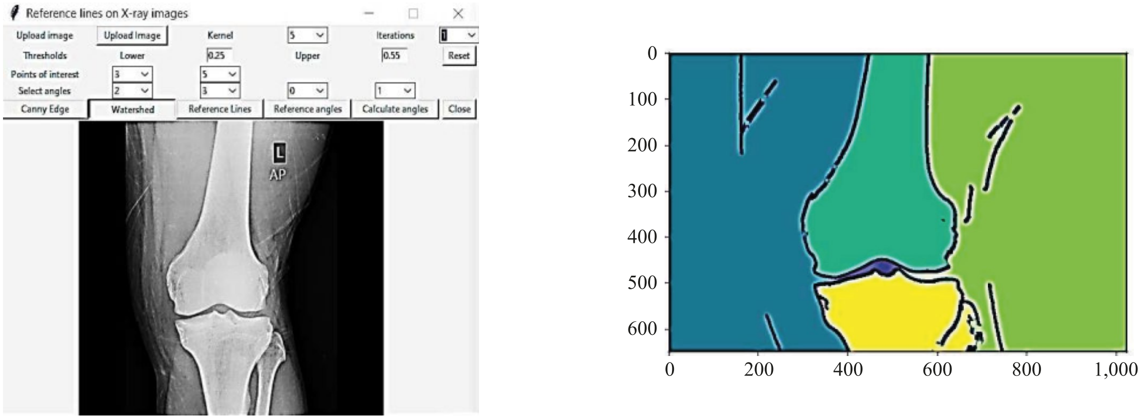

a) *b)*

Fig. 4. Watershed algorithm output:
a — original image; *b* — result of watersheds

Research Results. After using the watershed algorithm, boundaries were drawn for the points under study [12]. To construct reference lines, the extreme points were calculated along the boundary of the mark (selected region) of the bone. Then, the center of mass was calculated, the image was converted to binary format, and its center was found. Having determined the extreme points on four sides, we took the middle of the top of the upper bone, the middle of the base of the lower bone and drew a line.

We used the formula for calculating the angle between two lines and three coordinate points: *aa*, *bb* and *cc*. Two are the extreme points of both lines, and one is the common point of their intersection [13].

$$b = -a \times x_1 + y_1, \tag{2}$$

$$x_1 = y_1 - b \div a,\ x_2 = y_2 - b \div a, \tag{3}$$

$$a = 1.0 \times (y_2 - y_1) \div 1.0 \times (x_2 - x_1). \tag{4}$$

Figure 5 shows the result of constructing reference lines and angles on X-ray images.

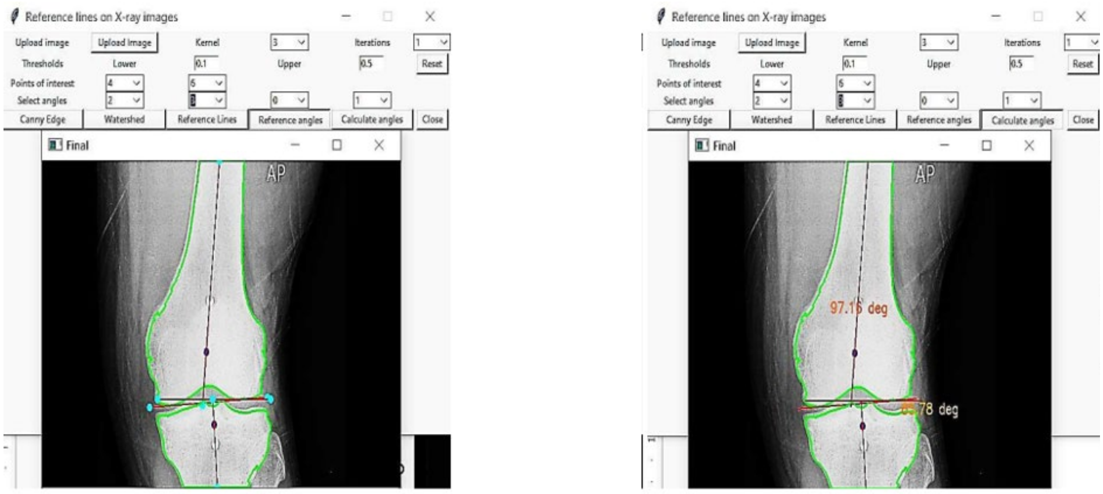

a) *b)*

Fig. 5. Results of using the improved watershed algorithm on X-ray images:
a — construction of reference lines; *b* — calculation of angles

The performance of the Canny edge detector [14] was compared to the results of the new algorithm proposed by the author. The higher performance of the latter solution is obvious. This is explained, firstly, by the improvement of the Canny operator. Secondly, the new method is integrated with an improved Gaussian filter. Therefore, there is no need for an additional filter, and the execution time of the algorithm is reduced. Its implementation has significantly increased the accuracy and yielded better results, specifically for images of radial lines with high noise levels.

The new solution was implemented at Al-Basel Hospital in Latakia, Syria. Images from two X-ray machines were used. The program was applied to X-ray images of 500 patients. In 490 cases, no manual processing was required, i.e., the accuracy of the results was 98%. Image processing took about 20 seconds.

The proposed algorithm is implemented in Python with a graphic interface. The scheme for creating reference lines and angles for processing X-ray images of the knee joint is designed to improve the interpretation of X-ray images (Fig. 6).

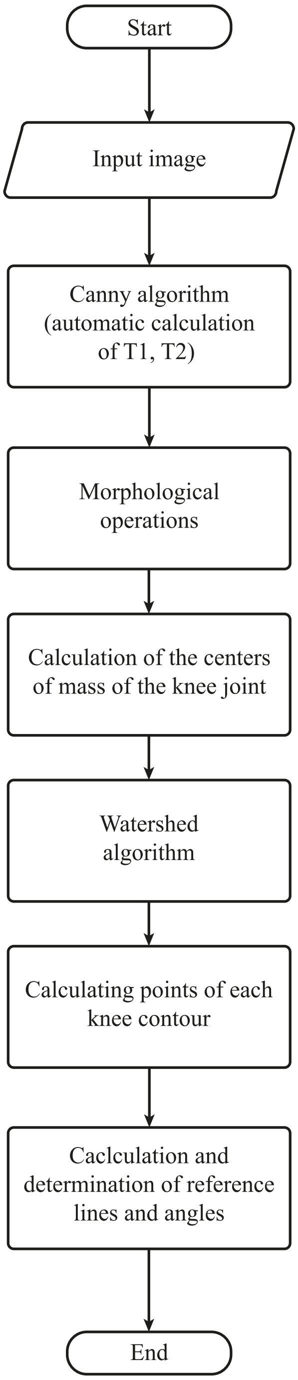

Fig. 6. Improved algorithm for creating reference lines and angles for processing knee joint X-ray images

Discussion and Conclusion. A new approach to knee X-ray imaging is being used at Al-Basel Hospital (Latakia, Syria). The practice has shown the value of advanced automated image analysis in improving diagnostic accuracy. It should be noted that even an earlier version of the program effectively identified bone abnormalities that were missed by visual analysis [15]. With the help of the proposed solution, orthopedists can qualitatively work through subtle factors indicating violations, as well as combinations of indicators that can cause confusion and hinder the detection of pathology. It follows that the use of the approach described in this article allows us to reasonably expect an increase in the quality of medical services in the field of orthopedics and surgery. Specialists receive tools for more precise planning and execution of operations. In addition, the new solution opens up opportunities for better organization of conservative treatment taking into account the individual characteristics of the pathology.

Scientific research in this line should be continued to expand diagnostic capabilities and a range of treatment strategies for musculoskeletal diseases. Of particular interest is achieving absolute, i.e., 100% accuracy in algorithmic determination of the lines. The time for image processing should also be reduced. Optimization of computational processes will provide obtaining results faster, which is particularly important in emergency diagnostics. In addition, it is advisable to refine the method for analyzing more complex clinical cases. Another promising direction is adapting the algorithm for analyzing other joints, such as hip or shoulder joints.

References

1. Al-Temimi Ammar Mudheher Sadek, Pilidi VS. On an Algorithm for Structure Analysis of X-ray Medical Images. *University News. North-Caucasian Region. Technical Sciences Series.* 2018;197(1):23–28. https://doi.org/10.17213/0321-2653-2018-1-23-28

2. Jassam KI. Removal of Random Noise from Conventional Digital X-Ray Images. *International Archives of Photogrammetry and Remote Sensing*. 1993;29:113–118. https://doi.org/n10y2021/7227

3. Ruiyuan Liu, Jian Mao. Research on Improved Canny Edge Detection Algorithm. In: *Proc. 2nd International Conference on Electronic Information Technology and Computer Engineering, (EITCE). MATEC Web of Conferences.* 2018;232(4):03053. https://doi.org/10.1051/matecconf/201823203053

4. Kulesh PN, Solomin LN. Relationships between Reference Lines Altered during Leg Shape Correction as Requested by the Patient. *Orthopaedic Genius.* 2021;27(3):390–397. https://doi.org/10.18019/1028-4427-2021-27-3-390-397

5. Riganti S, Nasto LA, Mannino S, Brunenghi GM, Boero S. Correction of Complex Lower Limb Angular Deformities with or without Length Discrepancy in Children Using the TL-HEX Hexapod System : Comparison of Clinical and Radiographical Results. *Journal of Pediatric Orthopaedics B*. 2019;28(3):214–220. https://doi.org/10.1097/BPB.0000000000000573

6. Gaidel AB, Pervushkin SS. Research of the Textural Features for the Bony Tissue Diseases Diagnostics Using the Roentgenograms. *Computer Optics*. 2013;37(1):133–119. https://doi.org/10.18287/0134-2452-2013-37-1-113-119

7. Weibin Rong, Zhanjing Li, Wei Zhang, Lining Sun. An improved Canny Edge Detection Algorithm. In: *Proc. IEEE International Conference on Mechatronics and Automation (ICMA).* New York City: IEEE; 2014. P. 577–582. https://doi.org/10.1109/ICMA.2014.6885761

8. Kaur EK, Mutenja V, Gill EIS. Fuzzy Logic Based Image Edge Detection Algorithm in MATLAB. *International Journal of Computer Applications.* 2010;1(22):55–58. http://doi.org/10.5120/442-675

9. Haibo Zhou, Hao Ying. A Method for Deriving the Analytical Structure of a Broad Class of Typical Interval Type-2 Mamdani Fuzzy Controllers. *IEEE Transactions on Fuzzy Systems.* 2013;21(3):447–458. http://doi.org/10.1109/TFUZZ.2012.2226891

10. Gonzalez RC, Woods RE. *Digital Image Processing*. Moscow: Tekhnosfera; 2005. 1072 p. (In Russ.)

11. Abdelwahed Motwakel, Adnan Shaout, Gasm Elseed Ibrahim Mohamed. Dry Fingerprint Image Enhancement Using Fuzzy Morphology. *International Journal of Knowledge Engineering and Data Mining.* 2016;4(1):40–53. https://doi.org/10.1504/IJKEDM.2016.082074

12. Suhas S, Venugopal CR. An Efficient MRI Noise Removal Technique Using Linear and Nonlinear Filters. *International Journal of Computer Applications.* 2018;179(15):17–20. https://doi.org/10.5120/IJCA2018915777

13. Anam S, Uchino E, Misawa H, Suetake N. Texture Analysis and Modified Level Set Method for Automatic Detection of Bone Boundaries in Hand Radiographs. *International Journal of Advanced Computer Science and Applications*. 2014;5(10): 117–126. https://doi.org/10.14569/IJACSA.2014.051017

14. Al-Temimi Ammar Mudheher Sadek, Pilidi VS. Automating the Process of Determining the Reference Lines on the X-ray Medical Images. *Engineering Journal of Don.* 2017;44(1):27–36. URL: http://www.ivdon.ru/uploads/article/pdf/IVD_55_Temimi_Pelidi.pdf_02dcdf3989.pdf (accessed: 25.05.2024).

15. Mannaa AS, Muratova GV. Development of Algorithm for Constructing Reference Lines and Angles for Knee Joints on X-ray Images. *Bulletin of Higher Education Institutes. North-Caucasian Region. Natural Sciences.* 2023;218(2):15–20. https://doi.org/10.18522/1026-2237-2023-2-15-20

About the Author:

Ali Sajae Mannaa, Postgraduate Student, Department of Informatics and Computational Experiment, Vorovich Institute of Mathematics, Mechanics and Computer Sciences, Southern Federal University (21e, Zorge Str., Rostov-on-Don, 344015, Russian Federation), SPIN-code, ORCID, ScopusID, ResearcherID, mannaa@sfedu.ru

Conflict of Interest Statement: **the author claimed no conflict of interest.**

The author has read and approved the final manuscript.

Об авторе:

Али Сажи Маннаа, аспирант кафедры информатики и вычислительного эксперимента института математики, механики и компьютерных наук им. И.И. Воровича Южного федерального университета (344015, г. Ростов-на-Дону, ул. Зорге 21е, д. 1001), SPIN-код, ORCID, ScopusID, ResearcherID, mannaa@sfedu.ru

Конфликт интересов: **автор заявляет об отсутствии конфликта интересов.**

Автор прочитал и одобрил окончательный вариант рукописи.

Received / Поступила в редакцию 29.05.2024
Reviewed / Поступила после рецензирования 17.06.2024
Accepted / Принята к публикации 26.06.2024